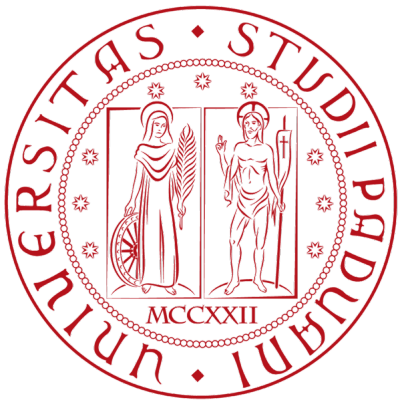

Università degli Studi di Padova

Department of Physics and Astronomy "Galileo Galilei"

Master Degree in Physics

Final Dissertation

NP effects at the MUonE experiment at CERN

Thesis supervisor:
Prof. Paride Paradisi

Candidate:
Lorenzo Mai
1205209

Academic Year 2019-2020

Ad A.
Guardami affrontare questa vita come fossi ancora qua.

Contents

Introduction

The Standard Model (SM) of particle physics has been experimentally tested with high precision in a successful way and the recent observation of a state compatible with the Higgs boson seems to validate this theory. Nevertheless it cannot provide a complete description of Nature and today it is commonly shared the idea that it is not a fundamental theory, but rather its low-energy version valid up to a certain energy scale Λ. A lot of hints, in particular the solution to the hierarchy problem, points towards the presence of new physics (NP) at $\Lambda \sim$ TeV scale; the Large Hadron Collider (LHC) at CERN has already tested this range of energies, reaching $\sqrt{s} \sim 14$ TeV but, unfortunately, no evidences of NP have been found so far.
Among the issues which characterize the SM, that of the anomalous magnetic moment of the muon represents a very long standing problem. In particular, the discrepancy between the theoretical prediction and the experimental result is of 3.3σ. However it is still not clear whether this inconsistency is due to the hadronic uncertainties which affect a_μ or it is an hint of NP. This problem led to the proposal of the experiment MUonE, whose goal is to extract a precise value of a_μ^{Had} using a new method based on the analysis of μe collisions. However, the precision expected for this experiment raises the question whether NP could pollute MUonE measurements. This work aims to analyze this issue studying NP effects in muon-electron scattering due to both heavy and light mediators, depending on whether their mass is higher or lower than $\mathcal{O}$ (1 GeV), which is the energy scale of the MUonE experiment.
After a revision of the fundamental theoretical concepts of the SM in Ch. (1) and the explanation of the muon $g-2$ anomaly in Ch. (2), the thesis will be split in two parts. In the first part, see Ch. (3), I will discuss heavy mediators. Here I assume that modes have typical mass of $\Lambda \sim 1$ TeV and, therefore, it is possible to exploit an EFT approach constructing the most general Lagrangian invariant under the full SM gauge group $G_{\text{SM}} = SU(3)_C \otimes SU(2)_L \otimes U(1)_Y$. Once computed the NP corrections to the $\mu^\pm e^- \to \mu^\pm e^-$ cross section, I evaluate the correlated corrections to both the total cross section and the forward-backward asymmetry of the process $e^+e^- \to \mu^+\mu^-$, which are constrained by LEP bounds. Finally I will focus also on lepton flavor violating (LFV) effects in muon-electron collisions such as the process $\mu^+e^- \to \mu^-e^+$.
In the second part, see Ch. (4), I will concentrate on light NP mediators, for which the model-independent EFT approach cannot be applied. In particular I will focus on popular scenarios containing either light (pseudo)scalars, referred to as axion-like particles (ALPs), or light (axial)vector bosons, such as the so-called dark-photons and light Z'. Using existing direct and indirect bounds on masses and couplings of these light particles, I establish the maximum sizes of these light NP effects allowed in μe collisions.

The work of this thesis extends and generalises the results appeared in the paper:

A. Masiero, P. Paradisi and M. Passera, "New physics at the MUonE experiment at CERN," https://arxiv.org/pdf/2002.05418.pdf.

Chapter 1

The Standard Model

The Standard Model (SM) of particle physics is a very successful theory. Its predictions have been tested in the last forty years with an increasing precision and they have shown an amazing agreement with the experimental results for a wide range of phenomena. The coronation of the SM rely in the discovery of the Higgs boson in 2012 [1, 2], the missing piece of this theory which was theorised fifty years before. Nevertheless, today it is commonly shared and accepted the idea that the SM can't be the fundamental theory which physicists were looking for, rather its low energy effective version: indeed this model isn't able to provide a complete description of Nature when going to very high energies, which implies that it needs a UV completion. The key point is to understand at what energy scale New Physics (NP) appears and what specific generalization of the SM is required.
This chapter is dedicated to a concise review the Electroweak (EW) and Flavor sectors of the SM, which will be presented in Sec. (1.1), being the basis over which this entire work is built; in Sec.(1.2), instead, the reasons why a BSM theory is needed will be briefly mentioned and explained.

1.1 Electroweak and Flavor sectors of the SM

The Electroweak sector of the SM is based on the gauge symmetry $SU(2)_L \otimes U(1)_Y$ and its particle content consists in three charged leptons (electron, muon and tau) with the corresponding neutrinos, six quarks (up, down, charm, strange, top, bottom), one scalar boson (Higgs) and four vector bosons (B_μ, W^i_μ). The fermionic matter content is divided into three generations of doublets and singlets according to the transformation properties of the fields under the gauge group. Denoting them as $\psi(T, Y)$, where T and Y are, respectively, their representations under $SU(2)_L$ and $U(1)_Y$ and the hypercharge satisfies $Y = Q - T_3$, this organization reads

$$l^p\left(2, -\frac{1}{2}\right) \quad e^p_R\,(1, -1) \quad q^p\left(2, \frac{1}{6}\right) \quad u^p_R\left(1, \frac{2}{3}\right) \quad d^p_R\left(1, -\frac{1}{3}\right), \tag{1.1}$$

where $p = 1, 2, 3$ run over the three generations and the two doublets are explicitly $l^p = (\nu^p_L, e^p_L)$, $q^p = (u^p_L, d^p_L)$; also the Higgs fields is charged under the EW gauge group with $\phi = (2, 1/2)$.

The EW Lagrangian in the interaction basis is

$$\begin{aligned}\mathcal{L}_{\rm SM}^{\rm EW} = &-\frac{1}{4}W^i_{\mu\nu}W^{i\mu\nu} - \frac{1}{4}B_{\mu\nu}B^{\mu\nu} + (D_\mu\phi)^\dagger(D^\mu\phi) + \sum_\psi \bar{\psi}i\not{D}\psi + \\ &- \lambda\left(\phi^\dagger\phi - \frac{v^2}{2}\right)^2 - \left[\bar{q}_{Lp}y_u^{pr}\tilde{\phi}u_{Rr} + \bar{q}_{Lp}y_d^{pr}\phi d_{Rr} + \bar{l}_{Lp}y_e^{pr}\phi e_{Rr} + h.c.\right]\end{aligned} \tag{1.2}$$

where W^i_μ and B_μ are, respectively, the gauge fields associated to $SU(2)_L$ and $U(1)_Y$, while the two covariant derivatives read

$$D_\mu\psi = \left(\partial_\mu + i\frac{g}{2}\sigma_i W^i_\mu + ig'Y_\psi B_\mu\right)\psi, \tag{1.3}$$

$$D_\mu\phi = \left(\partial_\mu + i\frac{g}{2}\sigma_i W^i_\mu + i\frac{g'}{2}B_\mu\right)\phi. \tag{1.4}$$

In the Lagrangian of Eq. (1.2) there are no mass terms for both fermions and vector bosons, since they would violate the gauge symmetry; nevertheless they can still be generated via Spontaneous Symmetry Breaking (SSB) mechanism once the scalar field ϕ gets a non-zero vacuum expectation value (VEV), i.e.

$$\langle\phi\rangle = v = \sqrt{\frac{-\mu^2}{\lambda}} = 246\ \text{GeV}. \tag{1.5}$$

Then, parametrizing the field as an excitation around this vacuum (imposing directly the unitary gauge) as

$$\phi(x) = \frac{v + H(x)}{\sqrt{2}} \tag{1.6}$$

and replacing it in the initial Lagrangian, it is possible to find the mass spectrum of the theory, which reads

$$M_W^2 = \frac{v^2g^2}{4}, \quad M_Z^2 = \frac{v^2(g+g')^2}{4}, \quad M_\gamma = 0, \quad M_H^2 = 2\lambda v^2. \tag{1.7}$$

Another interesting way to test the SM concerns its flavor sector.
If all the Yukawa couplings were null the SM Lagrangian would enjoy a global $U(3)^5 = U(3)_l^2 \otimes U(3)_q^3$ flavor symmetry, corresponding to the independent unitary rotations of the fermion fields in flavor space; nevertheless, being $y_\psi \neq 0$ and in general non-diagonal, this symmetry is explicitly broken. As a consequence, the residual flavor symmetry group of $\mathcal{L}_{\rm SM}$ is $G_F = U(1)_B \otimes U(1)_e \otimes U(1)_\mu \otimes U(1)_\tau$, where the four $U(1)$ groups are associated, respectively, to the baryon number and lepton family number conservation.
This interaction with the scalar field allows also leptons and quarks to receive mass but it is possible to read the spectrum only after the diagonalization of the Yukawa matrices by means of a field rotation. The new basis is known (quite obviously) as *mass basis* and it can be recovered once the fields are rotated through the unitary matrices L_ψ and R_ψ as

$$u'_L = L_u u_L, \quad d'_L = L_d d_L, \quad e'_L = L_e e_L \tag{1.8}$$

$$u'_R = R_u u_R, \quad d'_R = R_d d_R, \quad e'_R = R_e e_R \tag{1.9}$$

in such a way that for every fermion the new matrix $\tilde{y}_\psi = L_\psi y_\psi R_\psi^\dagger$ is diagonal. Then the fermion mass terms read

$$m_{\psi^i} = \frac{v\tilde{y_{\psi^i}}}{\sqrt{2}} \tag{1.10}$$

where i, as usual, run over the three generations.
The rotation to the mass basis must be performed also in all the other sectors of the SM. Nevertheless it turns out that only the charge currents are affected by this change of basis, since the kinetic terms and the neutral currents (both electromagnetic and weak) transform as[1]

$$\bar{\psi}_L\gamma^\mu\psi_L \to \bar{\psi}_L L_\psi^\dagger\gamma^\mu L_\psi\psi_L = \bar{\psi}_L\gamma^\mu\psi_L \tag{1.11}$$

where it has been exploited the fact that the rotation matrix L_ψ is unitary and that it commutes with the gammas (belonging to different spaces). Clearly this does not happen in the case of the charge sector: indeed, given the current J_μ^- the explicit rotation leads to

$$\bar{u}_L\gamma^\mu d_L + \bar{\nu}_L\gamma^\mu e_L \to \bar{u}_L L_u^\dagger\gamma^\mu L_d d_L + \bar{\nu}_L L_\nu^\dagger\gamma^\mu L_e e_L = \bar{u}_L\gamma^\mu V_{CKM} d_L + \bar{\nu}_L\gamma^\mu U_{PMNS} e_L \tag{1.12}$$

where $V_{\text{CKM}} \equiv L_u^\dagger L_d$ and $U_{\text{PMNS}} \equiv L_\nu^\dagger L_e$ are, respectively, the *Cabibbo-Kobayashi-Maskawa* and *Pontecorvo–Maki–Nakagawa–Sakata* mixing matrices. As a consequence, while in the interaction basis the charge current are flavor diagonal, in the mass basis tree level Flavor Changing Charged Current (FCCC) transitions arise due to the presence of V_{CKM}. This matrix is of crucial importance in flavor physics, because it is the only source of flavor-changing transitions in the SM. The most used parametrizations are the *standard parametrization*, which uses three angles θ_i and a complex phase δ, and the *Wolfenstein parametrization*, where the CKM matrix elements are expanded in powers of the small parameter $\lambda = |V_{us}| \approx 0.22$ [3]. The latter has the remarkable property of exhibiting the strong hierarchy between the CKM matrix elements. Explicitly it is

$$V_{\text{CKM}} = \begin{pmatrix} 1-\frac{\lambda^2}{2} & \lambda & A\lambda^3(\rho-i\eta) \\ -\lambda & 1-\frac{\lambda^2}{2} & A\lambda^2 \\ A\lambda^3(1-\rho-i\eta) & -A\lambda^2 & 1 \end{pmatrix} + \mathcal{O}\left(\lambda^4\right), \tag{1.13}$$

where A, ρ, η are real parameters of order one; however, sometimes it is convenient to deal with the rescaled variables $\bar{\rho}$ and $\bar{\eta}$ provided by

$$\bar{\rho} = \rho\left(1-\frac{\lambda^2}{2}\right) + \mathcal{O}\left(\lambda^4\right) \quad \bar{\eta} = \eta\left(1-\frac{\lambda^2}{2}\right) + \mathcal{O}\left(\lambda^4\right).$$

Since V_{CKM} is unitary, the following relations hold:

$$\sum_{k=1\ldots3} V_{ik}^* V_{ki} = 1 \qquad \sum_{k=1\ldots3} V_{ik}^* V_{kj\neq i} = 0. \tag{1.14}$$

These relations are a specific feature of the SM and their experimental verification is a powerful consistency check of the model. Among them,

$$V_{ud}V_{ub}^* + V_{cd}V_{cb}^* + V_{td}V_{tb}^* = 0 \quad \leftrightarrow \quad [\bar{\rho}+i\bar{\eta}] + [(1-\bar{\rho})-i\bar{\eta}] + 1 = 0 \tag{1.15}$$

is the phenomenologically most interesting one, because it involves the sum of three terms of the same order in λ. It is usually represented as a triangle, known as CKM triangle, in the complex $(\bar{\rho}, \bar{\eta})$ plane:

[1] The same is true also for the "right-handed" structures.

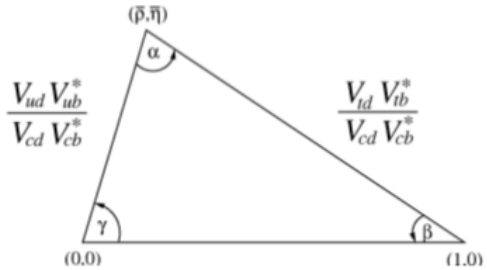

Figure 1.1

The angles and sides can be extracted from appropriate flavor observables in such a way that Eq. (1.15) can be experimentally tested. The values of λ and A are known with good accuracy [4] and this allows to express all the observables sensitive to the CKM matrix elements in terms of $\bar{\rho}$ and $\bar{\eta}$ only. The resulting constraints are shown in the plot of Fig. (1.2), which clearly shows that they are all consistent with a unique value of those parameters ($\bar{\rho} = 0.153 \pm 0.013$, $\bar{\eta} = 0.343 \pm 0.011$), implying the fact that the SM provides an excellent description of the flavor sector.

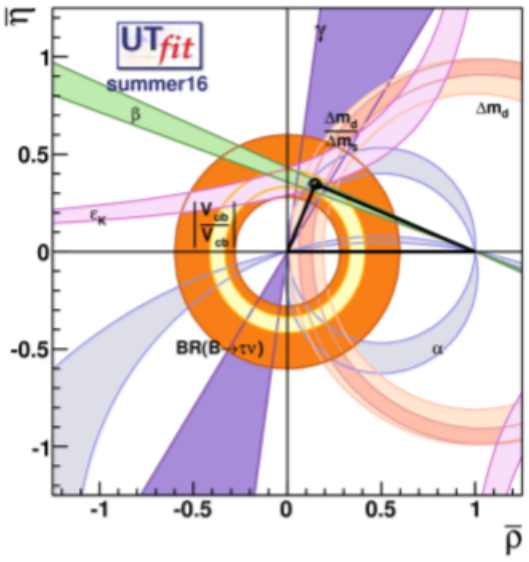

Figure 1.2

1.2 Why going beyond the SM

As briefly aforementioned, although all the theoretical successes the SM not only is not able to provide a complete description of nature, but it also presents some discrepancies with the experimental results. Here I will discuss some of its most important issues:

- *Hierarchy problem*: from a theoretical point of view, it can be expected a bigger value for the Higgs mass respect to the experimental one ($m_h \approx 126$ GeV) due to the fact that its one-loop contribution provide a correction to the bare value which

is $\propto \Lambda^2$, with Λ the scale at which NP appears. If there is no new physics up to the Planck scale ($M_P \sim 10^{19}$ GeV), this correction would be several orders of magnitude higher than the experimental value and, for this reason, a fine tuning is required; otherwise, invoking the naturalness hypothesis, NP should appear at $\Lambda \sim$ TeV. Nevertheless other possible solutions have been proposed throughout the years, from SuperSymmetry to composite Higgs models.

- *Neutrinos' nature and masses*: in the SM neutrinos are massless particles but, as shown by a lot of different experiments which observe the phenomenon of neutrino flavor oscillation, they should actually be massive. The need to explain how a neutrino gets its mass arises also the question about its nature: indeed, if we suppose that right-handed neutrinos ν_R exist, it is possible to give mass to them as for the other fermions, thanks to the SSB. However, knowing that $m_\nu \sim 10^{-1}$ eV, it turns out that there is a naturalness problem in this sector of the SM, being $\frac{m_\nu}{m_t} = \frac{y_\nu}{y_t} \sim 10^{-12}$. This issue can be solved supposing that neutrinos are Majorana fields, i.e. they coincide with the corresponding charge conjugate field, which get their mass through *See-saw* mechanism. However the experiments have not yet pointed out the nature of neutrinos and, so, also the question about their mass remains open.

- *Dark Matter and Dark Energy*: nowadays there is the strong evidence that only the $\sim 5\%$ of the total energy budget of the universe is due to ordinary matter, i.e. the particle content of the SM, while the remaining part is constituted for the $\sim 27\%$ by Dark Matter (DM) and for the $\sim 68\%$ by Dark Energy (DE). However the nature of DM and DE is still not known and a lot of models are continuously proposed in order to solve this issue; in particular, the most interesting and promising ones in the DM sector concern supersymmetric particles and the *axion* scenario.

- *Strong CP problem*: the existence of a four dimension term which arises in the QCD sector of the SM Lagrangian, i.e. $\theta_{\text{QCD}} G^a_{\mu\nu} G^{a\mu\nu}$, leads to CP violation. In order to take into account the cross-section of CP violating processes, one should adjust by hand the theta parameter as $\theta_{\text{QCD}} \sim 10^{-10}$, which is unnaturally small.

- *Baryon Asymmetry*: this is one of the most known and precise cosmological observations we have and it consists in a tiny excess of matter over the antimatter. It is still not clear which kind of dynamical mechanism caused this asymmetry[2] but, for sure, every model which tries to explain it should satisfy the Sakharov conditions of B, C, CP violation and of departure from thermal equilibrium. Although the SM satisfies all of them, the amount of asymmetry generated turns out to be incompatible with the measured ones, leaving the question still open.

- *Muon* $g-2$: this is a long standing inconsistency between the experimental value of the muonic anomalous magnetic moment and the corresponding SM prediction. At the moment the discrepancy is of 3.3σ but it is still not clear whether it is a consequence of the fact that NP is showing in this channel or an imprecise extracted value of the leading order hadronic contribution a_μ^{HLO}.

[2]The hypothesis that the universe have been always asymmetric do not hold: indeed, if we suppose that after the Big Bang there was already more matter than antimatter, we must also consider that the inflation would have washed out this asymmetry, leaving an equal amount of particles and anti-particles once ended.

Chapter 2

The muon $g-2$ and the MUonE experiment

This chapter is devoted to the discussion of the muonic $g-2$ problem, recalling firstly in Sec. (2.1) the comparison between the experimental value of the anomaly a_μ and its theoretical prediction provided by the SM; particular attention will be put on the hadronic contribution and the current methods for its extraction. Secondly, in Sec. (2.2) it will be discussed a new experiment thought to provide a refined and more precise prediction of the SM to compare with the experimental value: MUonE.

2.1 The anomalous magnetic moment of the muon

From the Dirac equation in an external electromagnetic field, i.e.

$$(i\not{D} - m)\psi = 0, \tag{2.1}$$

it is possible to predict a muonic magnetic moment $\vec{\mu}_\mu = g_\mu |e| \vec{S}/2m_\mu$, where $\vec{S}$ is the spin operator and g_μ is the gyromagnetic factor of the muon. At the tree level, simply taking the non relativistic limit of Eq. (2.1), it is easy to obtain $g_\mu = 2$; however, loops effects introduce a small but still significant deviation to this TL value which can be parametrized by the anomaly

$$a_\mu \equiv \frac{g_\mu - 2}{2}. \tag{2.2}$$

This quantity, known as anomalous magnetic moment, can be accurately measured in the experiments, but also precisely predicted in the SM; their comparison provides an excellent tool to test this theory at quantum level and significant deviations could be symptom of NP. The E821 experiment at Brookhaven National Lab (BNL) studied the precession of muons in a constant external magnetic field, finding [5]

$$a_\mu^{\text{exp}} = (11659209.1 \pm 6.3) \times 10^{-10}. \tag{2.3}$$

The error achieved by the BNL E821 experiment, $\delta a_\mu^{exp} = 6.3 \times 10^{-10}$, corresponds to 0.54 ppm and it is dominated by the available statistics; nevertheless, the preparations for new experiments at J-PARC [33] and Fermilab [34], which aim to measure the $g-2$ of the muon with a precision of 0.14 ppm (or even better), have already started.

On the theoretical side, the SM value for a_μ is generally divided into the three parts

$$a_\mu = a_\mu^{\text{QED}} + a_\mu^{\text{EW}} + a_\mu^{\text{Had}},$$

each one linked to a specific sector of the SM; they will be analyzed in a while. The final theoretical prediction is

$$a_\mu^{\text{SM}} = (11659183 \pm 4.8) \times 10^{-10}, \tag{2.4}$$

and its difference with the experimental result reads

$$\Delta a_\mu = a_\mu^{\text{exp}} - a_\mu^{\text{SM}} = (26.1 \pm 7.9) \times 10^{-10} \sim 3.3\sigma. \tag{2.5}$$

A summary plot [29] reporting the current status of the anomalous magnetic moment of the muon can be found in Fig. (2.1)

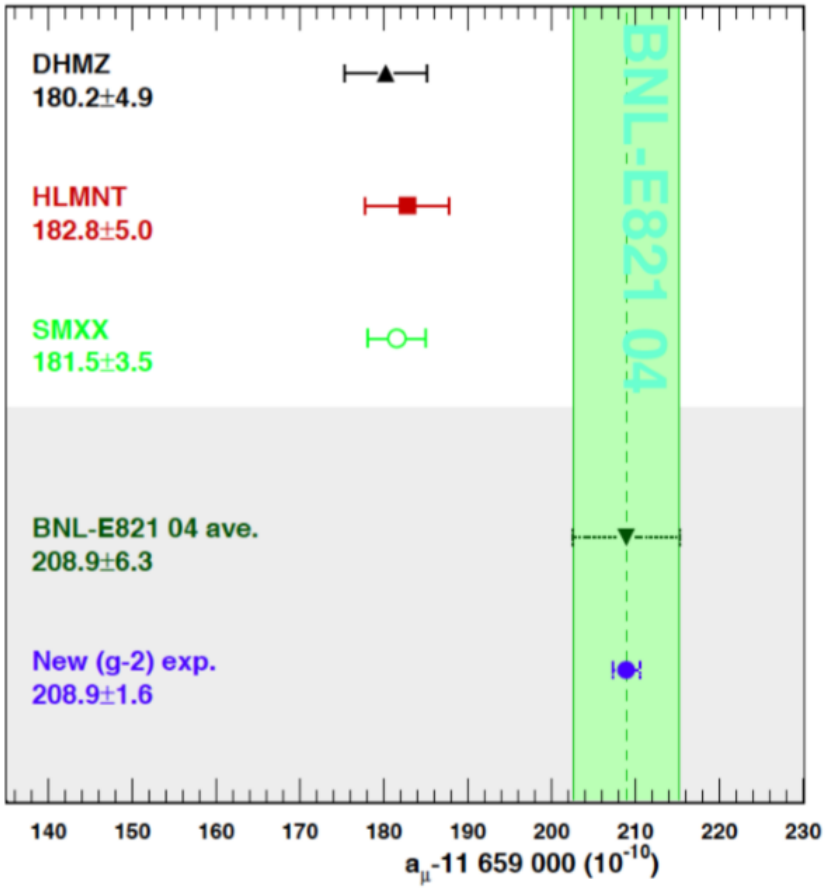

Figure 2.1: Comparison between the SM prediction and the experimental value of a_μ. DHMZ [30] and HLMNT [31] are two theoretical estimations, while SMXX [32] corresponds to their average; its reduced error is due to the improvements on the hadronic cross section measurement. BNL-E821 04 ave. is the current experimental value of a_μ and New $(g-2)$ exp. is the same central value with a fourfold improved precision, as planned by the future experiments at Fermilab and J-PARC.

2.1.1 QED contribution

Quantum Electrodynamics provides the largest fraction of the contribution by far. It can be subdivided order-by-order as follows [6]:

$$a_\mu^{\mathrm{QED}} = \sum_j c_j \left(\frac{\alpha}{\pi}\right)^j \tag{2.6}$$

where the coefficients c_j are sum of terms which can be either constants or functions of m_μ/m_i $(i = e, \tau)$. In [6] it is present a detailed review of all the contributions up to $j = 5$; in the following I will report a very brief summary, being the QED contribution not the main result on which this thesis is focused, specifying essentially only the numerical values of these coefficients.
At one loop there is only one diagram, which is nothing else that the vertex correction to the three point function. It provides the Schwinger term, with $c_1 = 1/2$. At two loops there are nine QED diagrams [7–9]: seven of them contain muons and photons, while the remaining two involve the vacuum polarisation of the virtual photon with a fermionic loop (with both e and τ). All these contributions has been computed analytically, providing

$$c_2 = 0.765857423(16).$$

At three-loops there are more than 100 diagrams, 36 of which are vacuum polarisations and 12 light-by-light diagrams. The corresponding coefficient can be still calculated analytically [10–12] and it results

$$c_3 = 24.05050982(28). \tag{2.7}$$

Starting from four loops, numerical methods and Monte Carlo simulations for the computation of the more than 1000 diagrams becomes necessary, being almost all of them not known analytically [13, 14]. The fourth coefficient is

$$c_4 = 130.8734(60). \tag{2.8}$$

Finally, at five loop level there are more than 12000 diagram which can contribute. Their numerical evaluation was performed in [15] and it provides

$$c_5 = 751.917(932). \tag{2.9}$$

Summing all the computations together, the QED contribution turns out to be

$$a_\mu^{\mathrm{QED}} = 11658471.8859(.0026)(.0009)(.0017)(.0006) \times 10^{-10}, \tag{2.10}$$

where the uncertainties are consequence of the experimental errors in the measurement of α and of the lepton masses, but also of the numerical errors for the four and five loop terms.

2.1.2 EW contribution

Differently from the electromagnetic interactions, the EW ones are characterized by the presence of massive mediators $(W^\pm, Z, h)$; as a consequence, these contributions to the

anomalous magnetic moment of the muon are suppressed by factors $\left(\frac{m_\mu}{m_W}\right)^2$. This can be seen clearly in the one-loop EW diagrams which involve the W and Z bosons, the neutrinos and the Higgs h. These contributions have been computed analytically in [16–20] and their sum reads

$$a_\mu^{\mathrm{EW}} = \frac{G_\mu m_\mu^2}{8\sqrt{2}\pi^2}\left[\frac{5}{3}+\frac{1}{3}\left(1-4\sin^2\theta_{\mathrm{W}}\right)^2+\mathcal{O}\left(\frac{m_\mu^2}{M_W^2}\right)+\mathcal{O}\left(\frac{m_\mu^2}{m_H^2}\right)\right] \tag{2.11}$$

where $\sin^2\theta_W = 1 - M_W^2/M_Z^2 \approx 0.223$ and $G_\mu = 1.166 \times 10^{-5}$ GeV^{-2}. Taking the corrections $\mathcal{O}\left(\frac{m_\mu^2}{M_{W,Z,h}^2}\right)$ to be negligible allows to find

$$a_{\mu\ 1-\mathrm{loop}}^{\mathrm{EW}} = (19.482 \pm 0.001) \times 10^{-10} \tag{2.12}$$

where the uncertainty are related to the measure of the Weinberg angle.
At the two loop level there is already an elevated number of diagrams: indeed, being the SM a non-abelian theory, it is possible to construct a lot of different structures by means of the three and four interactions among gauge bosons. Moreover, although the presence of the aforementioned suppression, the leading order two loop contribution [21] involve diagrams which contain a fermionic triangle loop, yielding a factor $\log(m_{W,Z}/m_\psi)$ at the amplitude level. It enhances the two loop contribution to the same order of the one loop, but with an opposite sign:

$$a_{\mu\ 2-loop}^{\mathrm{EW}} = (-41.2 \pm 0.1) \times 10^{-10}$$

Finally, the total EW contribution results

$$a_\mu^{\mathrm{EW}} = (15.36 \pm 0.1) \times 10^{-10}. \tag{2.13}$$

2.1.3 Hadronic contribution

The most important contributions to the anomalous magnetic moment coming from strong interactions are due to QED diagrams with quark loops (HVP) at leading order and the so-called hadronic light-by light scattering (HLbL)

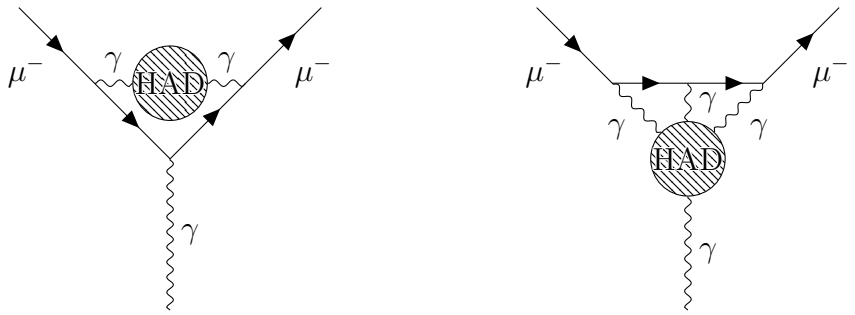

HVP effects at higher orders have been computed but they turn out to be at least 10^2 times smaller than the leading order [22].
There are various alternative ways to evaluate these contributions:

- **HVP**

  These contributions can be extracted indirectly by examining the e^+e^- annihilations by means of dispersion integral, a result based on analyticity and unitarity of the S matrix [25–27]; in the following subsection this procedure will be discussed quite in detail.
  The result is
  $$a_\mu^{\text{HVP}} = (693.9 \pm 4) \times 10^{-10}$$

- **HLbL**

  They have been extracted by using the Resonance Lagrangian Approach. This method is based on Chiral Perturbation theory (the EFT of quark-confined states governed by the chiral symmetries of QCD) extended to higher energies and augmented with vector resonances. They are estimated as [22]:
  $$a_\mu^{\text{HLbL}} = (10.3 \pm 2.9) \times 10^{-10}.$$

Both these theoretical techniques can be compared with the Lattice QCD (LQCD) approach, which aims to obtain the contributions by directly calculating the path-integrals of the confined quarks and gluons using the rules of high-energy QCD [23]. Although this technique is naturally all-inclusive regarding the hadronic processes, it is limited by computational complexity, causing a lack of precision.

2.1.3.a How to extract the HLO

This subsection is devoted to describing the method employed in the past for the indirect extraction of the leading order HVP contribution to a_μ and, subsequently, to layout a novel method [24] that forms the basis of the proposed MUonE experiment.
First of all, a generic vacuum polarisation (VP) function is usually denoted as $\Pi(q^2)$. Since the SM is a renormalisable theory, the bad divergent behaviour at large momenta is regulated by the introduction of a proper counterterm which generates an analogous diagram, only with the symbol $\otimes$ indicating the counterterm insertion in place of the vacuum polarisation function:

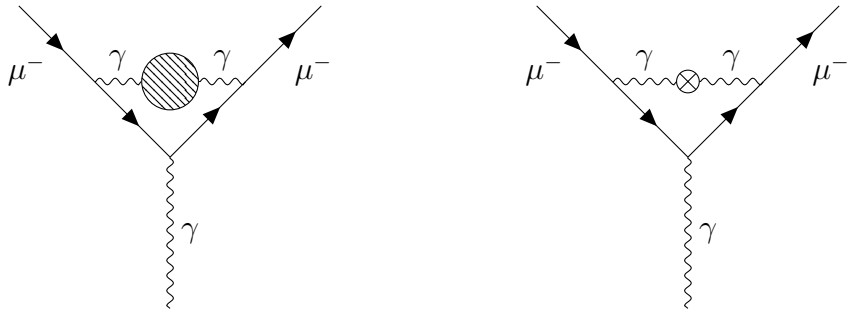

Only the sum of these two diagrams allows to get rid of any unphysical divergences at large momenta. By imposing that the loop correction be vanishing in the low-momentum transfer limit (which is a consistency with the classical limit), this counterterm turns

out to be $-\Pi(0)$. Therefore from now on it will be directly considered the renormalised quantity

$$\bar{\Pi}(q^2) = \Pi(q^2) - \Pi(0) = \frac{q^2}{\pi}\int_{s_0}^{+\infty} ds \frac{\mathrm{Im}[\Pi(s)]}{s\,(s - q^2 - i\varepsilon)}, \tag{2.14}$$

where s_0 is the starting point of the lightest branch cut.
Now, let's consider e^+e^- annihilation with a vacuum-polarisation insertion. Exploiting the optical theorem, diagrammatically this reads

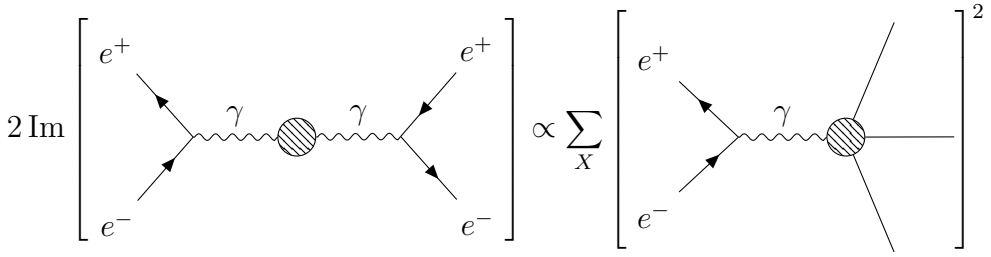

and it is telling us that the imaginary part of the vacuum polarisation is proportional to the cross-section of the process $e^+e^- \to$ generic particles. Since for the final purpose we are interested in the hadronic vacuum polarization, the attention will be put only to the particular case of $e^+e^- \to$ hadrons.
Usually the hadron-production cross section is measured in units of the cross-section of the process $e^+e^- \to \mu^+\mu^-$ in the $m_e = 0$ limit. It is, then, suitable to define the $\mathcal{R}_\gamma(s)$ factor

$$\mathcal{R}_\gamma(s) := \frac{\sigma\left(e^+e^- \to \gamma \to \text{hadrons}\right)}{\sigma\left(e^+e^- \to \gamma \to \mu^+\mu^-\right)} = \frac{\sigma\left(e^+e^- \to \gamma \to \text{hadrons}\right)}{\frac{4\pi\alpha^2}{3s}}. \tag{2.15}$$

Plugging (2.14) and (2.15) together, once exploited analytically the relation provided by the optical theorem, it is possible to find

$$\bar{\Pi}(q^2) = \Pi(q^2) - \Pi(0) = \frac{\alpha q^2}{3\pi}\int_{4m_\pi^2}^{+\infty} ds \frac{\mathcal{R}_\gamma(s)}{s\,(s - q^2 - i\varepsilon)} \tag{2.16}$$

where s_0 now starts at the π mass, since the pions are the lightest hadrons that can be produced.
Now, it is possible to derive the expression for the HVP corrections to a_μ. The amplitude can be easily recovered from that of the QED three point vertex function modifying the internal photon propagator with the insertion of the renormalised VP function $\bar{\Pi}(q^2)$ as a multiplicative factor:

$$\begin{aligned}
&-ie\bar{u}\left(p_2\right)\Gamma^\mu\left(p_1,p_2\right)u\left(p_1\right) = \\
&= ie\mu^{\varepsilon/2}\int\frac{d^Dq}{(2\pi)^D}\frac{-ig_{\alpha\beta}}{q^2}\left[\bar{\Pi}\left(q^2\right)\right]\bar{u}\left(p_2\right)\left[\gamma^\beta\frac{i\left[\left(\not{q}+\not{p}_2\right)+m_\mu\right]}{\left(q+p_2\right)^2-m_\mu}\gamma^\mu\frac{i\left[\left(\not{q}+\not{p}_1\right)+m_\mu\right]}{\left(q+p_1\right)^2-m_\mu}\gamma^\alpha\right]u\left(p_1\right) = \\
&= -ie\mu^{\varepsilon/2}\frac{\alpha}{3\pi}\int_{4m_\pi^2}^{+\infty}\frac{ds}{s}\mathcal{R}_\gamma(s)\int\frac{d^Dq}{(2\pi)^D}\frac{-ig_{\alpha\beta}}{q^2-s}\times \\
&\times\bar{u}\left(p_2\right)\left[\gamma^\beta\frac{i\left[\left(\not{q}+\not{p}_2\right)+m_\mu\right]}{\left(q+p_2\right)^2-m_\mu}\gamma^\mu\frac{i\left[\left(\not{q}+\not{p}_1\right)+m_\mu\right]}{\left(q+p_1\right)^2-m_\mu}\gamma^\alpha\right]u\left(p_1\right) = \\
&= \frac{\alpha^2}{3\pi^2}\int_{4m_\pi^2}^{+\infty}\frac{ds}{s}\mathcal{R}_\gamma(s)\bar{u}\left(p_2\right)\left[F_1\left(k^2,s\right)\gamma^\mu+\frac{i}{2m_\mu}F_2\left(k^2,s\right)\sigma^{\mu\nu}\gamma_\nu\right]u\left(p_1\right).
\end{aligned} \tag{2.17}$$

where the result has been expressed in terms of the two form factors $F_{1,2}$. In order to find the g-factor it is necessary to send $k \to 0$ and to recall that in this limit $F_1(0,s) = 1$, for consistency with the renormalisation conditions. The F_1 factor reproduces the tree-level contribution, therefore to find the anomaly one focuses on the $F_2(0,s)$ contribution. The standard way in literature to express such a result is:

$$a_\mu^{\mathrm{HLO}} = \frac{\alpha^2}{3\pi^2}\int_{4m_\pi^2}^{+\infty}\frac{ds}{s}\mathcal{R}_\gamma(s)K_\mu^{(2)}(s) \tag{2.18}$$

$$K_\mu^{(2)}(s) = \int_0^1 dx \frac{x^2(1-x)}{x^2+(1-x)s/m_\mu^2}$$

This result shows its utility once splitted into two parts in the integration range by setting the reference scale $\tilde{s}$ upon which QCD can be computed perturbatively. Then, there will be two contributions: the high-energy term, in which the $\mathcal{R}_\gamma$ factor can be computed analytically, and the low energy one, in which $\mathcal{R}_\gamma$ can be measured experimentally by annihilating e^+e^- pairs and measuring the relative cross-sections Nevertheless, the measure of the latter contribution is not easy to perform and the experimental difficulties in its analysis constitutes the big uncertainty in the SM prediction. Indeed $\mathcal{R}_\gamma$ is highly fluctuating at low energy due to the presence of a lot of resonances and threshold effects, as it can been seen by the plot

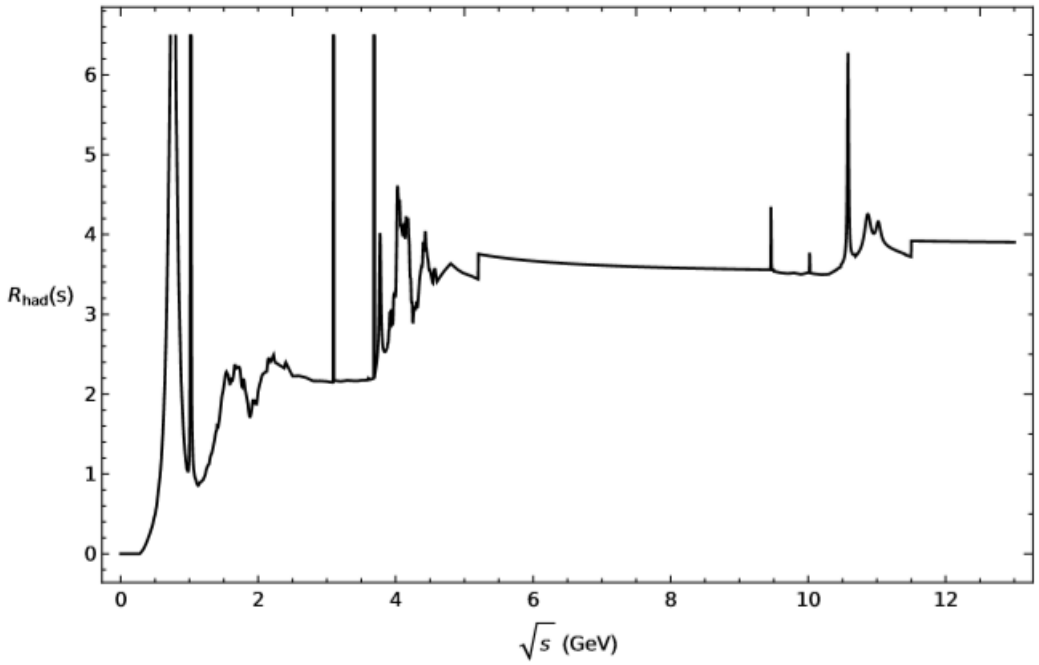

Figure 2.2: Behaviour of the function $\mathcal{R}_\gamma$ in the non-perturbative region $\sqrt{s} \in [0, 13]$ GeV. Note the high number of resonances in correspondence of mesons production thresholds; on the other side, the region with $\sqrt{s} > 13$ GeV is well reproduced by perturbative QCD.

2.2 The MUonE experiment

The MUonE experiment [35] has been thought as an alternative and competitive way to extract the leading hadronic contribution to a_μ without relying on the measure of the cross section for the process $e^+e^- \to hadrons$, being its behaviour at low energies the responsible of the big uncertainty in the SM prediction.
However, before entering in the detailed description of this experiment, let's firstly discuss the kinematics of the process.

2.2.1 Kinematics

MUonE is a fixed target experiment in which energetic muons scatter with electrons at rest. The process can be schematically written as

$$e^-(p_1) + \mu^-(p_2) \to e^-(p_3) + \mu^-(p_4),$$

with the three Mandelstam variables which are simply

$$s = (p_1 + p_2)^2 = (p_3 + p_4)^2, \quad t = (p_1 - p_3)^2 = (p_2 - p_4)^2, \quad u = (p_1 - p_4)^2 = (p_2 - p_3)^2$$

and which satisfy $s + t + u = 2m_\mu^2 + 2m_e^2$.
In the reference frame of the laboratory, the momenta of the involved particles are explicitly

- $p_1^\mu = (m_e, 0)$
- $p_2^\mu = (E_\mu, \vec{p_\mu})$
- $p_3^\mu = (E'_e, \vec{p_e}')$
- $p_4^\mu = (E'_\mu, \vec{p_\mu}')$

whit, as usual, the dispersion relation $E_i = \sqrt{m_i^2 + |\vec{p_i}|^2}$.
In the experiment the energy of the incoming muon flux is $E_\mu = 150$ GeV (which is a typical energy available at the M2 beam line in CERN's North Area); then, given $E_e^{'}$ the recoil energy of the electrons, it follows

$$s = 2m_e E_\mu + m_\mu^2 + m_e^2 = 0.164 \text{ GeV}^2, \qquad t = -2m_e(E_e^{'} - m_e) \tag{2.19}$$

with

$$t_{min} < t < 0 \quad \text{and} \quad t_{min} = -\frac{\lambda(s, m_e^2, m_\mu^2)}{s} = -0.143 \text{ GeV}^2, \tag{2.20}$$

where $\lambda(x, y, z) = x^2 + y^2 + z^2 - 2xy - 2yz - 2xz$ is the Källen function. Moreover, it is also convenient to define the variable x, which is related to t by

$$x(t) = \left(1 - \sqrt{1 - \frac{4m_\mu^2}{t}}\right) \frac{t}{2m_\mu^2}. \tag{2.21}$$

The conservation of the total four-momentum implies explicitly the two equations

$$\begin{cases} m_e + E_\mu = E'_e + E'_\mu \Rightarrow E_\mu = T_e + E'_\mu \\ \vec{p_\mu} = \vec{p_e}' + \vec{p_\mu}' \end{cases}, \tag{2.22}$$

where in the first one the definition of kinetic energy $E'_e = m_e + T_e$ has been used. Rewriting the second equation as $\vec{p_\mu}' = \vec{p_\mu} - \vec{p_e}'$, it follows the equality

$$\left|\vec{p_\mu}'\right|^2 = \left|\vec{p_e}'\right|^2 + |\vec{p_\mu}|^2 - 2\left|\vec{p_e}'\right||\vec{p_\mu}|\cos\theta_e, \tag{2.23}$$

where θ_e is the diffusion angle of the electron respect to the direction of the incident muon; exploiting also the energy conservation, this angle satisfies the relation

$$\cos\theta_e = \frac{\left|\vec{p_e}'\right|^2 + |\vec{p_\mu}|^2 - \left|\vec{p_\mu}'\right|^2}{2\left|\vec{p_e}'\right||\vec{p_\mu}|}. \tag{2.24}$$

The diffusion angle of the muon, θ_μ, can be obtained proceeding in the same way, this time rewriting the second equation of (2.22) as $\vec{p_\mu} - \vec{p_\mu}' = \vec{p_e}'$ and, again, squaring it:

$$\cos\theta_\mu = \frac{\left|\vec{p_\mu}'\right|^2 + |\vec{p_\mu}|^2 - \left|\vec{p_e}'\right|^2}{2\left|\vec{p_\mu}'\right||\vec{p_\mu}|}. \tag{2.25}$$

Now let's see how to find the maximum value for these two angles. In order to achieve this purpose, it is necessary to equate the value of the Mandelstam variable s in the laboratory frame (s_{lab}) with that in the center of mass frame (s_{cm}), where their explicit expression are

$$s_{lab} = (E_\mu + m)^2 - |\vec{p}_\mu|^2 = m_\mu^2 + m_e^2 + 2E_\mu m_e$$

$$s_{cm} = (E^*_\mu + E^*_e)^2,$$

with $E_{e,\mu} = \sqrt{p^{*2} + m^2_{e,\mu}}$; a little bit of easy algebra leads to

$$p^{*2} = \frac{m_e^2(E_\mu - m_\mu)}{m_e^2 m_\mu^2 + 2m_e E_e}. \tag{2.26}$$

The maximum angles exist if and only if the condition

$$\beta = \frac{\sqrt{E_\mu^2 - m_\mu^2}}{E_\mu + m_e} > \beta^*_{e,\mu} = \frac{p^*}{\sqrt{p^{*2} + m^2_{e,\mu}}} \tag{2.27}$$

is satisfied; inserting Eq. (2.26) in $\beta_{e,\mu}$ it follows

$$\beta_e = \beta, \qquad \beta_\mu = \frac{\sqrt{E_\mu^2 - m_\mu^2}}{E_\mu + m_e\left(\frac{m_\mu^2}{m_e^2}\right)} < \beta \tag{2.28}$$

from which, using the general relation $\sin\theta^{max}_{e,\mu} = \frac{\beta^*_{e,\mu}\gamma^*_{e,\mu}}{\beta\gamma}$, it is possible to find

$$\sin\theta^{max}_\mu = \frac{m_e}{m_\mu}, \qquad \sin\theta^{max}_e = 1 \Rightarrow \theta^{max}_{e,\mu} = 90^\circ. \tag{2.29}$$

Another important quantity that can be found is the energy E'_e of the diffused electrons as a function of the angle θ_e. This can be done using the Lorentz transformation $E^*_e = \gamma(E'_e - \beta p'_e\cos\theta_e) = \gamma m_e$, where it has been used the fact that in the center of mass frame

the energy of the electron is the same before and after the scattering (E_e^*). Solving for E'_e it can be found:

$$E'_e(\theta_e) = m_e \left(\frac{1 + \beta^2 \cos {\theta_e}^2}{1 - \beta^2 \cos {\theta_e}^2} \right), \tag{2.30}$$

from which it follows $E'_e(\theta_e^{max}) = m_e$. Moreover, using again the Lorentz transformation provided just above, together with the explicit expression for β present in (2.27), it is possible to see that the kinetic energy takes its maximum value for $\cos\theta^* = 1$, which has explicit expression

$$T_e^{max} = \frac{2m_e(E_\mu^2 - m_\mu^2)}{2m_e E_\mu + m_e^2 + m_\mu^2}. \tag{2.31}$$

This results is strictly linked to the difference $\Delta E_e = E_e^{'max} - E_e^{'min} = 2\gamma\beta p^*$; indeed, inserting the usual quantities already derived, it turns out to be exactly T_e^{max}:

$$\Delta E_e = \frac{2m_e(E_\mu^2 - m_\mu^2)}{2m_e E_\mu + m_e^2 + m_\mu^2} \equiv T_e^{max}. \tag{2.32}$$

This results should not surprise since, noticing that $T_e^{min} = 0$, it follows immediately from $\Delta E_e = T_e^{max} - T_e^{min}$.

2.2.2 Theoretical motivations for MUonE

Having discusses the basic, but still fundamental, kinematical features of the μe scattering, we can now turn on the theoretical motivations for this experiment.
As aforementioned, the idea which has motivated the proposal of MUonE relies in the needed to find an alternative way to $e^+e^- \to hadrons$ processes for the extraction og a_μ^{Had}. This can be achieved noticing that, once took again the previous results, a_μ^{HLO} can be related to the running of α_{QED} working in the space-like region. Switching the s and x integrations [36] in Eq. (2.18) it is possible to obtain

$$a_\mu^{\text{HLO}} = \frac{\alpha}{\pi} \int_0^1 dx (x-1) \bar{\Pi}_{\text{Had}}[t(x)], \tag{2.33}$$

with

$$t(x) = \frac{x^2 m_\mu^2}{x-1} < 0, \tag{2.34}$$

where the integral is expressed in terms of the renormalised HVP function with the space-like variable t, in contrast to the time-like variable s of the previous relation.
Let us now take a look at the running of the QED coupling constant α, another well-understood effect of radiative corrections. It is written down at a specified squared momentum transfer q^2 in terms of α measured at a different squared momentum transfer and the general VP function

$$\alpha(t) = \frac{\alpha(0)}{1 - \Delta\alpha(t)} \tag{2.35}$$
$$-\Delta\alpha(q^2) = \text{Re}[\bar{\Pi}(q^2)].$$

$\Delta\alpha$ has various contribution, depending on the kinds of VP functions at play. In particular, $\Delta\alpha_{\text{QED}}$, given by the QED corrections to the photon propagator, is very well known and

its contribution can be factorised from the whole running in order to isolate the hadronic contribution $\Delta\alpha_{\text{Had}}$.
The corrections to α must depend only on the real part of $\bar{\Pi}$, since the VP function can acquire a non-vanishing imaginary part whenever $q^2 > 4m^2$, with m the mass of some massive particle involved in the VP. Nevertheless, if the transferred momentum q^2 is space-like, then $\bar{\Pi}(q^2)$ can be safely identified with its real part, since by the same unitarity-based reasoning the imaginary part would vanish in that kinematic region.
Based on these considerations, it is possible to lay out a procedure to find out the Hadronic VP correction to a_μ by actually measuring the hadronic contribution to the running of α. Firstly $\Delta\alpha$ has to been measure with space-like square momentum transfer t; then, the known QED contribution must be subtracted and the resulting quantity

$$\Delta\alpha_{\text{Had}}(t) = \text{Re}[\Pi_{\text{Had}}(t)] \equiv \bar{\Pi}_{\text{Had}}(t) \tag{2.36}$$

is then substituted into Eq. (2.33), bringing to

$$a_\mu^{\text{HLO}} = \frac{\alpha}{\pi}\int_0^1 dx(x-1)\Delta\alpha_{\text{Had}}[t(x)] \tag{2.37}$$

Although it is based on Eq. (2.18), this is a very different approach respect to the previous one and it presents also an important benefit: the radiative corrections keep the hadrons fully-virtual, as opposed to having final hadronic states which can, in general, give rise to very complex subsequent processes. The advantage of studying space-like momentum transfer rather than time-like is evident from Fig. (2.3): the space-like momentum forbids resonances, which allows the photonic VP function to be smooth in its domain (lower panel). On the contrary, the time-like region opens up the possibility for resonances, pair production and threshold behaviour that cause spikes and troths in the VP function (upper panel).

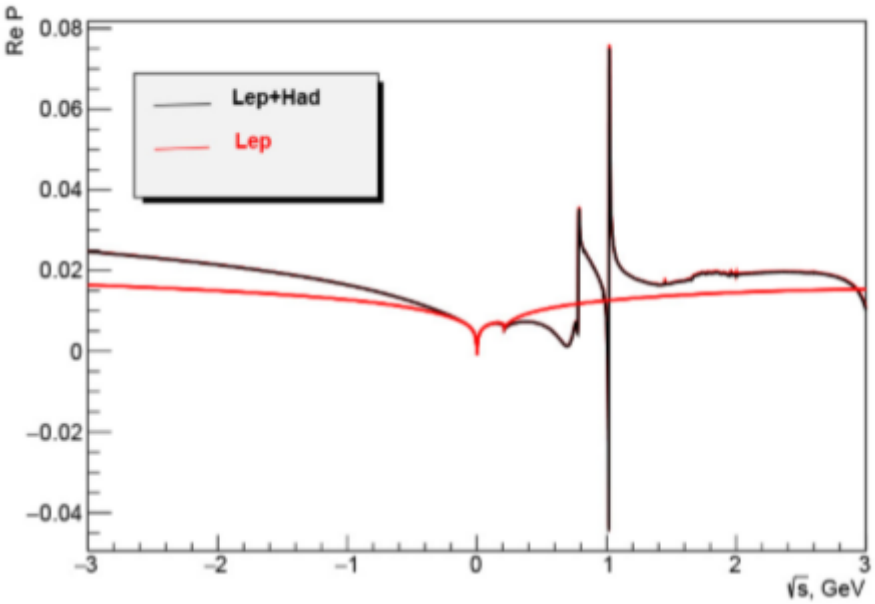

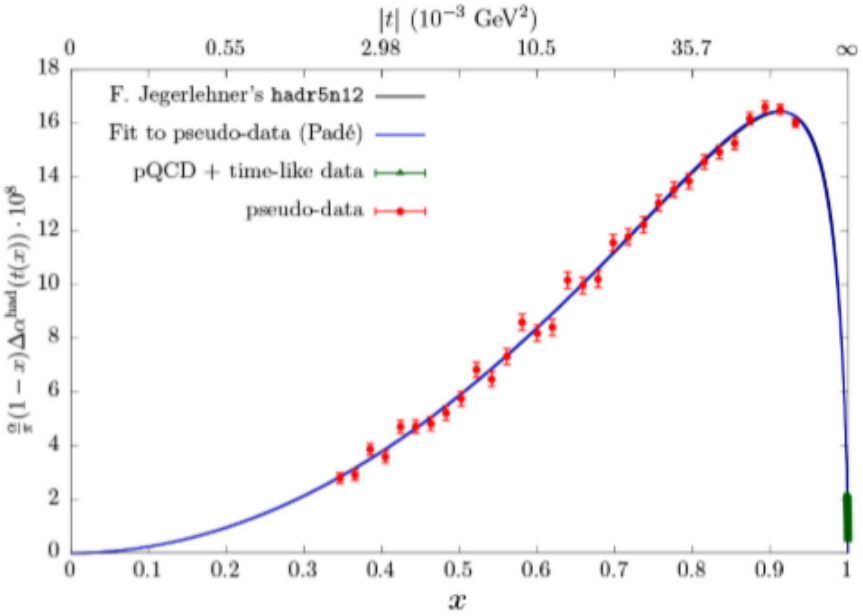

Figure 2.3

A precise value of (2.37) entails an accurate value of $\alpha(t)$ in the space-like region through the measure of the cross section of some physical process. An option could be the Bhabha scattering $e^+e^- \to e^+e^-$ which, however, is still characterized by an s channel contribution in addition to the desired t channel:

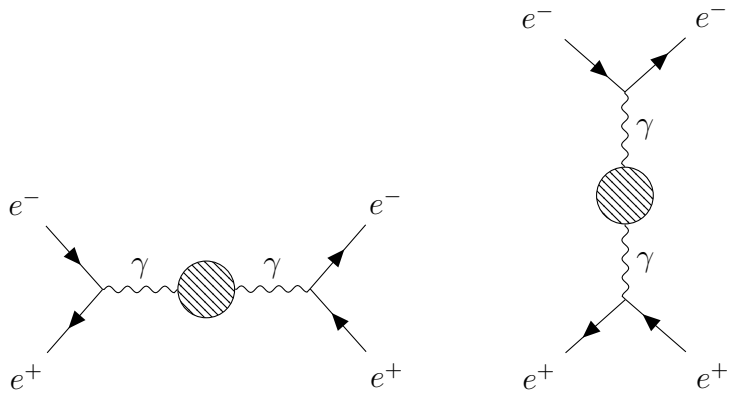

To be competitive with time-like measurements, a space-like estimate of a_μ must be given with an accuracy of $\sim 1\%$. Given the peak value of $\Delta\alpha_{\text{Had}}$ to be $\sim 10^{-3}$, the experimental precision in the cross-section measurement needs to be of the order 10^{-5} or 10 ppm [29]; however, there are no currently existing e^+e^- collider which can provide such a high level of accuracy.
A more practical alternative is represented by the muon-electron elastic scattering $\mu^\pm e^- \to \mu^\pm e^-$ [3]:

[3] In the diagram I only reported the process $\mu^- e^- \to \mu^- e^-$; its partner process has the same structure, with a switched muonic current's flow.

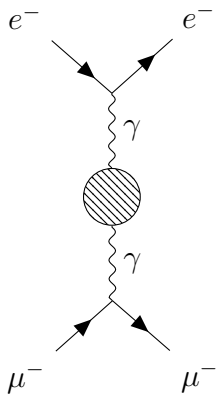

Not only this scattering is a pure t channel process, but also the required precision could already be potentially achieved at existing facilities.
The experiment would take the form of a fixed-target collision [29]: a high-energy (150-200 GeV) muon beam is already available at CERN's North area and it will be directed on a fixed target, enabling the measurement of the differential cross-section of muons which scatter with the electrons in the atomic orbitals of the layer; in the following section it will be reported a quite detailed analysis on the kinematics. The MUonE experiment [37] aims to extract the running $\alpha(t)$ by measuring the cross-section with a precision of ~ 10 ppm to provide a $\sim 1\%$ estimate of a_μ^{HLO} , in order to be competitive with the new upcoming $g-2$ experiments. However, the precision expected for this experiment raises the question whether NP could pollute the measurements or not. This work aims to analyze this issue, studying NP effects in muon-electron scattering due to both heavy and light mediators, depending on whether their mass is higher or lower than $\mathcal{O}$ (1 GeV), which is the energy scale of the MUonE experiment. Since in the former case it is possible to employ an effective field theory (EFT) approach, in the next chapter this tool will be briefly reviewed.

Chapter 3

Heavy new physics effects at MUonE

As mentioned in the last chapter, this work aims to analyze possible signals of NP in μe scatterings due to heavy and light mediators, depending on whether their mass is higher or lower than $\mathcal{O}(1\text{ GeV})$. In the former case it will be employed an effective field theory (EFT) formalism, whose main theoretical aspects will be recalled in Sec. (3.1), constructing the most general effective Lagrangian invariant under the electromagnetic gauge group $U(1)_{em}$. After the computation of the NP contributions to the $\mu^{\pm}e^{-} \to \mu^{\pm}e^{-}$ differential cross section in Sec. (3.4), corrections to correlated observable, as the total cross section and the forward-backward asymmetry of the process $e^{+}e^{-} \to \mu^{+}\mu^{-}$, will be computed; then, from the comparison with the experimental results, NP will be constrained and, subsequently, it will be evaluated whether it could affect MUonE measurements or not. The same analysis will be carried out also for lepton-flavor violation (LFV) NP effects in Sec. (3.5).
The case related to light mediators will be discussed in the following chapter.

3.1 Effective Field Theories

The basic idea under the construction of an effective field theory (EFT) is that, whenever there is a situation in which it is necessary to deal with a quantum field theory (QFT) with two (or more) very different energy or length scales, it is possible to construct a simpler theory by performing an expansion in the ratio of these scales. I will provide immediately an illustrative example, reconnecting to what mentioned in the introduction. As a consequence of the fact that the Standard Model of particles physics leaves many questions unanswered, it is very probable that there should exist some BSM physics involving new heavy particles with masses $\Lambda \gg v$, i.e. much above the scale of electroweak symmetry breaking. While the complete Lagrangian of the UV theory is at present a pure utopia, we can construct its low-energy version – the so called SMEFT – by extending the usual SM Lagrangian with higher dimensional local operators built out the field content of this theory:

$$\mathcal{L}_{\text{SMEFT}} = \mathcal{L}_{\text{SM}} + \sum_{n\geq 1}\sum_{i}\frac{\mathcal{C}_i^{(n)}}{\Lambda^n}\mathcal{Q}_i^{(n)}, \tag{3.1}$$

where $\mathcal{Q}_i^{(n)}$ are all the possible operators of dimension $D = 4 + n$ which must respect the symmetries of the Standard Model, such as Lorentz and gauge invariance. There is, of course, an infinite set of such operators but, at the same time, there exists only a finite set of them (which forms a complete basis) for each dimension D; moreover, the contributions

of these operators to any given observable are suppressed by powers of $(v/\Lambda)^{D-4}$ in relation to those of the Standard Model. On the other side, the $\mathcal{C}_i^{(n)}$ are known as *Wilson coefficient* and they are the dimensionless couplings which contain all the information about the short-distance physics which has been integrated out. The above equation is useful only because the infinite sum over n can be truncated at some value n_{max} since matrix elements of the operators $\mathcal{Q}_i^{(n)}$ scale like powers of m, where $m \ll \Lambda$ represents the characteristic scale of the low-energy effective theory ($m = v$ in the case of SMEFT), i.e.

$$\langle f|\mathcal{Q}_i^{(n)}|i\rangle \sim m^{n+\delta}, \tag{3.2}$$

where δ is set by the external states; truncating the sum at n_{max} one makes an error of order $(m/\Lambda)^n \ll 1$ relative to the leading term.
In this work I will deal only with operators up to $D = 6$, since $D \geq 7$ operators are suppressed by higher powers of the inverse of Λ.

3.1.1 Running couplings

Essentially, in constructing the effective Lagrangian of Eq. (3.1) the contributions from virtual particles are split up into short and long distance modes as

$$\int_0^\infty \frac{d\omega}{\omega} = \int_0^\Lambda \frac{d\omega}{\omega} + \int_\Lambda^\infty \frac{d\omega}{\omega}, \tag{3.3}$$

where the first term is sensitive to IR physics and is absorbed into the matrix elements $\langle\mathcal{Q}_i^{(n)}\rangle$, while the second is sensitive to UV physics and it is absorbed into the Wilson coefficients $\mathcal{C}_i^{(n)}$. However, let's suppose that we are performing a measurement at a reference energy scale E such that $m \ll E < \Lambda$. We can then integrate out the high-energy fluctuations of the light Standard Model fields (with frequencies $\omega > E$) from the generating functional because they will not be needed as source terms for external states. This yields a different effective Lagrangian which, however, has the same operators $\mathcal{Q}_i^{(n)}$ (since any Standard Model particles haven't been removed). What changes is the split-up of modes, which now reads

$$\int_0^\infty \frac{d\omega}{\omega} = \int_0^E \frac{d\omega}{\omega} + \int_E^\infty \frac{d\omega}{\omega}, \tag{3.4}$$

As a consequence, the values of the Wilson coefficients and operators matrix elements need to be different, but in such a way that

$$\mathcal{L}_{\text{EFT}} = \sum_{n=0}\sum_i \frac{\mathcal{C}_i^{(n)}(E)}{\Lambda^n}\mathcal{Q}_i^{(n)}(E) = \sum_{n=0}\sum_i \frac{\mathcal{C}_i^{(n)}(\Lambda)}{\Lambda^n}\mathcal{Q}_i^{(n)}(\Lambda). \tag{3.5}$$

Generally speaking, the effective Lagrangian that has to be studied is

$$\mathcal{L}_{\text{EFT}} = \sum_{n=0}\sum_i \frac{\mathcal{C}_i^{(n)}(\mu)}{\Lambda^n}\mathcal{Q}_i^{(n)}(\mu), \tag{3.6}$$

whose matrix elements are, by construction, independent of the arbitrary factorization scale μ (with $m \leq \mu \leq \Lambda$). Here $\mathcal{Q}_i^{(n)}(\mu)$ are renormalized composite operators defined in dimensional regularization with the $\bar{\text{MS}}$ scheme, while $\mathcal{C}_i^{(n)}(\mu)$ are the corresponding

renormalized Wilson coefficients. The scale μ serves as the renormalization scale for these quantities, but at the same time it is the factorization scale which separates short-distance (high-energy) from long-distance (low-energy) contributions.
Here a couple of comments are appropriate. First of all, the terms with $n = 0$ are just those of the renormalizable Lagrangian of the low-energy theory. As a consequence, parameters such as $\alpha_s(\mu)$ or $m(\mu)$ might contain some information about short-distance physics through their scale dependence. An example is provided by the μ dependence of gauge couplings and mass parameters in supersymmetric extensions of the Standard Model, suggesting a unification of the strong and electroweak forces at a scale $\Lambda \sim 10^{16}$ GeV. Secondly, operators with $n \geq 1$ are those which start to be interesting, since their coefficients tell us something about the fundamental high-energy scale Λ. The most evident example is that of the weak interactions at low energy. These are described by four-fermion operators with mass dimension $D = 6$, whose coefficients are proportional to the Fermi constant $\sqrt{2}G_F = 1/v^2$. The numerical value of G_F indicates the fundamental mass scale of EW symmetry breaking, allowing to estimate the masses of the heavy weak gauge bosons $W^{\pm}$ and Z long before these particles were discovered.
At any fixed n, the basis $\mathcal{Q}_i^{(n)}(\mu)$ of composite operators can be renormalized in the standard way, allowing, however, for the possibility of *operator mixing*:

$$\mathcal{Q}_{i,0}^{(n)} = \sum_j Z_{ij}^{(n)}(\mu)\mathcal{Q}_j^{(n)}(\mu). \tag{3.7}$$

The operators with the subscript "0" on the left-hand side are bare operators, while those on the right-hand side are the renormalized ones. In the presence of operator mixing, in the renormalization of $\mathcal{Q}_{i,0}^{(n)}$ other operators $\mathcal{Q}_j^{(n)}(\mu)$, with $i \neq j$, are needed as counterterms[4]. Moroever, in dimensional regularization there is no mixing between operators of different dimension D and, consequently, this regularization method is as the most convenient one[5].

3.1.2 Anomalous dimension and RG evolution equation for the Wilson coefficients

From the fact that the bare operators on the left-hand side of Eq. (3.7) are scale independent, it follows that

$$\frac{dZ_{ij}(\mu)}{d\ln\mu}\mathcal{Q}_j(\mu) + Z_{ij}(\mu)\frac{d\mathcal{Q}_j(\mu)}{d\ln\mu} = 0, \tag{3.8}$$

which can be solved to give

$$\frac{d\mathcal{Q}_k(\mu)}{d\ln\mu} = -\left(Z^{-1}\right)_{ki}(\mu)\frac{dZ_{ij}(\mu)}{d\ln\mu}\mathcal{Q}_j(\mu) \equiv -\gamma_{kj}(\mu)\mathcal{Q}_j(\mu). \tag{3.9}$$

In matrix notation, this simply reads

$$\frac{d\overrightarrow{\mathcal{Q}}(\mu)}{d\ln\mu} = -\gamma(\mu)\overrightarrow{\mathcal{Q}}(\mu), \quad \text{with} \quad \gamma(\mu) = Z^{-1}(\mu)\frac{dZ(\mu)}{d\ln\mu}. \tag{3.10}$$

[4]Let's note that the renormalization constants $Z_{ij}^{(n)}$ contain a wave-function renormalization factor $Z_a^{1/2}$ for each component field contained in the composite operators, in addition to renormalization factors absorbing the UV divergences of the 1PI loop corrections to the operator matrix elements.

[5]In order to have an handle notation, from now on I will drop always the superscript "(n)".

The quantity γ is called the *anomalous-dimension matrix* of the composite operators and it can be obtained from the coefficient of the $1/\epsilon$ pole term in Z.
Since the effective Lagrangian is μ independent by construction, for every $n \geq 0$

$$\frac{d\mathcal{C}_i(\mu)}{d\ln\mu}\mathcal{Q}_i(\mu) + \mathcal{C}_i(\mu)\frac{d\mathcal{Q}_i(\mu)}{d\ln\mu} = \left[\frac{d\mathcal{C}_i(\mu)}{d\ln\mu}\delta_{ij} - \mathcal{C}_i(\mu)\gamma_{ij}(\mu)\right]\mathcal{Q}_j(\mu) = 0. \tag{3.11}$$

which, exploiting the linear independence of the basis operators, leads to

$$\dot{\mathcal{C}}_i = \mu\frac{d\mathcal{C}_i}{d\mu} = \gamma_{ij}\mathcal{C}_j. \tag{3.12}$$

Using ordinary perturbation theory, the differential equation (3.12) can be formally solved, imposing as initial condition $\mathcal{C}_i(\Lambda)$ once computed by matching the full theory with the effective one, obtaining

$$\mathcal{C}_i(\mu) = Pexp\left[\int_{x=\Lambda}^{x=\mu} dx\frac{\gamma(x)}{\beta(x)}\right]_{ij}\mathcal{C}_j(\Lambda), \tag{3.13}$$

where P denotes the coupling constant ordering of the anomalous dimension matrix. It is worth to stress again on the fact that the operator renormalization produces an operator mixing thanks to the anomalous dimension matrix γ_{ij}: this implies that operators that weren't present at the scale Λ can arise at different scales due to the evolution of their coefficients, as aa consequence of the fact that their running may contain coefficients of other operators which were present at Λ scale.
Finally, in order to obtain the theory at low energy, the *matching* procedure must be employed. To determine the values of the coefficients $\mathcal{C}_i$ it is necessary to compute the amplitudes $\mathcal{M}$ at a given order of both the modified theory (by the integration of heavy degrees of freedom) and the constructed EFT:

$$\mathcal{M} = \langle f_n\,|\mathcal{L}|\,i_n\rangle = \sum_i \mathcal{C}_i\,\langle f_n\,|\mathcal{Q}_i|\,i_n\rangle + h.c. \tag{3.14}$$

In general, in order to obtain $\mathcal{L}_{EFT}$ at the generic scale μ, one have to solve (3.12) in the LLA limit, obtaining

$$\mathcal{C}_i(\mu) = \mathcal{C}_i(\Lambda) + \dot{\mathcal{C}}_i(\Lambda)\ln\frac{\Lambda}{\mu}. \tag{3.15}$$

Fulfilling the matching condition, the Lagrangian is obtained once summed over all the possible coefficients and flavor structures:

$$\mathcal{L}_{\text{EFT}} = \frac{1}{\Lambda^2}\sum_i\sum_{prst}\mathcal{C}^i_{prst}(\mu)\mathcal{Q}^i_{prst}. \tag{3.16}$$

3.2 SM cross section and experimental sensitivity

Let's start the discussion firstly recalling the SM prediction for the differential cross section of the process

$$e^-(p_1) + \mu^-(p_2) \to e^-(p_3) + \mu^-(p_4),$$

where the electron and muon masses will be now respectively denoted as m and M.
In the following I will refer to the differential cross section $d\sigma/dt$, which is given by the general formula

$$\frac{d\sigma}{dt} = \frac{1}{16\pi}\frac{1}{\lambda(s, m^2, M^2)}\left|\overline{\mathcal{M}}\right|^2, \tag{3.17}$$

where $|\overline{\mathcal{M}}|^2$ is the unpolarized squared matrix element, i.e.

$$|\overline{\mathcal{M}}|^2 = \frac{1}{4}\sum_{spin} \mathcal{M}^*\mathcal{M}.$$

In principle, in the SM this process can be mediated by the photon γ, the weak Z boson and the Higgs boson H

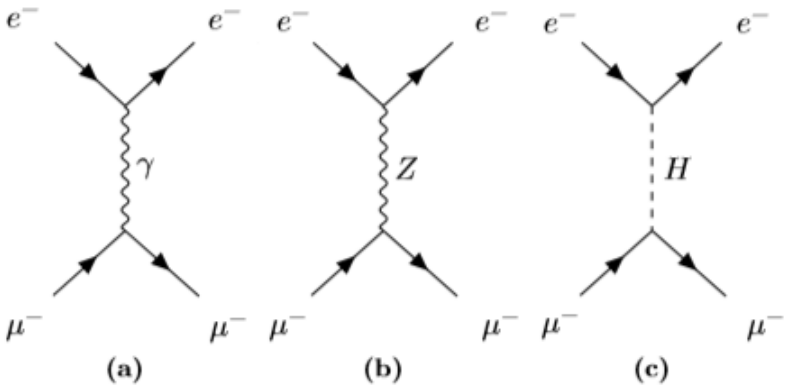

and the total unpolarized squared matrix element reads

$$|\overline{\mathcal{M}}_{tot}|^2 = \frac{1}{4}\sum_{spins}(|\mathcal{M}_\gamma|^2+|\mathcal{M}_Z|^2+|\mathcal{M}_H|^2+2\mathrm{Re}[\mathcal{M}_\gamma^*\mathcal{M}_Z]+2\mathrm{Re}[\mathcal{M}_\gamma^*\mathcal{M}_H]+2\mathrm{Re}[\mathcal{M}_Z^*\mathcal{M}_H]). \tag{3.18}$$

Nonetheless, only the pure photon and the interference with the Z boson contributions can be seen at MUonE since the other ones require a sensibility greater respect to that of the experiment (10 ppm). In the following subsections I will report a brief recap of these contributions.

3.2.1 QED contribution

The amplitude for the scattering mediated by the photon γ is simply

$$\mathcal{M}_\gamma = \frac{ie^2}{t}\bar{u}(p_3)\gamma^\mu u(p_1)\bar{u}(p_4)\gamma_\mu u(p_2) \tag{3.19}$$

from which it follows, after the computations of the two traces, that

$$\left|\overline{\mathcal{M}}_\gamma\right|^2 = \frac{64\pi^2\alpha^2}{t^2}f(s,t) \tag{3.20}$$

where $f(s,t) = t^2/2 + st + (M^2 + m^2 - s)^2$. Combining Eq. (3.17) with the result just found, it is possible to find the total QED contribution

$$\frac{d\sigma_0}{dt} = \frac{4\pi\alpha^2}{t^2}\frac{f(s,t)}{\lambda(s, m^2, M^2)} \tag{3.21}$$

3.2.2 Weak Z boson contribution

In this case, the full amplitude is

$$\mathcal{M}_Z = i\left(\frac{ig}{2c_W}\right)^2 \bar{u}\left(p_3\right)\gamma^\mu\left(g_V^e - g_A^e\gamma^5\right)u\left(p_1\right)\frac{\left(-g_{\mu\nu} + \frac{P_\mu P_\nu}{M_Z^2}\right)}{t - M_Z^2}\bar{u}\left(p_4\right)\gamma^\nu\left(g_V^\mu - g_A^\mu\gamma^5\right)u\left(p_2\right) \tag{3.22}$$

where $P = p_1 - p_3 = p_2 - p_4$ and c_W is the cosine of the Weimberg angle; moreover it has been assumed that

$$g_V^e = g_V^\mu = \frac{1}{4} - s_W^2 \qquad g_A^e = g_A^\mu = \frac{1}{4}. \tag{3.23}$$

Since the working condition is that of $|P|^2 \ll M_Z^2$, Eq. (3.22) can be rewritten employing the Fermi theory as

$$\mathcal{M}_Z = -\frac{4iG_F}{\sqrt{2}}\bar{u}\left(p_3\right)\gamma^\mu\left(g_V^e - g_A^e\gamma^5\right)u\left(p_1\right)\bar{u}\left(p_4\right)\gamma_\mu\left(g_V^\mu - g_A^\mu\gamma^5\right)u\left(p_2\right). \tag{3.24}$$

Then, the interference term with the photon is

$$\overline{\mathcal{M}}_{\gamma Z} = 2\mathrm{Re}[\mathcal{M}_\gamma^*\mathcal{M}_Z] = \left|\bar{\mathcal{M}}_\gamma\right|^2\delta_Z^- \tag{3.25}$$

where the explicit expression for the relative contribution δ_Z^- to the total differential cross section reads

$$\delta_Z^- = -\frac{G_F t}{4\pi\alpha\sqrt{2}}\left[a_\theta^2 - \frac{t(s-u)}{2f(s,t)}\right]. \tag{3.26}$$

The plot for δ_Z^- as a function of t in the range of interest is

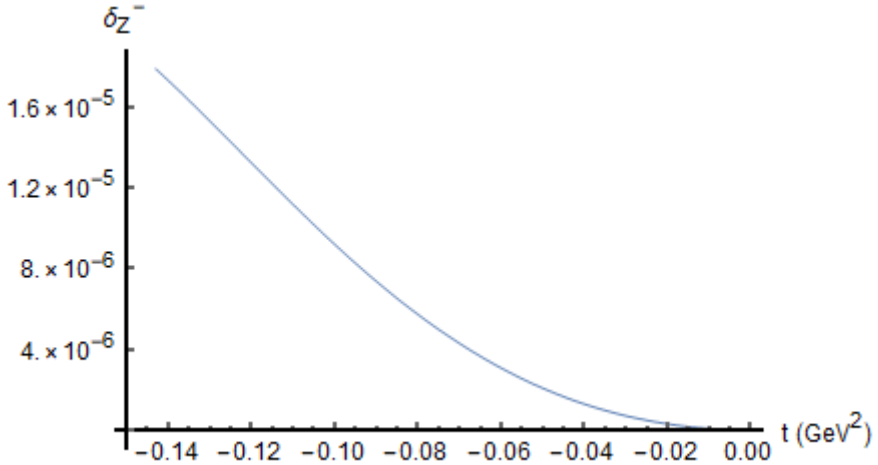

Figure 3.1

From Fig. (3.1) it is possible to note that δ_Z is at most $\sim 1.6 \times 10^{-5}$ (in correspondence of $t = t_{min} = -0.143$ GeV^2) and, therefore, the $Z - \gamma$ interference is barely detectable. Moreover, the pure Z contribution of $\left|\bar{\mathcal{M}}_Z\right|^2$ can be safely neglected, being $\mathcal{O}(G_F^2)$.

3.2.3 Weak W^+ boson contribution

Since the experiment is characterized by an incoming beam of both $\mu^\pm$, in the case of scattering between positive muons and electrons there could be also the process $\mu^+e^- \to \nu_e\bar{\nu}_\mu$. This time the scattering is mediated by the W^+ boson and its corresponding tree level diagram is

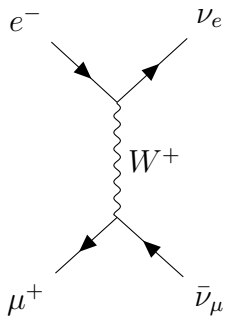

Also in this case, being $|t| \ll m_W^2$, it is possible to employ the Fermi theory; proceeding in this way, the amplitude simply reads

$$\mathcal{M}_{\bar{\nu}\nu} = -\frac{iG_F}{\sqrt{2}}\bar{u}(p_3)\gamma^\mu(1-\gamma_5)u(p_1)\bar{v}(p_4)\gamma_\mu(1-\gamma_5)v(p_2). \tag{3.27}$$

It is already clear that the cross section for this process will be highly suppressed by the presence of G_F^2: indeed, after a little bit of simple algebra and neglecting $\mathcal{O}(m^2/s)$ terms, it is possible to find

$$\sigma(\mu^+e^- \to \nu_e\bar{\nu}_\mu) = \frac{G_F^2(M^2+2s)}{12\pi} \sim 10^{-12}\ \text{GeV}^{-2} \tag{3.28}$$

for $s = 0.164\ \text{GeV}^2$, which is several order of magnitude smaller compared to the pure QED one ($\sigma_0 \sim 10^{-2}\ \text{GeV}^{-2}$), similarly to the pure Z contribution in μe scattering; therefore, this process can be safely neglected.

3.2.4 Higgs contribution

The amplitude for diagram (c) can be easily written as

$$\mathcal{M}_H = -\frac{imM}{v^2}\bar{u}(p_3)u(p_1)\frac{1}{t-m_H^2}\bar{u}(p_4)u(p_2). \tag{3.29}$$

All the Higgs contributions, the pure one in $\left|\bar{\mathcal{M}}_H\right|^2$ and also the two interference with γ and Z, can be neglected; indeed, taking the ratio of the Higgs amplitude respect to that of the Z boson, i.e.

$$\frac{\mathcal{M}_H}{\mathcal{M}_Z} \propto \frac{mM}{M_Z^2}\frac{t-M_Z^2}{t-M_H^2} \overset{t\ll M_{Z,H}^2}{\approx} \frac{5\times10^{-5}}{(125)^2} \tag{3.30}$$

it is possible to note that it is already very suppressed, implying that all the Higgs contributions are beyond the resolution of MUonE.
Then, the total SM differential cross section at LO reads

$$\frac{d\bar{\sigma}_{\text{LO}}}{dt} = \frac{d\sigma_0}{dt}\left(1+\delta_Z^-\right) \tag{3.31}$$

3.2.5 $\mu^- e^- \to \mu^- e^-$ vs $\mu^+ e^- \to \mu^+ e^-$ cross section

So far it has been only discussed the scattering of muons with electrons; nevertheless, as mentioned a couple of times and remembered in subsection (3.2.3), in the incident beam there could be either muons and antimuons. However, the QED and weak contributions to the μe scattering behave differently in considering μ^+ instead of μ^-. Indeed, while Eq. (3.21) holds also for antimuons, as a result of the QED invariance under both charge conjugation (C) and parity (P), the same is not true for the Z contribution (3.26), being parity violated by weak interactions [6]. As a consequence, the total differential cross section for the $\mu^- e^- \to \mu^- e^-$ and $\mu^+ e^- \to \mu^+ e^-$ processes will have the same QED part and a different weak one. In particular, after a very easy computation, the general result reads

$$\frac{d\sigma^{\pm}_{\text{LO}}}{dt} = \frac{d\sigma_0}{dt}\left(1 + \delta^{\pm}_Z\right), \tag{3.32}$$

where the weak contribution is

$$\delta^{\pm}_Z = -\frac{G_F t}{4\pi\alpha\sqrt{2}}\left[a^2_\theta \pm \frac{t(s-u)}{2f(s,t)}\right]. \tag{3.33}$$

For sake of clarification, from now on it will be reported the computations and the corresponding plots only for muons; nevertheless, the final results for both muons and antimuons will still be provided.

3.3 NLO contributions

Next-to-leading order (NLO) QED corrections to Eq. (3.32) has been computed a long time ago in [11-17]; however in those computations there have been made some very specific assumptions, as a vanishing electron mass, the soft approximation, and so on. A more recent and general calculation of the full set of NLO QED and EW corrections, where some of these simplifications are relaxed, can be found in [59].
The only hadronic contribution to Eq. (3.32) at NLO is provided by the LO QED diagram with one HVP insertion in the virtual photon propagator, i.e.

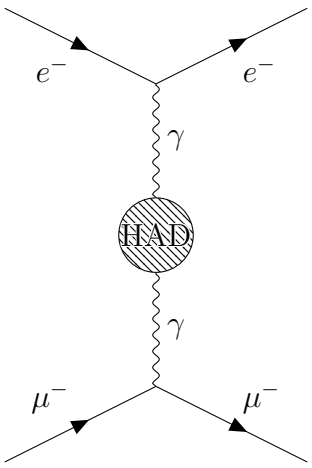

[6] Notice that the question does not even arise in the case in which the mediator is W^+.

This contribution can be evaluated simply remembering the factorization property for the VP function already used in Eq. (2.17), which holds both for leptonic and hadronic VP, leading to an amplitude

$$\mathcal{M}_{\rm NLO,H} = \mathcal{M}_\gamma[\bar{\Pi}_{\rm Had}(t)]. \tag{3.34}$$

It is now easy to obtain the contribution to the total unpolarized amplitude squared, which is given by the interference term with the pure QED:

$$\overline{\mathcal{M}}_{\rm NLO,H} = \frac{1}{4}\sum_{spin} 2{\rm Re}(\mathcal{M}_\gamma^* \mathcal{M}_{\rm NLO,H}) = -2\bar{\Pi}_{\rm Had}(t)|\bar{\mathcal{M}}_\gamma|^2 = 2\Delta\alpha_{\rm Had}(t)|\overline{\mathcal{M}}_\gamma|^2 \tag{3.35}$$

3.4 Heavy NP mediators

In this section I will analyze possible heavy NP effects in low-energy collisions of positive and negative muons with electrons. The mass Λ of the mediators are assumed to be much larger than $\mathcal{O}(1{\rm GeV})$, allowing the employment of an EFT approach in order to take into account the leading NP contributions.

3.4.1 Effective Lagrangian

The most general effective Lagrangian for charged leptons which is invariant under the electromagnetic gauge group $U(1)_{em}$ can be written, up to $D = 6$ operators, as

$$\begin{aligned}\mathcal{L}_{\rm LEFT} = \frac{1}{\Lambda^2}\Big[& d_1^{prst}\,(\bar{e}_{pL}e_{rR})\,(\bar{e}_{sL}e_{tR}) + h.c. + \,. \\ & d_2^{prst}\,(\bar{e}_{pL}\gamma^\mu e_{rL})\,(\bar{e}_{sL}\gamma^\mu e_{tL}) + \\ & d_3^{prst}\,(\bar{e}_{pL}\gamma^\mu e_{rL})\,(\bar{e}_{sR}\gamma^\mu e_{tR}) + \\ & d_4^{prst}\,(\bar{e}_{pR}\gamma^\mu e_{rR})\,(\bar{e}_{sR}\gamma^\mu e_{tR})\Big] + \\ & \frac{d_0^{pr}}{\Lambda}\,(\bar{e}_{pL}\sigma^{\mu\nu}e_{rR})\,F_{\mu\nu} + h.c.\end{aligned} \tag{3.36}$$

where, again, p, r, s, t are flavor indices. The dipole operators can contribute at tree level to the μe scattering through a double operator insertion; nevertheless all of them can be safely neglected thanks to the current tight experimental constraints on the leptonic dipole moments. Moreover, also semileptonic operators should be, in principle, added to Eq. (3.36); however they can contribute only at loop level through the generation of operators already present in $\mathcal{L}_{\rm LEFT}$, but this time suppressed by $1/\Lambda^4$. Then, they can be neglected without problems.
Once assured that the Lagrangian of Eq. (3.36) is sufficient for our purpose, it is possible to open it and to explicit the flavor indices in order to select the structures of interest. Using the Fierz Identities (A.1), the starting Larangian can be written as the sum of two contributions:

$$\mathcal{L}_{\rm LEFT} = \mathcal{L}_{\rm LFC} + \mathcal{L}_{\rm LFV} \tag{3.37}$$

where the lepton flavor conserving (LFC) piece reads

$$\begin{aligned}\mathcal{L}_{\rm LFC} = \frac{1}{\Lambda^2}\Big[& (a_1 + ia_2)\,(\bar{\mu}_L\mu_R)\,(\bar{e}_L e_R) + h.c. + \\ & (a_3 + ia_4)\,(\bar{\mu}_L e_R)\,(\bar{e}_L\mu_R) + h.c. + \\ & (a_5 + ia_6)\,(\bar{\mu}_L\mu_R)\,(\bar{e}_R e_L) + h.c. + \\ & a_7\,(\bar{\mu}_L\gamma^\mu\mu_L)\,(\bar{e}_L\gamma_\mu e_L) + a_8\,(\bar{\mu}_R\gamma^\mu\mu_R)\,(\bar{e}_R\gamma_\mu e_R) + \\ & a_9\,(\bar{\mu}_L\gamma^\mu\mu_L)\,(\bar{e}_R\gamma_\mu e_R) + a_{10}\,(\bar{\mu}_R\gamma^\mu\mu_R)\,(\bar{e}_L\gamma_\mu e_L)\Big]\end{aligned} \tag{3.38}$$

while the lepton flavor violating (LFV) one is

$$\begin{aligned}\mathcal{L}_{\rm LFV} = \frac{1}{\Lambda^2}\Big[& b_1\,(\bar{\mu}_L e_R)\,(\bar{\mu}_L e_R) + b_2\,(\bar{\mu}_R e_L)\,(\bar{\mu}_R e_L) + \\ & b_3\,(\bar{\mu}_L e_R)\,(\bar{\mu}_R e_L) + b_4\,(\bar{\mu}_L\gamma^\mu e_L)\,(\bar{\mu}_L\gamma_\mu e_L) + \\ & b_5\,(\bar{\mu}_R\gamma^\mu e_R)\,(\bar{\mu}_R\gamma_\mu e_R) + h.c.\Big].\end{aligned} \tag{3.39}$$

While Eq. (3.38) contributes to the process $\mu^\pm e^- \to \mu^\pm e^-$, Eq. (3.39) violates the electron and muon family numbers of two units (but still preserving the total lepton number), generating, for example, the scatterings $\mu^+e^- \to \mu^-e^+$ and $e^-e^- \to \mu^-\mu^-$; here, the dimensionless coefficients a_k (with $k = 1, .., 10$) are real while b_l (with $l = 1, .., 5$) are complex. Let's note that, having in mind the μe elastic scattering, only flavor structures with two electrons and two muons have been taken into account; however, from Eq. (3.36) also operators with one (three) electron and three (one) muons can arise, providing the additional LFV processes $\mu^\pm e^- \to e^\pm e^-$ and $\mu^\pm e^- \to \mu^\pm\mu^-$. Nevertheless both of them are highly constrained by the experimental bounds [60] of the processes $\mu \to e\gamma$ and $\mu \to 3e$, which are

$$\mathrm{Br}(\mu^+ \to e^+\gamma) \leq 4.2 \times 10^{-13} \quad \text{and} \quad \mathrm{Br}(\mu^+ \to e^+e^-e^+) \leq 1 \times 10^{-12}.$$

Since they are very rare processes and our purpose relies in trying to understand under what conditions NP effects are maximum in μe scattering, from now on only the Lagrangians (3.38) and (3.39) will be considered.

3.4.2 Heavy NP in $\mu^\pm e^- \to \mu^\pm e^-$ scattering

The leading corrections induced by $\mathcal{L}_{\rm LFC}$ to the LO QED differential cross section $d\sigma_0/dt$ are given by[7]

$$\frac{d\sigma^\pm_{\rm LFC}}{dt} = \frac{d\sigma_0}{dt}\delta^\pm_{\rm LFC} \tag{3.40}$$

where, once defined $z^+ = s$ and $z^- = u$,

$$\begin{aligned}\delta^\pm_{\rm LFC} = \frac{t}{8\pi\alpha\Lambda^2}\frac{1}{f(s,t)}[& 2mMa_S(z^\mp - z^\pm) \\ & + 2mMa_T(z^\pm - t - M^2 - m^2) \\ & + a_V f(s,t) + \frac{a_A}{2}t(z^\pm - z^\mp)]\end{aligned} \tag{3.41}$$

[7]The detailed computation can be found in (A.2).

with the coefficients $a_{S,V,T,A}$ defined as

$$\begin{aligned} a_S &= a_1 + a_5 \\ a_T &= a_3 \\ a_V &= a_7 + a_8 + a_9 + a_{10} \\ a_A &= a_7 + a_8 - a_9 - a_{10}. \end{aligned} \tag{3.42}$$

In Eq. (3.41) terms suppressed by $(t/\Lambda^2)^2$ and a_θ^2 have been neglected. It is interesting to see that by means of the EFT approach we are taking into account all possible NP contributions due to heavy mediators of mass $\sim \Lambda$ independently on their nature. Indeed if, for example, the heavy DOF which has been integrated out was a scalar (pseudoscalar), we would end up with the same contribution of Eq. (3.41) simply with $a_1 = a_5$ ($a_1 = -a_5$) and with all the other a_k equal to zero; as a consequence, for a heavy scalar δ_{LFC} depends only on a_S, while for a pseudoscalar it would be null. An explicit example of this can be provided using the Higgs boson as a mediator. The amplitude for this process is (3.29) and the corresponding interference with the photon ones lead to the unpolarized squared matrix element

$$\overline{\mathcal{M}}_{\gamma H} \overset{t \ll M_H^2}{\approx} \frac{32\pi\alpha m^2 M^2}{v^2 M_H^2 t}(s-u). \tag{3.43}$$

Then, the corresponding shift to the total differential cross section is

$$\frac{d\sigma^-}{dt} = \frac{d\sigma_0}{dt}\delta^-_{\gamma H}$$

with

$$\delta^-_{\gamma H} = \frac{t}{8\pi\alpha}\frac{1}{f(s,t)}\left[2mMa(s-u)\right], \tag{3.44}$$

where it has been defined $a = 2mM/M_H^2$ and $\Lambda^2 = 1/(\sqrt{2}G_F)$. The reasonment done above is true also for other kind of particles: the leading effect of a heavy vector (axial) boson to δ_{LFC} is obtained choosing $a_7 = a_8 = a_9 = a_{10}$ ($a_7 = a_8 = -a_9 = -a_{10}$) and all other $a_k = 0$. Therefore, for a heavy (axial) vector, δ_{LFC} depends only on the parameter (a_A) a_V. Similarly, the coefficient a_T is introduced taking into account heavy spin-1 tensor particles.

A necessary condition for NP to affect the measurements of the MUonE experiment is that they are larger than the expected experimental resolution of $\mathcal{O}(10^{-5})$. Barring large accidental cancellations among the $a_{S,T,V,A}$ contributions to $\delta^{\pm}_{\text{LFC}}$, at MUonE's energies this implies

$$|a_{A,V}| \gtrsim 10\left(\frac{\Lambda}{1\text{TeV}}\right)^2 \qquad |a_{S,T}| \gtrsim 10^4\left(\frac{\Lambda}{1\text{TeV}}\right)^2. \tag{3.45}$$

This is well illustrated by the following plots where, respectively, values of the coefficients which are lower (3.2) and comparable (3.3) to the bounds of (3.45) are taken into account.

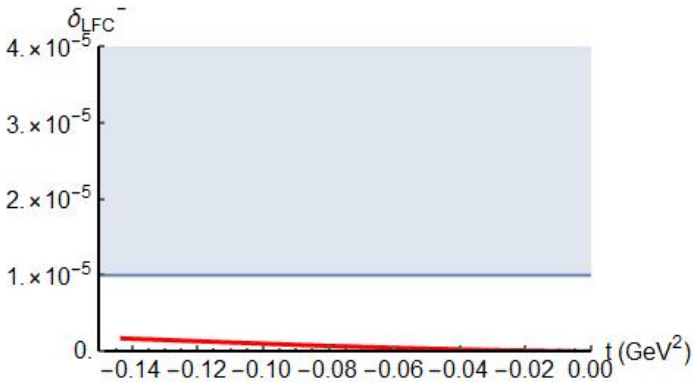

Figure 3.2: The red line represents the NP contribution to the μe differential cross section, while the blue area is the sensitivity range of MUonE. In this case $\Lambda \sim 10^2$ GeV and $a_A = a_V = a_S = a_T = 10^{-2}$; as expected, choosing values of the parameters that are smaller than the lower bounds (3.45), makes the NP contribution not detectable at MUonE.

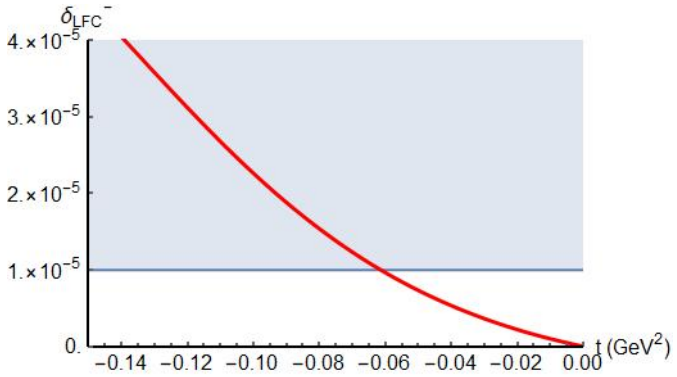

Figure 3.3: The red line represents the NP contribution to the μe differential cross section, while the blue area is the sensitivity range of MUonE. In this case $\Lambda \sim 10^2$ GeV and $a_A = a_V = 10^{-1}$ and $a_S = a_T = 10^2$; as expected, choosing values of the parameters which correspond to the lower bounds (3.45), makes the NP contribution detectable at MUonE.

Another interesting way to observe it consists in plotting δ_{LFC}^{-} as a function of both t and the coefficients $a_{A,V,S,T}$.

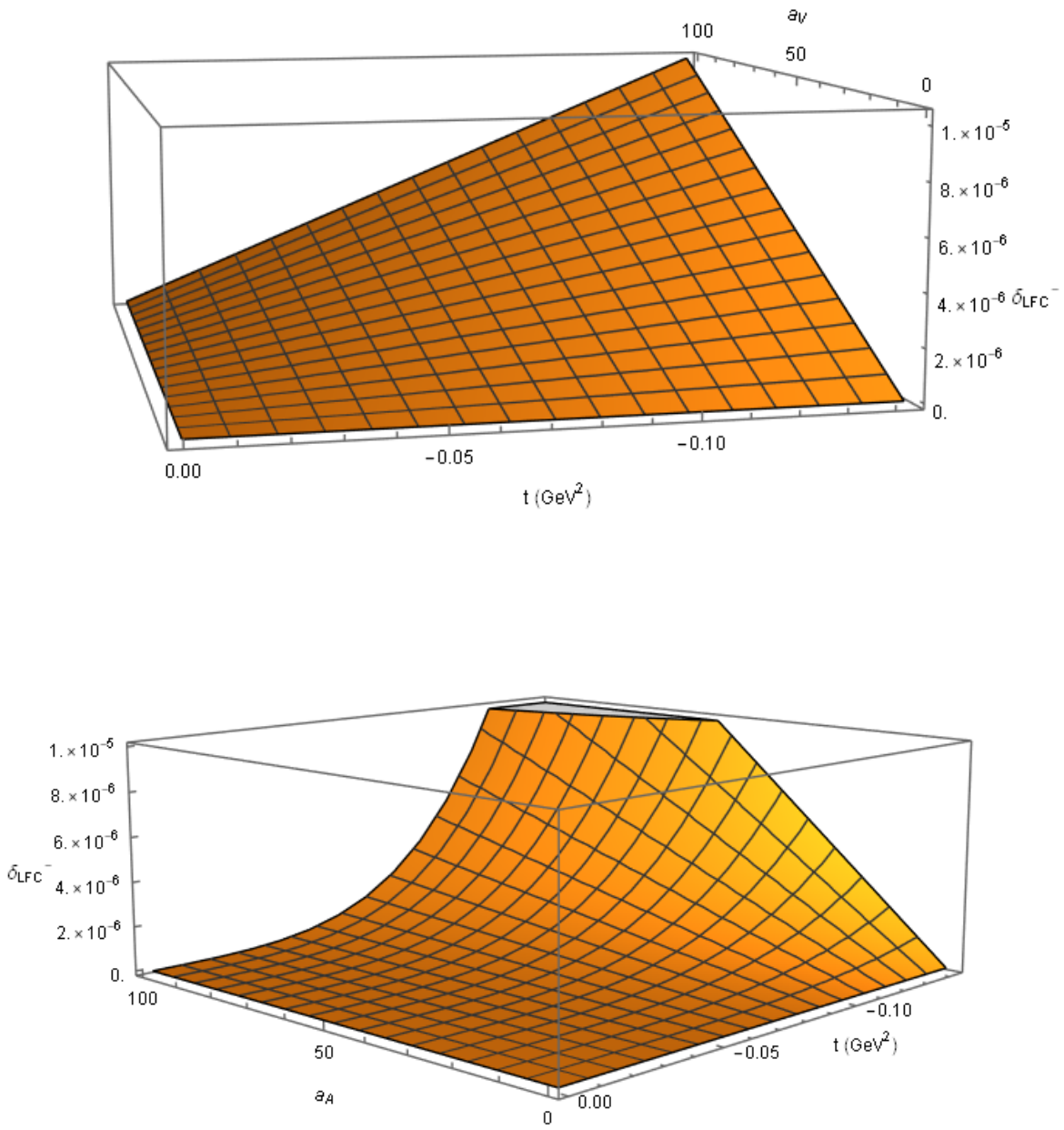

Figure 3.4: The two plots represent the dependence of δ^-_{LFC} on t and a_V (up) or a_A (down). As it can be seen, δ^-_{LFC} reach MUonE sensitivity of $\mathcal{O}\,(10^{-5})$ only for $t \to t_{min}$ and if the Wilson coefficients take the lower bound of (3.45).

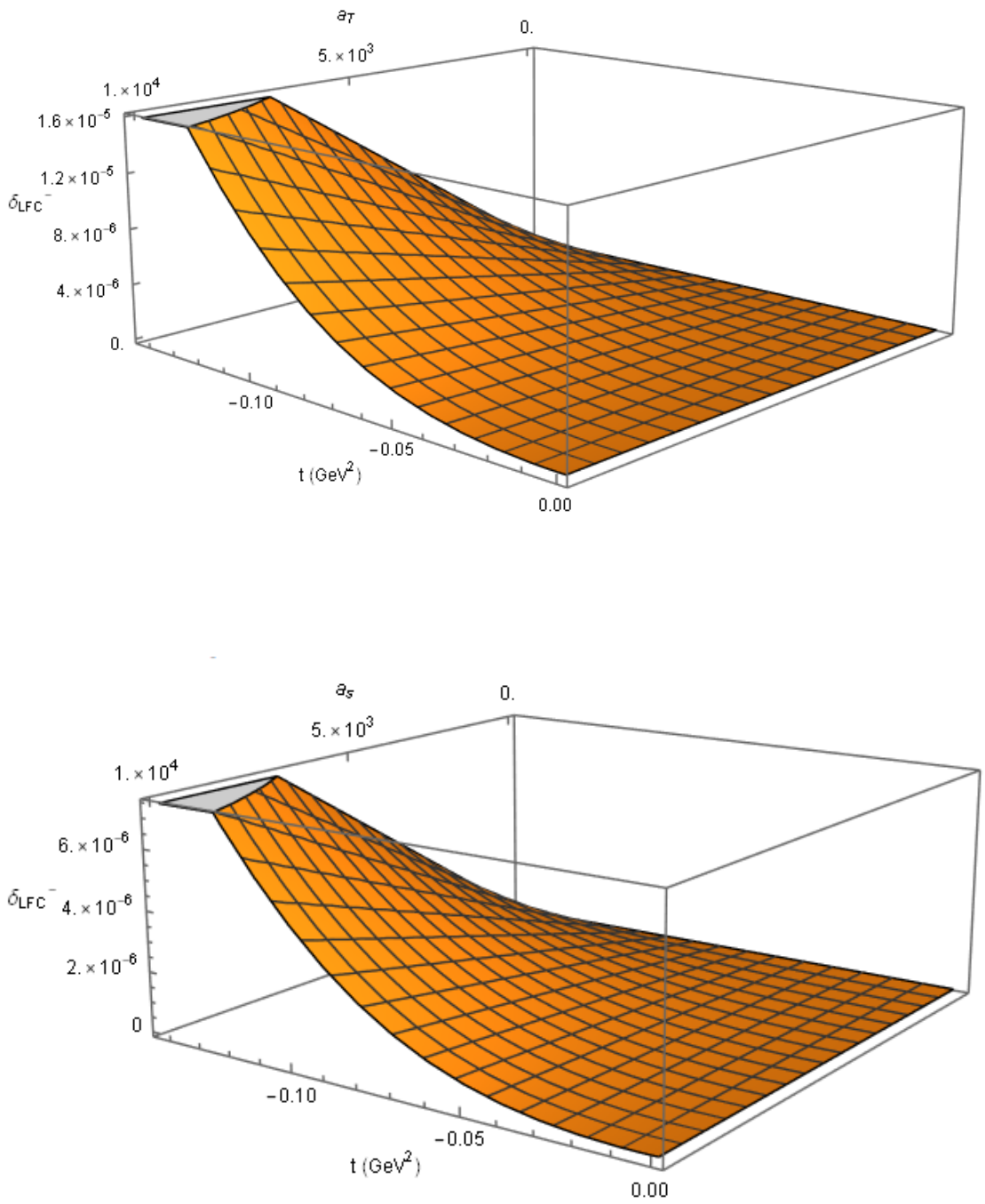

Figure 3.5: The two plots represent the dependence of δ^-_{LFC} on t and a_T (up) or a_S (down). As it can be seen, δ^-_{LFC} reach MUonE sensitivity of $\mathcal{O}\left(10^{-5}\right)$ only for $t \to t_{min}$ and if the Wilson coefficients take the lower bound of (3.45).

Nevertheless these bounds should be immediately compared to those obtained requiring the perturbativity and the unitarity of the theory: the former brings to the condition $|a_k|, |b_l| \leq 16\pi^2$, while the latter implies:

$$\frac{|a_k|, |b_l|}{\Lambda^2} < \frac{16\pi\eta_{k,l}}{s} \tag{3.46}$$

with $\eta_{k,l}$ coefficients of $\mathcal{O}(1)$. The perturbativity bounds immediately exclude any kind of pollution to the elastic μe scattering cross section from both a_T and a_S which can be, then, safely neglected; this fact allows to define also two observables in order to prove separately both a_A and a_V. This can be done simply taking Eq. (3.41) and evaluating at the endpoint $t = t_{min}$ the two quantities

$$\begin{aligned}(\delta^+_{\rm LFC} + \delta^-_{\rm LFC})_{t_{min}} &= \frac{a_V}{4\pi\alpha\Lambda^2} t_{min} \\ (\delta^+_{\rm LFC} - \delta^-_{\rm LFC})_{t_{min}} &= \frac{a_A}{4\pi\alpha\Lambda^2}(t_{min} - 2M^2 + 2s),\end{aligned}$$

where the electron mass m has been neglected.

3.4.3 Heavy NP in $e^+e^- \to \mu^+\mu^-$

The LFC Lagrangian of Eq. (3.38) contributes also to the process $e^+e^- \to \mu^+\mu^-$, whose cross section and forward-backward asymmetry $A_{\rm FB}$ have been widely studied and precisely measured at LEP.
At energies $\sqrt{s} \gg M$, both the electron and muon masses can be neglected and the total cross section reads [8]

$$\sigma(e^+e^- \to \mu^+\mu^-) = \sigma_{\rm SM} + \sigma_{\rm NP}, \tag{3.47}$$

where

$$\begin{aligned}\sigma_{\rm SM} &= \frac{4\pi\alpha^2}{3s} + \frac{\alpha G_F}{3\sqrt{2}} \frac{a_\theta^2 M_Z^2}{s - M_Z^2} + \frac{G_F^2}{96\pi}\left(a_\theta^2 + 1\right)^2 \frac{s M_Z^4}{\left(s - M_Z^2\right)^2} \\ \sigma_{\rm NP} &= \frac{1}{\Lambda^2}\left(a_V \frac{\alpha}{6} + a_A \frac{G_F}{48\pi\sqrt{2}} \frac{s M_Z^2}{s - M_Z^2}\right).\end{aligned} \tag{3.48}$$

Similarly, it is possible to compute the the new asymmetry, which is

$$A_{\rm FB} = A_{\rm FB}^{\rm SM}\left[1 + \frac{r(s)}{\Lambda^2}\left(\frac{a_A\left(s - M_Z^2\right)}{\sqrt{2} G_F M_Z^2} - \frac{a_V s}{16\pi\alpha}\right)\right], \tag{3.49}$$

with

$$A_{\rm FB}^{\rm SM} = \frac{3 s G_F M_Z^2\left[4\pi\alpha\sqrt{2}\left(s - M_Z^2\right) + a_\theta^2 s G_F M_Z^2\right]}{128\pi^2\alpha^2\left(s - M_Z^2\right)^2 + \left(a_\theta^2 + 1\right)^2 s^2 G_F^2 M_Z^4 + 16\pi\alpha\sqrt{2} a_\theta^2 G_F M_Z^2 s\left(s - M_Z^2\right)}$$

the usual full SM prediction, and

$$r(s) = \frac{128\pi^2\alpha^2\left(s - M_Z^2\right)^2 - s^2 G_F^2 M_Z^4}{128\pi^2\alpha^2\left(s - M_Z^2\right)^2 + s^2 G_F^2 M_Z^4}.$$

It is worth to underline that in the NP contributions all the suppressed terms, as $(s/\Lambda^2)^2$ and those multiplied by a_θ, have been systematically neglected. For a detailed computations of the NP contributions to both the cross section and the forward-backward asymmetry check (A.4).

[8] The detailed computations can be found in (A.3) and (A.4)

NP effects on these two observables can be constrained by means of a comparison of the LEP-II data [38], which read

$$\frac{\sigma\left(e^+e^- \to \mu^+\mu^-\right)_{\rm EXP}}{\sigma\left(e^+e^- \to \mu^+\mu^-\right)_{\rm SM}} = 0.9936 \pm 0.0141 \tag{3.50}$$

$$\frac{A_{\rm FB}^{\rm EXP}\left(e^+e^- \to \mu^+\mu^-\right)}{A_{\rm FB}^{\rm SM}\left(e^+e^- \to \mu^+\mu^-\right)} = 0.9925 \pm 0.0212 \tag{3.51}$$

where these two values refer to the the mean value of those ratios in the energy range $130 \leq \sqrt{s} \leq 207$ GeV. Imposing these two constraints at the 2σ level, it follows that the coefficients $a_{A,V}$ must satisfy the bound

$$|a_{A,V}| \lesssim 1 \left(\frac{\Lambda}{1\ \text{TeV}}\right)^2 . \tag{3.52}$$

It is immediate to see that this requirement doesn't allow to fullfill the condition (3.45), making NP not detectable at MUonE. Hereafter I report two exemplary plots which show the consistence with this bound:

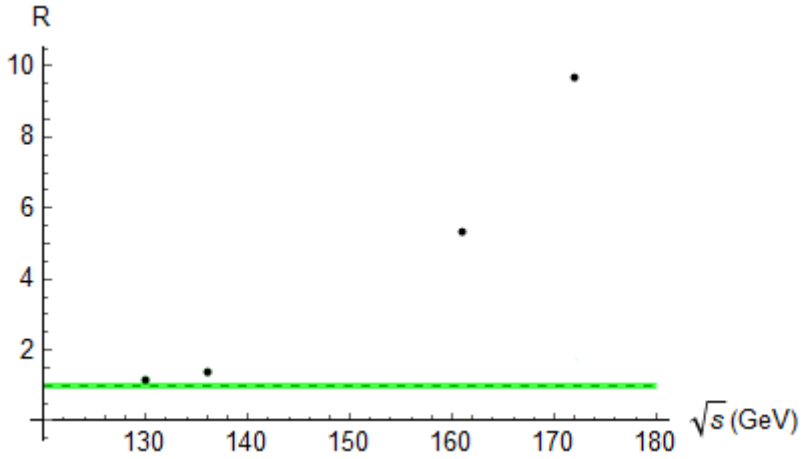

Figure 3.6: The black dashed line represents the averaged ratio R between the experimental value of $A_{\rm FB}$ and its SM prediction for the data taken at the following energies: $130, 136, 161, 172, 183, 189, 192, 196, 200, 202, 205, 207$ GeV; the green boundary represents the experimental uncertainty; the black dots correspond to the ratio of the experimental $A_{\rm FB}$ with the new prediction for this observable (i.e. that with NP contributions) with $a_A = a_V = 10$. They turn out to be absolutely not consistent with the experimental bounds.

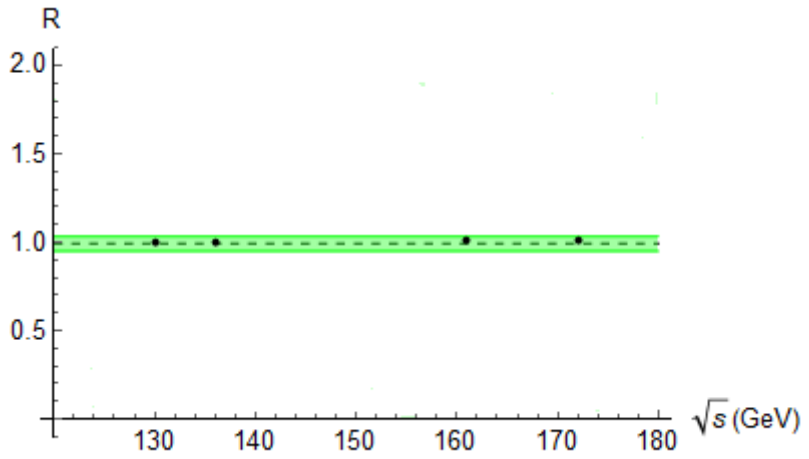

Figure 3.7: The red dashed line represents the averaged ratio R between the experimental value of $A_{\rm FB}$ and its SM prediction for the data taken at the following energies: 130, 136, 161, 172, 183, 189, 192, 196, 200, 202, 205, 207 GeV; the green boundary represents the experimental uncertainty; the black dots correspond to the ratio of the experimental $A_{\rm FB}$ with the new prediction for this observable (i.e. that with NP contributions) with $a_A = a_V = 1$. They turn out to be consistent with the experimental bound, differently from the previous case where $a_A = a_V = 10$. This confirms the theoretical bounds provided by Eq.(3.52)

Let's now analyze the possibility of still having heavy new physics, but at energies well below the electroweak scale v.
Since we want to rely again on the EFT approach, it is necessary to require that $\sqrt{s} \ll \Lambda$; for this reason, LEP-II data cannot longer be used, differently from the of low-energy ones from PEP [39], PETRA [40] and TRISTAN [41], which ran at a center of mass energy $\sqrt{s} = 29, 35, 59$ GeV respectively. The measured values of $\sigma(e^+e^- \to \mu^+\mu^-)$ and of $A_{\rm FB}$ provides the following ratios

$$\frac{\sigma\left(e^+e^- \to \mu^+\mu^-\right)_{\rm EXP}}{\sigma\left(e^+e^- \to \mu^+\mu^-\right)_{\rm SM}} = \begin{cases} 0.994 \pm 0.022, & \sqrt{s} = 29 \text{ GeV} \\ 0.984 \pm 0.027, & \sqrt{s} = 35 \text{ GeV} \\ 0.987 \pm 0.019, & \sqrt{s} = 58 \text{ GeV} \end{cases} \tag{3.53}$$

$$\frac{A_{\rm FB}\left(e^+e^- \to \mu^+\mu^-\right)_{\rm EXP}}{A_{\rm FB}\left(e^+e^- \to \mu^+\mu^-\right)_{\rm SM}} = \begin{cases} 0.995 \pm 0.164, & \sqrt{s} = 29 \text{ GeV} \\ 1.076 \pm 0.170, & \sqrt{s} = 35 \text{ GeV} \\ 0.977 \pm 0.065, & \sqrt{s} = 58 \text{ GeV} \end{cases} \tag{3.54}$$

These experimental values are very useful to constrain the coefficients a_V and a_A; indeed, observing that $s \ll M_Z^2$, the two equations (3.47) and (3.49) can be safely approximated by

$$\sigma(e^+e^- \to \mu^+\mu^-) \approx \frac{4\pi\alpha^2}{3s} + \frac{\alpha a_V}{6\Lambda^2} \tag{3.55}$$

$$A_{\rm FB} \approx A_{\rm FB}^{\rm SM}\left(1 - \frac{a_A}{\sqrt{2}G_F\Lambda^2}\right) \tag{3.56}$$

allowing to probe separately a_A and a_V.
Once imposed PEP bounds it is possible to find that these two coefficients must satisfy

$$|a_V| \lesssim \left(\frac{\Lambda}{\text{TeV}}\right)^2, \quad |a_A| \lesssim 10^{-2}\left(\frac{\Lambda}{\text{TeV}}\right)^2 \tag{3.57}$$

which, as seen before, do not allow visible NP effects at MUonE, since they would provide $\delta_{\rm LFC} < 10^{-5}$. Nevertheless it is important to underline that what has just been discusses is true for $\sqrt{s} \ll \Lambda < v$, i.e. for $\Lambda \geq 100$ GeV, since for smaller values the EFT approach would break down.
At mass scales below ~ 100 GeV new particles are strongly disfavoured by LEP bounds. In this scenario, the effective couplings a_V and a_A can be present only through the exchange of a vector boson U that couples to leptons in a "V-A way", i.e. $\bar{\ell}\gamma^\mu(g_V^{'(\ell)} - g_A^{'(\mu)})\ell U_\ell$. Equations (3.47) and (3.49) are still true, once replaced $a_X/\Lambda^2 \to 4g_X^e g_X^\mu/(s - M_U^2)$, with $X = V, A$. These couplings are constrained by both LHC experiments (for the mass range $10 \lesssim M_U \lesssim 50$ GeV) [42] and the BaBar experiments ($M_U \lesssim 10$ GeV) [43]; in the former case it is possible to refer to Fig. 6 of [42], which provides the bounds for the pure vector coupling g_V as a function of M_U, while for the latter one it is available the upper bound $g_V \lesssim 7 \times 10^{-4}$. In both cases, assuming that these constraints hold also for g_A and barring accidental cancellations, it easily follows that contributions of NP lying below v do not affect μe scattering at MUonE.

3.5 Heavy NP and LFV effects

After the detailed analysis of $\mathcal{L}_{\rm LFC}$ and the possibility to pollute MUonE measurements, in this section the attention is turned on the LFV case provided by (3.39). As already mentioned, $\mathcal{L}_{\rm LFV}$ violates both the electron and muon family numbers by two units (still preserving the total lepton number) generating, for example, the processes $\mu^\pm e^- \to e^\pm e^-$ and $\mu^\pm e^- \to \mu^\pm \mu^-$. Although there are no relevant experimental bounds on these two processes, the coefficients of $\mathcal{L}_{\rm LFV}$ can be still constrained analyzing the muonium-antimuonium (Mu $-$ $\overline{\rm Mu}$) oscillation (with Mu and $\overline{\rm Mu}$ which refer, respectively, to μ^+e^- and μ^-e^+ bound states)[9].
It has been shown by Feinberg and Weimberg [46] that the time integrated probability for the Mu $-$ $\overline{\rm Mu}$ oscillation satisfies

$$P({\rm Mu} - \overline{\rm Mu}) \simeq \frac{2|\langle \overline{\rm Mu}|\mathcal{L}_{\rm LFV}|{\rm Mu}\rangle|^2}{\Gamma_\mu^2} \tag{3.58}$$

where $\Gamma_\mu = G_F^2 M^5/192\pi^3 \approx 3 \times 10^{-19}$GeV is nothing else that the muon decay rate. The evaluation of the matrix element provides[10]

$$|\langle \overline{\rm Mu}|\mathcal{L}_{\rm LFV}|{\rm Mu}\rangle| = \frac{|b_1 + b_2 - 3b_3 + 4b_4 + 4b_5|}{2\pi a_0^3 \Lambda^2} \tag{3.59}$$

where $a_0 = (\alpha m)^{-1}$; then, exploiting all the numerical values, the prediction for the oscillation probability reads

$$P({\rm Mu} - \overline{\rm Mu}) \approx 10^{-9} \left(\frac{1{\rm TeV}}{\Lambda}\right)^4 |b_1 + b_2 - 3b_3 + 4b_4 + 4b_5|^2 \tag{3.60}$$

which has to be compared with the current experimental bound [47]

$$P({\rm Mu} - \overline{\rm Mu}) \leq 8.2 \times 10^{-11} \tag{3.61}$$

[9] Historically this phenomenon has been predicted by Pontecovo [44] in 1957, well before the discovery of muonium [45] in 1960.
[10] See (A.5) for details on the computation.

at the 90% of C.L.. It is almost immediate to notice that (3.61) is satisfied by the theoretical prediction of P if and only if the coefficients do not exceed the values

$$|b_{1,2}| \lesssim 0.3 \left(\frac{\Lambda}{1\text{TeV}}\right)^2, \quad |b_{3,4,5}| \lesssim 0.1 \left(\frac{\Lambda}{1\text{TeV}}\right)^2. \tag{3.62}$$

Also in this case, in order to understand whether NP flavor violation effects can affect MUonE measurements, it is necessary to check if, saturating the bounds of Eq. (3.62), the dominant contribution to the $\mu^+e^- \to \mu^-e^+$ differential cross section is higher than $\mathcal{O}(10^{-5})$.
The five amplitudes associated to the terms of (3.39) are

$$\begin{aligned}
\mathcal{M}_1 &= \frac{ib_1}{4\Lambda^2}\bar{u}(p_3)(1+\gamma_5)u(p_1)\bar{v}(p_2)(1+\gamma_5)v(p_4)\\
\mathcal{M}_2 &= \frac{ib_2}{4\Lambda^2}\bar{u}(p_3)(1-\gamma_5)u(p_1)\bar{v}(p_2)(1-\gamma_5)v(p_4)\\
\mathcal{M}_3 &= \frac{ib_3}{4\Lambda^2}\bar{u}(p_3)(1+\gamma_5)u(p_1)\bar{v}p(_2)(1-\gamma_5)v(p_4)\\
\mathcal{M}_4 &= \frac{ib_4}{4\Lambda^2}\bar{u}(p_3)\gamma^\mu(1-\gamma_5)u(p_1)\bar{v}(p_2)\gamma_\mu(1-\gamma_5)v(p_4)\\
\mathcal{M}_5 &= \frac{ib_5}{4\Lambda^2}\bar{u}(p_3)\gamma^\mu(1+\gamma_5)u(p_1)\bar{v}(p_2)\gamma_\mu(1+\gamma_5)v(p_4).
\end{aligned}$$

In this case it is convenient to perform the computations by means of Mathematica, being the calculation of the unpolarized squared amplitude very long and easily subject to errors, even working with the simplification of $m = M = 0$. In this limit, the final result of the amplitude, combined with the usual reference formulas in (A.1), provides

$$\frac{d\sigma_{\text{LFV}}}{dt} = \frac{d\sigma_0}{dt}\delta_{\text{LFV}}, \tag{3.63}$$

where

$$\delta_{\text{LFV}} = \left(\frac{t}{8\pi\alpha\Lambda^2}\right)^2 \sum_{l=1}^{5} |b_l|^2 c_l(s,t), \qquad c_{1,2,3}(s,t) = \frac{t^2}{f(s,t)}, \qquad c_{4,5}(s,t) = \frac{(s+t)^2}{f(s,t)}. \tag{3.64}$$

Being the functions $c_{1,2,3}(s,t)$ and $c_{4,5}(s,t)$ (at most) of order $\mathcal{O}(10^{-1})$ and $\mathcal{O}(1)$ respectively, it's easy to check that the MUonE measurements can be affected by NP LFV effects if

$$|b_{1,2,3}| \gtrsim 10^4 \left(\frac{\Lambda}{1\text{TeV}}\right)^2, \quad |b_{4,5}| \gtrsim 10^3 \left(\frac{\Lambda}{1\text{TeV}}\right)^2 \tag{3.65}$$

which, however, are excluded by the experimental bound on the muonium-antimuonium in Eq. (3.62).

3.6 NP above the EW scale

So far it has been investigated the case of NP at scales $\Lambda \lesssim v$, where $v \sim 246$ GeV is the electroweak VEV; in such a scenario, the construction of the most general effective

Lagrangian requires to add operators up to dimension $D = 6$ invariant only under the electromagnetic gauge group $U(1)_{em}$, leading to Eq. (3.37), (3.38) and (3.39).
Nevertheless, if NP lies above the EW scale, the effective Lagrangian must be invariant under the full SM gauge group; the full list of all the 59 $D = 6$ operators which satisfy this requirement can be found in (A.7) while the detailed way to construct them is well illustred and explained in [61] and [62]. The previous expressions must be substituted with

$$\begin{aligned}\mathcal{L}_{\text{SMEFT}} = \frac{1}{\Lambda^2}\Big[& c_{\ell\ell}^{prst}\left(\bar{\ell}_{pL}\gamma^{\mu}\ell_{rL}\right)\left(\bar{\ell}_{sL}\gamma_{\mu}\ell_{tL}\right) + \\ & c_{\ell e}^{prst}\left(\bar{\ell}_{pL}\gamma^{\mu}\ell_{rL}\right)\left(\bar{e}_{sR}\gamma_{\mu}e_{tR}\right) + \\ & c_{ee}^{prst}\left(\bar{e}_{pR}\gamma^{\mu}e_{rR}\right)\left(\bar{e}_{sR}\gamma_{\mu}e_{tR}\right)\Big],\end{aligned} \tag{3.66}$$

where ℓ and e are the $SU(2)_L$ doublet and singlet respectively. As for the previous case, the Lagrangian should contain also semileptonic operators, as $\left(\bar{\ell}_{pL}\gamma^{\mu}\ell_{rL}\right)\left(\bar{q}_{sL}\gamma_{\mu}q_{tL}\right)$; however, their contribution to the μe scattering can takes place only at loop level, allowing us to safely neglect them since only the largest possible NP contributions are interesting. It is clear that this Lagrangian cannot contain again the four-lepton scalar operators present in the case of $U(1)_{em}$, being not invariant under the full SM group; moreover, having enlarged the symmetries of the theory, i.e. restricted the number of allowed operators, it is almost obvious that some of them will be no more present. Indeed, matching the Wilson coefficients of $\mathcal{L}_{\text{SMEFT}}$ and $\mathcal{L}_{\text{LFC}}$ at tree level, it is possible to find

$$\begin{aligned} a_1 &= a_2 = a_3 = a_4 = 0, \\ a_5 + ia_6 &= -2c_{\ell e}^{2112}, \\ a_7 &= c_{\ell\ell}^{1122} + c_{\ell\ell}^{2211} + c_{\ell\ell}^{1221} + c_{\ell\ell}^{2112}, \\ a_8 &= c_{ee}^{1122} + c_{ee}^{2211}, \\ a_9 &= c_{\ell e}^{2211}, \\ a_{10} &= c_{\ell e}^{1122}, \end{aligned} \tag{3.67}$$

while the matching with $\mathcal{L}_{\text{LFV}}$ reads

$$\begin{aligned} b_1 = b_2 = 0, \qquad & b_3 = -2c_{\ell e}^{2121}, \\ b_4 = 2c_{\ell\ell}^{2121}, \qquad & b_5 = c_{ee}^{2121}. \end{aligned} \tag{3.68}$$

In this scenario, then, the results of Eqs. (3.41), (3.47) and (3.49) are still correct, with the exception that now $a_S = a_5$ and $a_T = 0$; similarly, in the LFV sector Eq. (3.60) is valid, this time with the lack of the coefficients b_1 and b_2.
Another interesting fact, which arises as a result of the underlying $SU(2)_L$, symmetry is that $\mathcal{L}_{\text{SMEFT}}$ contains interactions with neutrinos; using directly the relations provided by

(3.67), the most important ones are

$$\begin{aligned}\mathcal{L}^{\nu}_{\text{SMEFT}} = \frac{1}{\Lambda^2}[&a_9\,(\bar{\nu}_{\mu L}\gamma^{\mu}\nu_{\mu L})\,(\bar{e_R}\gamma_{\mu}e_R) + \\ &a_{11}\,(\bar{\nu}_{\mu L}\gamma^{\mu}\nu_{\mu L})\,(\bar{e_L}\gamma_{\mu}e_L) + \\ &a_{12}\,(\bar{\nu}_{eL}\gamma^{\mu}e_L)\,(\bar{\mu}_L\gamma_{\mu}\nu_{\mu_L}) + \\ &a_{12}\,(\bar{\nu}_{\mu L}\gamma^{\mu}e_L)\,(\bar{e}_L\gamma_{\mu}\nu_{e_L}) + ...],\end{aligned} \tag{3.69}$$

where the new real coefficients are

$$a_{11} = c_{\ell\ell}^{1122} + c_{\ell\ell}^{2211}, \qquad a_{12} = c_{\ell\ell}^{1221} + c_{\ell\ell}^{2112} \tag{3.70}$$

and the dots in Eq. (3.69) stand for terms contained in Eq. (3.66) but not phenomenologically relevant. The most interesting ones are the scattering $\nu_\mu e \to \nu_\mu e$, the annihilation $e^+e^- \to \bar{\nu}_\mu\nu_\mu$ and the decay $\mu \to e\bar{\nu}_e\nu_\mu$. The inclusion of NP effects in the latter process brings to a redefinition of the Fermi constant, replacing $G_F^0/\sqrt{2} = 1/(2v^2)$ with

$$\frac{G_F^0}{\sqrt{2}} = \frac{G_F}{\sqrt{2}} + \frac{a_{12}}{4\Lambda^2} \tag{3.71}$$

where G_F is the experimental value extracted from the measure of the decay rate. It is important to notice that this shift affects every observable linked to weak interactions and a very smart way to test such a NP contribution is to analyze observables which do not receive any direct NP effect, such as the tau decay $\tau \to \ell\bar{\nu}_\ell\nu_\tau$. Nevertheless, comparing with τ decay data it is possible to find the constraint

$$|a_{12}| \lesssim 0.5\left(\frac{\Lambda}{1\text{ TeV}}\right)^2 \tag{3.72}$$

which forbids any observable NP effect in μe scattering due to a_{12}. Indeed, the presence of this contribution would provide an additional term to the total cross section of the process $\mu^+e^- \to \bar{\nu}_\mu\nu_e$ which is almost similar to that of Eq. (3.28); the difference is only in the coefficient which, since we want to deal with the interference term, can be recovered substituting one $G_F/\sqrt{2}$ factor with $2a_{12}/(4\Lambda^2)$, providing

$$\sigma^{\text{NP}}(\mu^+e^- \to \bar{\nu}_\mu\nu_e) = \frac{G_F a_{12}(M^2+s)}{12\sqrt{2}\pi\Lambda^2}. \tag{3.73}$$

Imposing the previous bound, this contribution turns out to be smaller than its SM analogous, being $\sigma^{\text{NP}}(\mu^+e^- \to \bar{\nu}_\mu\nu_e) \sim 5\times10^{-14}\text{GeV}^{-2}$ and not detectable at MUonE.

3.6.1 Heavy NP in $\nu_\mu e^- \to \nu_\mu e^-$

As already mentioned, the Lagrangian of Eq. (3.66) gives rise to interactions correlated to the μe scattering which involve neutrinos. The first process to investigate is the scattering $\nu_\mu e^- \to \nu_\mu e^-$, described by the two Feynman diagrams:

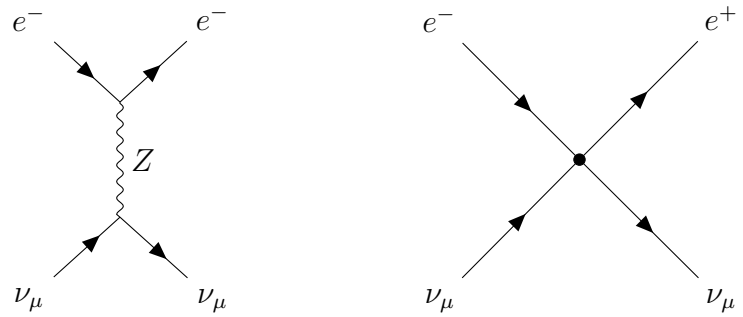

whose amplitudes are [11]

$$\mathcal{M}_Z = -\frac{iG_F^0}{\sqrt{2}}\frac{M_Z^2}{M_Z^2-t}\bar{u}(p_3)\gamma^\mu(1-\gamma_5)u(p_1)[g_L\bar{u}(p_4)\gamma_\mu(1-\gamma_5)u(p_2)+g_R\bar{u}(p_4)\gamma_\mu(1+\gamma_5)u(p_2)] \tag{3.74}$$

$$\mathcal{M}_{\rm NP} = \frac{ia_{12}}{4\Lambda^2}\bar{u}(p_3)\gamma^\mu(1-\gamma_5)u(p_1)[\bar{u}(p_4)\gamma_\mu(1-\gamma_5)u(p_2)+\bar{u}(p_4)\gamma_\mu(1+\gamma_5)u(p_2)] \tag{3.75}$$

so that the sum of them simply reads

$$\mathcal{M}_{tot} = -\frac{iG_F^0}{\sqrt{2}}\bar{u}(p_3)\gamma^\mu(1-\gamma_5)u(p_1)[g_L^{'}\bar{u}(p_4)\gamma_\mu(1-\gamma_5)u(p_2)+g_R^{'}\bar{u}(p_4)\gamma_\mu(1+\gamma_5)u(p_2)], \tag{3.76}$$

where the new chiral coefficients explicitly read

$$g_L^{'} = \left(s_\theta^2-\frac{1}{2}\right)\left(\frac{M_Z^2}{M_Z^2-t}\right)-\frac{\sqrt{2}a_{11}}{4G_F\Lambda^2}$$

$$g_R^{'} = s_\theta^2\left(\frac{M_Z^2}{M_Z^2-t}\right)-\frac{\sqrt{2}a_9}{4G_F\Lambda^2}.$$

The total amplitude (3.76) is the same of the weak one, but with different chiral coefficients; then, the total tree level cross section can be recovered directly from the SM one simply applying the replacements $g_{L,R}\to g_{L,R}^{'}$, leading to

$$\sigma(\nu_\mu e^-\to\nu_\mu e^-) = \frac{(G_F^0)^2 s}{\pi}\left(|g_L^{'}|^2+\frac{|g_R^{'}|^2}{3}\right). \tag{3.77}$$

Lastly, defining $g_{V,A}=g_L\pm g_R$ and imposing the experimental bounds $g_V=-0.040\pm0.015$ and $g_A=-0.507\pm0.014$ at the σ level, it follows, barring accidental cancellations,

$$|a_{9,11}|\lesssim\left(\frac{\Lambda}{1\text{ TeV}}\right)^2. \tag{3.78}$$

[11] From now on the superscript e will be removed and the chiral coefficients will refer only to the charge leptons

3.6.2 Heavy NP in $e^+e^- \to \nu_\mu\bar{\nu}_\mu$

The second interesting process to analyze is the annihilation $e^+e^- \to \nu_\mu\bar{\nu}_\mu$ since the presence of NP modifies the number of neutrinos N_ν.
The diagrams for this process are

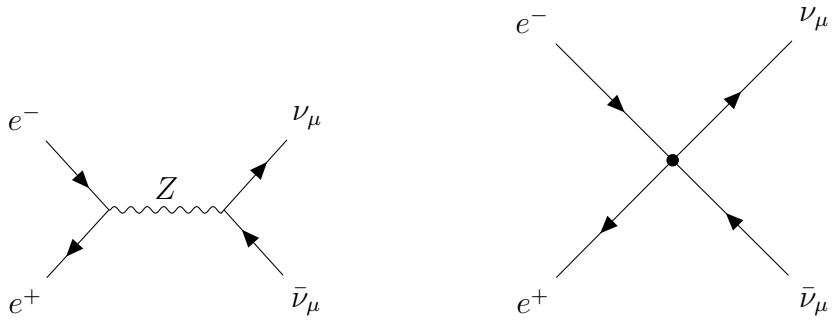

and the corresponding amplitudes

$$\mathcal{M}_Z = -\frac{iG_F^0}{\sqrt{2}}\frac{M_Z^2}{M_Z^2 - s}\bar{u}(p_3)\gamma^\mu(1-\gamma_5)v(p_4)[g_L\bar{v}(p_2)\gamma_\mu(1-\gamma_5)u(p_1) + g_R\bar{v}(p_2)\gamma_\mu(1+\gamma_5)u(p_1)] \tag{3.79}$$

$$\mathcal{M}_{\text{NP}} = \frac{i}{4\Lambda^2}\bar{u}(p_3)\gamma^\mu(1-\gamma_5)v(p_4)[a_9\bar{v}(p_2)\gamma_\mu(1-\gamma_5)u(p_1) + a_{11}\bar{v}(p_2)\gamma_\mu(1+\gamma_5)u(p_1)] \tag{3.80}$$

so that their sum reads

$$\mathcal{M}_{tot} = -\frac{iG_F^0}{\sqrt{2}}\bar{u}(p_3)\gamma^\mu(1-\gamma_5)v(p_4)[g_L^{'}\bar{v}(p_2)\gamma_\mu(1-\gamma_5)u(p_1) + g_R^{'}\bar{v}(p_2)\gamma_\mu(1+\gamma_5)u(p_1)], \tag{3.81}$$

where the new coefficients are still those provided above.
As for the previous process, also in this case the total amplitude is the same of the SM one, except for the new coefficients; then, making the proper substitutions, it is possible to immediately find

$$\sigma(e^+e^- \to \nu_\mu\bar{\nu}_\mu) = \frac{(G_F^0)^2 s}{6\pi}\left(|g_L^{'}|^2 + |g_R^{'}|^2\right). \tag{3.82}$$

Factorizing the SM contribution, this last result can be rewritten as

$$\sigma(e^+e^- \to \nu_\mu\bar{\nu}_\mu) = \sigma^{\text{SM}}(e^+e^- \to \nu_\mu\bar{\nu}_\mu)\left[1 + \frac{1}{\sqrt{2}G_F\Lambda^2}\left(\frac{s - M_Z^2}{M_Z^2}\right)\left(\frac{a_{11}g_L^{'} + a_9 g_R^{'}}{|g_L^{'}|^2 + |g_R^{'}|^2}\right)\right] \tag{3.83}$$

where terms $\propto 1/\Lambda^4$ have been neglected. Let's remember that in the SM the couplings of neutrinos to the Z boson are flavor blind, i.e. they are the same for every generation and not only for the muonic one; then, it is simple to define the total cross section

$$\sigma(e^+e^- \to \nu\bar{\nu}) = \sigma^{\text{SM}}(e^+e^- \to \nu\bar{\nu})\left[3 + \frac{1}{\sqrt{2}G_F\Lambda^2}\left(\frac{s - M_Z^2}{M_Z^2}\right)\left(\frac{a_{11}g_L^{'} + a_9 g_R^{e}}{|g_L^{e}|^2 + |g_R^{'}|^2}\right)\right],$$

which can be rearranged as

$$\sigma(e^+e^- \to \nu\bar{\nu}) = N_\nu \frac{(G_F)^2 s}{6\pi} \left(\frac{M_Z^2}{M_Z^2 - s}\right)^2 \left(|g_L^{'}|^2 + |g_R^{'}|^2\right) \tag{3.84}$$

once defined the new total number of neutrinos as

$$N_\nu = 3 + \frac{1}{\sqrt{2} G_F \Lambda^2} \left(\frac{s - M_Z^2}{M_Z^2}\right) \left(\frac{a_{11} g_L^{'} + a_9 g_R^{'}}{|g_L^{'}|^2 + |g_R^{'}|^2}\right). \tag{3.85}$$

Comparing this last result with the measurement $N_\nu = 2.92 \pm 0.05$ from LEP-II [38], it follows that the two coefficients a_9 and a_{11} must satisfy a more stringent bound respect to the previous one, which is

$$|a_{9,11}| \lesssim \left(\frac{\Lambda}{1\ \text{TeV}}\right)^2. \tag{3.86}$$

Chapter 4

Light new physics effects at MUonE

In this chapter I will focus on the analysis of light mediators, with masses of $\mathcal{O}(1\,\text{GeV})$, and their contributions on the low-energy μe scattering differential cross section. In this scenario the EFT approach is no more allowed and it is necessary to specify the spin and the interactions of the new mediators with the SM particles. In particular, I will take into account the cases of both a spin-0 and a spin-1 dynamical fields: in the former case the SM is supplemented by axion-like particles (ALPs) and it is discussed in Sec. (4.1), while the latter is representative of models with light Dark Photons or Z' vector bosons, which will be analyzed respectively in Sec. (4.2) and Sec. (4.3).

4.1 Axion-like particles

Axion-like particles (ALPs) represent a very interesting SM extension, where light pseudoscalar bosons arise naturally as pseudo-Nambu-Goldstone-Bosons of an underlying broken symmetry. These candidates are strongly motivated since they can give an answer to some of the open questions briefly described in Sec. (1.2) as, for example, the origin of dark matter and the hierarchy problem.
The most general Lagrangian describing the interactions of a spin zero particle Φ with leptons is

$$\mathcal{L}_{\Phi}^{\text{int.}} = \bar{\ell}_{iL}\left(C_R^{\Phi}\right)_{ij}\ell_{jR}\Phi + \bar{\ell}_{iR}\left(C_L^{\Phi}\right)_{ij}\ell_{jL}\Phi + h.c. \tag{4.1}$$

where C_R^{Φ} and C_L^{Φ} are off-diagonal matrices which induce LFV [48] and CP violating effects. Nevertheless, imposing both the flavor and CP conservation, i.e. requiring that $C_{L,R}^{ij} \propto \delta^{ij}$, it is possible to recover the standard and familiar expression

$$\mathcal{L}_{s,a}^{\text{int.}} = y_{sl}\bar{\ell}\ell s + y_{al}\bar{\ell}\gamma_5\ell a \tag{4.2}$$

with $s(a)$ a real scalar (pseudoscalar) particle, ℓ can be either e, μ and where it has been defined $y_{s\ell} = \text{Re}(C_R^s + C_L^s)_{\ell\ell}$ and $y_{a\ell} = \text{Im}(C_R^a - C_L^a)_{\ell\ell}$.
The TL contribution to the μe scattering differential cross section comes from a t channel exchange of both an a and a s particles due to $\mathcal{L}_{s,a}^{\text{int.}}$ [12]. The corresponding Feynman diagrams are simply

[12] Nonetheless, not imposing any constraint on flavor conservation would allow also LFV effects by means of t and s channel processes.

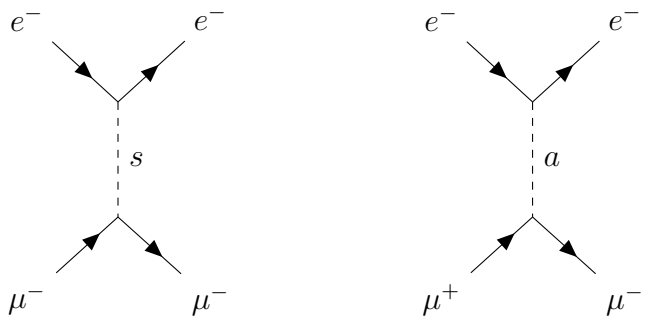

and the two related amplitudes read

$$\begin{aligned}\mathcal{M}_s &= -y_{se}y_{s\mu}\bar{u}(p_3)u(p_1)\frac{-i}{t-m_s^2}\bar{u}(p_4)u(p_2)\\ \mathcal{M}_a &= -y_{ae}y_{a\mu}\bar{u}(p_3)\gamma_5 u(p_1)\frac{-i}{t-m_a^2}\bar{u}(p_4)\gamma_5 u(p_2),\end{aligned} \tag{4.3}$$

providing a total amplitude

$$\mathcal{M} = \mathcal{M}_\gamma + \mathcal{M}_Z + \mathcal{M}_s + \mathcal{M}_a.$$

Then, the total unpolarized squared matrix element is

$$|\overline{\mathcal{M}}|^2 = |\overline{\mathcal{M}}_\gamma|^2 + \overline{\mathcal{M}}_{\gamma Z} + |\overline{\mathcal{M}}_s|^2 + \overline{\mathcal{M}}_{\gamma s} + |\overline{\mathcal{M}}_a|^2 \tag{4.4}$$

where the first two contributions (and also the absence of $|\bar{\mathcal{M}}_Z|^2$) have been already discussed in Sec. (3.2), while the other three terms are explicitly

$$\begin{aligned}|\overline{\mathcal{M}}_a|^2 &= \frac{t^2(y_{ae}y_{a\mu})^2}{(t-m_a^2)^2}\\ |\overline{\mathcal{M}}_s|^2 &= \frac{(y_{se}y_{s\mu})^2}{(t-m_s^2)^2}[(t-4M^2)(t-4m^2)]\\ \overline{\mathcal{M}}_{\gamma s} &= \frac{16\pi\alpha mM}{t}\frac{(y_{se}y_{s\mu})}{(t-m_s^2)}[t-2(M^2+m^2-s)].\end{aligned} \tag{4.5}$$

Actually in Eq. (4.4) there should be also $\overline{\mathcal{M}}_{\gamma a}$, $\overline{\mathcal{M}}_{sa}$, $\overline{\mathcal{M}}_{Zs(a)}$; nevertheless, the first two turn out to be exactly zero once computed the traces, while the other ones are highly suppressed by the presence of the factor $G_F mM g_{V(A)}^2$.
Finally, referring as usual to (A.1) for the reference formulas, the contribution to the differential cross section can be easily computed to be

$$\frac{d\sigma_{s,a}^{\pm}}{dt} = \frac{d\sigma_0}{dt}(1+\delta_{\rm LFC}^{\pm s}+\delta_{\rm LFC}^{\pm a}), \tag{4.6}$$

with

$$\begin{aligned}\delta_{\rm LFC}^{\pm s} = &\left(\frac{t}{8\pi\alpha}\right)^2\frac{(y_{se}y_{s\mu})^2}{(t-m_s^2)^2}\frac{(t-4m^2)\,(t-4M^2)}{f(s,t)}\\ &\pm\frac{y_{se}y_{s\mu}}{2\pi\alpha}\frac{mM}{(t-m_s^2)}\frac{(t^2-2t\,(m^2+M^2-s))}{f(s,t)}\end{aligned} \tag{4.7}$$

$$\delta_{\rm LFC}^{\pm a} = \left(\frac{t}{8\pi\alpha}\right)^2 \frac{(y_{ae}y_{a\mu})^2}{(t-m_a^2)^2}\frac{t^2}{f(s,t)}. \tag{4.8}$$

In order to understand whether these contributions can be detected at MUonE it is firstly necessary to have some upper bound for $y_{\Phi e}$ and $y_{\Phi\mu}$ (with $\Phi = s, a$). The most stringent constraint on the former comes from the electron $g-2$ and it can be found once calculated the contribution to the anomaly a_e coming from $\mathcal{L}_\Phi^{\rm int}$ (in the limit $m \ll m_\Phi$) and imposed the experimental bound $|\Delta a_e| < 10^{-12}$; it reads[13]

$$|y_{\Phi e}| \lesssim 5\times 10^{-4}\left(\frac{m_\Phi}{0.1\ \text{GeV}}\right). \tag{4.9}$$

Proceeding in a similar way, by means of the experimental value of the muonic $g-2$ and other low energy experimental constraints [53], it follows

$$|y_{\Phi\mu}| \lesssim 2\times 10^{-3} \tag{4.10}$$

for values of m_Φ smaller than a few GeV. The combination of these two bounds leads to $y_{\Phi e}y_{\Phi\mu} \leq 10^{-6}(m_\Phi/0.1\ \text{GeV})$, constraining $\delta_{\rm LFC}^\Phi \sim 10^{-7}$ and, so, not detectable at MUonE. Although the TL turned out to be not visible, it is important to underline the fact that it could not be the dominant contribution. This can happen if one of the two couplings $y_{\Phi\ell}$ is so small that it approaches zero; in this case, the leading contribution would be some one loop-induced vertex corrections.

At low energies, the general form of (4.2) for the description of ALP interactions with fermions and photons, up to dimension-5 operators, is

$$\mathcal{L}_{\rm ALP} = \frac{1}{2}\partial_\mu\Phi\partial^\mu\Phi - \frac{1}{2}m_\Phi^2\Phi^2 + \frac{e^2c_{\gamma\gamma}}{\Lambda}\Phi F_{\mu\nu}\tilde{F}^{\mu\nu} - \frac{\partial_\mu\Phi}{\Lambda}\sum_{\psi,i,j}\bar{\psi}_i\gamma^\mu(v_{ij}-a_{ij}\gamma_5)\psi_j \tag{4.11}$$

where Λ stands for the EFT cutoff, $\tilde{F}^{\mu\nu} = 1/2\epsilon^{\mu\nu\rho\sigma}F_{\rho\sigma}$ is the dual field strength tensor and the matrices v^{ij}, a^{ij} are hermitian and real. The interaction of the scalar field with fermions in this new Lagrangian, however, can still be brought back to that of (4.2) by means of the equation of motions. Indeed, the integration by part of this term lead to

$$\begin{aligned}
&-\frac{\partial_\mu\Phi}{\Lambda}\bar{\psi}_i\gamma^\mu(v_{ij}-a_{ij}\gamma_5)\psi_j \overset{\text{I.B.P.}}{=} +\frac{\Phi}{\Lambda}\partial_\mu\Big[\bar{\psi}_i\gamma^\mu(v_{ij}-a_{ij}\gamma_5)\psi_j\Big] + \text{total derivative} = \\
&= \frac{\Phi}{\Lambda}\Big[\bar{\psi}_i\overleftarrow{\partial\!\!\!/}(v_{ij}-a_{ij}\gamma_5)\psi_j + \bar{\psi}_i(v_{ij}+a_{ij}\gamma_5)\partial\!\!\!/\psi_j\Big] = -i\frac{\Phi}{\Lambda}\Big[(m_j-m_i)v_{ij} + (m_j+m_i)a_{ij}\gamma_5\Big],
\end{aligned} \tag{4.12}$$

where in the last passage it has been exploited the Dirac equation, while the total derivative has been neglected since the fields vanish at infinity; moreover, notice that the "old" couplings $y_{s\ell}$ and $y_{a\ell}$ are the equivalent (but not the same) of the "new" ones $-v_{ii}/\Lambda$ and $-a_{ii}/\Lambda$.

The Feynman rules for the two new interactions are

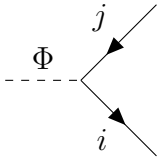

$$= \frac{1}{\Lambda}\Big[(m_j-m_i)v_{ij} + (m_j+m_i)a_{ij}\gamma_5\Big].$$

[13]For the explicit expression of the ALP contribution to the anomaly of a given fermion ψ_i see (4.25).

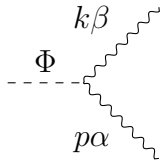

$$= -\frac{4ie^2}{\Lambda} c_{\gamma\gamma} p^\mu k^\nu \epsilon_{\mu\alpha\nu\beta}$$

However, since we are working in the LFC scenario, the condition $i = j$ must be always satisfied; this fact modifies the second Feynman rules, which now become simply $(2m/\Lambda)a_{ii}\gamma_5$. The relevant diagrams are

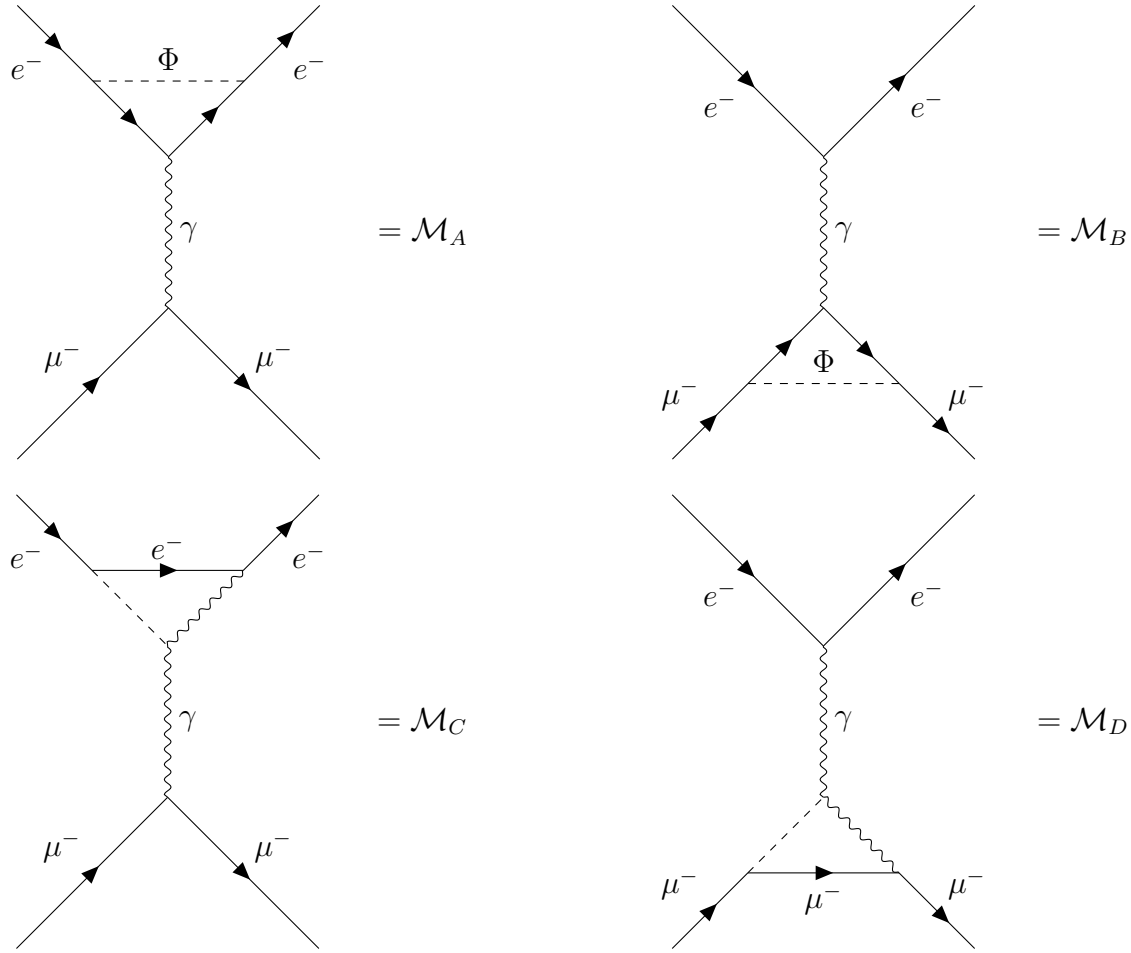

$= \mathcal{M}_A$

$= \mathcal{M}_B$

$= \mathcal{M}_C$

$= \mathcal{M}_D$

In the following I will assume that the very small coupling which tends to zero is a_{ee} and so it will be reported explicitly the results for $\mathcal{M}_B$ and $\mathcal{M}_D$; an analogous analysis can be brought on considering the opposite case, where the amplitudes $\mathcal{M}_A$ and $\mathcal{M}_C$ can be, respectively, recovered substituting $M \to m$. Focusing only on the part of the diagrams with the loop-vertex functions, which has, then, an uncontracted index[14], the amplitudes can be generally Lorentz-decomposed as

$$i\mathcal{M}^\rho = ie\bar{u}(p-q)\Sigma^\rho(q^2)u(p), \tag{4.13}$$

with

$$\Sigma^\rho_{ii}(q^2) = \left[\gamma_\sigma \mathcal{F}_1^{ii}\left(q^2\right)\left(g^{\rho\sigma} - \frac{q^\rho q^\sigma}{q^2}\right) + \frac{i\sigma^{\rho\sigma}q_\sigma}{2M}\mathcal{F}_2^{ii}\left(q^2\right)\right], \tag{4.14}$$

[14]Let's notice that it has been implicitly used the notation $\mathcal{M} = ie\bar{u}(p_4)\gamma_\rho u(p_2)\mathcal{M}^{\nabla\langle\iota}$.

where the explicit expressions of the two form factors $\mathcal{F}_{1,2}(q^2)$ depend on the fact that we are dealing with the linear ($\propto a$) or the quadratic ($\propto a^2$) contribution. The computation of the loop diagrams with *Mathematica* and *Package-X* leads to the expressions

$$\mathcal{F}_{1\,\mu\mu}^{\text{quad}}(q^2) = \frac{a_{\mu\mu}^2 M^2}{4\pi^2\Lambda^2}\Big[B_0(q^2;M,M) + \frac{A_0(m_\Phi) - A_0(M)}{M^2} + m_\Phi^2 C_0(M^2,q^2,M^2;m_\Phi,M,M) + \\ + 2C_{00}(M^2,M^2,q^2;m_\Phi,M,M) - 2M^2 C_{11}(M^2,M^2,q^2;m_\Phi,M,M)\Big] \tag{4.15}$$

$$\mathcal{F}_{2\,\mu\mu}^{\text{quad}}(q^2) = \frac{a_{\mu\mu}^2 M^3}{4\pi^2\Lambda^2}\Big[C_{22}(M^2,q^2,M^2;m_\Phi,M,M) + 2C_{12}(M^2,q^2,M^2;m_\Phi,M,M) + \\ + C_{11}(M^2,q^2,M^2;m_\Phi,M,M)\Big] \tag{4.16}$$

for the quadratic term and

$$\mathcal{F}_{1\,\mu\mu}^{\text{lin}}(q^2) = -q^2\frac{e^2 c_{\gamma\gamma} a_{\mu\mu} M^2}{4\pi^2\Lambda^2}\Big[C_{11}(M^2,M^2,q^2;0,M,m_\Phi) + C_{11}(M^2,M^2,q^2;m_\Phi,M,0)\Big] \tag{4.17}$$

$$\mathcal{F}_{2\,\mu\mu}^{\text{lin}}(q^2) = -\frac{e^2 c_{\gamma\gamma} a_{\mu\mu} M^2}{2\pi^2\Lambda^2}\Big[2C_{00}(M^2,M^2,q^2;m_\Phi,M,M) + M^2 C_{11}(M^2,q^2,M^2;m_\Phi,M,M) + \\ + 2C_{00}(M^2,M^2,q^2;m_\Phi,M,0) + M^2 C_{11}(M^2,M^2,q^2;m_\Phi,M,0)\Big] \tag{4.18}$$

for the linear one, where the results have been left in term of the Passarino-Veltman (PAVE) functions. In the explicit form of $\mathcal{F}_{1,2\,\mu\mu}^{\text{lin}}$, the functions C_{00} and C_{11} appear two times, but they depend on different sets: this is a consequence of the fact that there is also another diagram which should be considered, which is similar to the fourth one but with the exchange of the photon and the scalar in the loop.
One can also compute the 1-loop corrections to the two diagrams with amplitudes (4.3) in which the mediator is the ALP; however, without making any calculation, it is easy to understand that these kind of contributions would be very small and, indeed, applying the previous bounds they turn out to lie far beyond the sensitivity of MUonE. Indeed, going back to the previous notation, the typical amplitude would be $\mathcal{M}_\Phi^{\text{1-loop}} \propto y_{\Phi\ell}^2 \mathcal{M}_\Phi$, where Φ can be either s, a.
The total amplitudes would, then, be[15]

$$\mathcal{M}_B = ie\mathcal{M}_B^\rho \bar{u}(p_3)\gamma_\rho u(p_1) = \frac{\alpha a^2 M^2}{\pi\Lambda^2} P \tag{4.19}$$

$$\mathcal{M}_D = ie\mathcal{M}_D^\rho \bar{u}(p_3)\gamma_\rho u(p_1) = \frac{4\alpha^2 c_{\gamma\gamma} a M^2}{\Lambda^2} L \tag{4.20}$$

where in P and L are contained the spinorial structures and the explicit expressions of the PAVE functions. Now it is possible to compute the shift δ_{ALP} which is induced in the SM differential cross section by these diagrams. Since all of them can be parametrized

[15]For sake of convention, from now on it will be aadopted $a_{\mu\mu} = a$

by (4.13), the computation can be performed only one time and, then, depending on the contribution we want to analyze the proper form factors will be employed. The only relevant "product of diagrams" is that with the SM one mediated by the photon [16], i.e. it is necessary to compute

$$\bar{\mathcal{M}}_{\text{int}} = \frac{1}{4} 2\,\text{Re} \sum_{spin} \mathcal{M}_{\gamma}^{*} \mathcal{M} \tag{4.21}$$

which, after the computation of the traces and the differential cross section through the formulas in (A.1), provides

$$\delta_{\text{ALP}} = 2\mathcal{F}_1. \tag{4.22}$$

In order to understand whether these contributions can be detectable at MUonE it is necessary, as usual, to check if there are allowed values of a and m_Φ (from experimental bounds on other observables) for which $\delta_{\text{ALP}} \sim 10^{-5}$.
First of all, the evaluation of the PAVEs contained in the squared bracket of Eqs. (4.19) and (4.20), respectively denoted as S_{quad} and S_{lin}, as a function of the ALP's mass and t provides the interesting plots

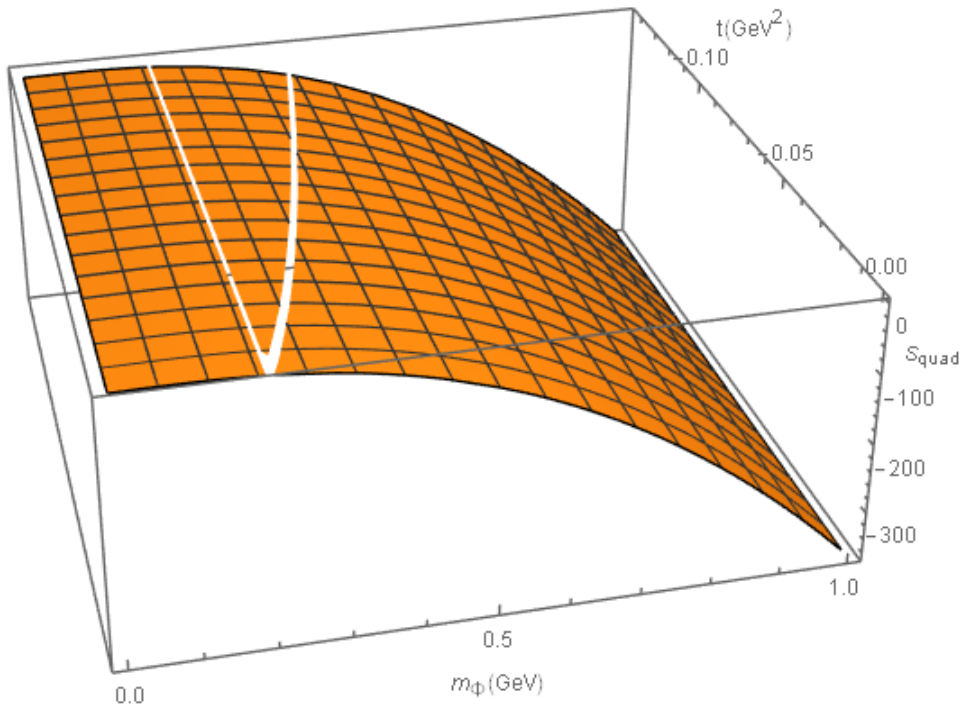

Figure 4.1: Dependence of P on t and the ALP's mass. The "cut" in the graph is a consequence of particular combinations of the couple (t, m_Φ) for which the PAVE functions are not defined; consequently, they are forbidden.

[16] Let's remember that in this regime of energies the weak contribution is suppressed by the presence of G_F.

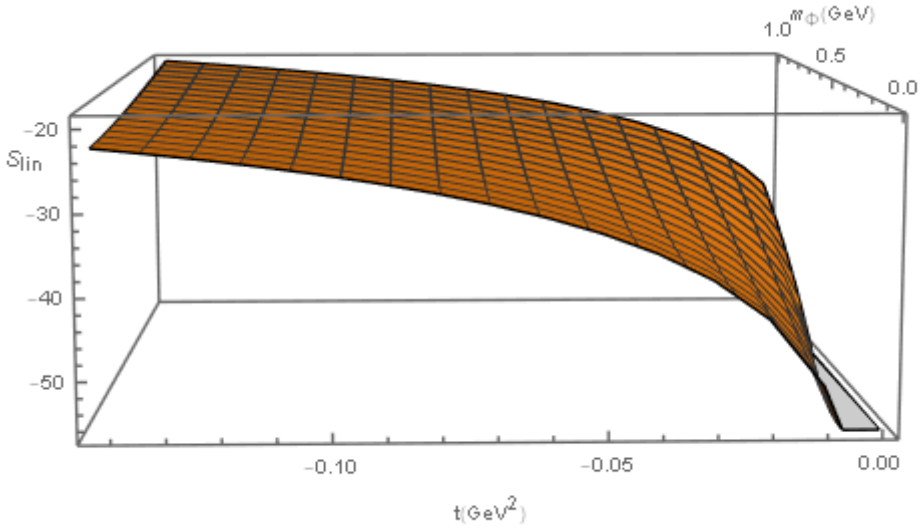

Figure 4.2: Dependence of L on t and the ALP's mass.

In Fig. (4.1) it is possible to note that, for a given value of the ALP's mass in the range $m_\Phi \in [0, 1]$ GeV, the value of P is left unaffected by that of $t \in [-0.143, 0]\,\text{GeV}^2$; in addition roughly speaking $|P| \in [0, 10^2]$. Similar conclusions hold also for Fig. (4.2), where $|L| \sim 10^{-1}$.
From these two plots, then, it is clear that loop induced vertex functions allowed by ALPs can be detected at MUonE if and only if the conditions

$$\frac{\alpha a^2 M^2}{\pi \Lambda^2} \gtrsim 10^{-7} \tag{4.23}$$

for the quadratic contribution and

$$\frac{4\alpha^2 c_{\gamma\gamma} a M^2}{\Lambda^2} \gtrsim 10^{-6} \tag{4.24}$$

for the linear one are satisfied.
At this point, however, the couplings a and $c_{\gamma\gamma}$ can still take whatever value, always under the conditions of perturbativity and unitariry; for this reason, the first step to understand whether the requirements (4.23) and (4.24) are satisfied consists in constraining them by means of the experimental measures of some other observables. The most suitable one in the LFC scenario is, probably, the lepton anomaly Δa_{ℓ_i}: the idea is simply to constrain the two couplings requiring that the contributions to this anomaly coming from the Lagrangian (4.11) are within the experimental bounds.
First of all, from the computations of the loop induced diagrams already performed, the contribution to the lepton anomaly for a given flavor i is

$$(\Delta a_{\ell_i}) = -\frac{m_{\ell_i}^2}{16\pi^2\Lambda^2}\left[64\pi\alpha_{\text{em}} c_{\gamma\gamma} a_{ii}\left(\log\frac{\Lambda^2}{m_{\ell_i}^2} - h_2(x_i)\right) + 4\,|a_{ii}|^2\, h_1(x_i)\right] \tag{4.25}$$

where, given $x_i = (m_\Phi/m_i)^2$,

$$h_1(x) = 1 + 2x - (x-1)x\log x + 2x(x-3)\sqrt{\frac{x}{x-4}}\log\left(\frac{\sqrt{x}+\sqrt{x-4}}{2}\right) \tag{4.26}$$

$$h_2(x) = 1 + \frac{x^2}{6}\log x - \frac{x}{3} - \frac{x+2}{3}\sqrt{(x-4)x}\log\left(\frac{\sqrt{x}+\sqrt{x-4}}{2}\right). \tag{4.27}$$

Now, since we are dealing with $a = a_{\mu\mu}$, the bound $|\Delta a_\mu| \lesssim 10^{-9}$ must be employed. For the reference maximum value $m_\Phi = 1$ GeV, barring accidental cancellations, this requirement applied to the quadratic contribution leads to

$$a \lesssim 10\left(\frac{\Lambda}{1\text{ TeV}}\right) \tag{4.28}$$

which, once applied to the linear one, implies

$$c_{\gamma\gamma} \lesssim 10\left(\frac{\Lambda}{1\text{ TeV}}\right). \tag{4.29}$$

For a little bit smaller ALP's mass, $m_\Phi = 10^{-1}$ and $m_\Phi = 10^{-2}$, the bounds are similar and they read

$$a \lesssim 1\left(\frac{\Lambda}{1\text{ TeV}}\right) \tag{4.30}$$

which, once applied to the linear one, implies

$$c_{\gamma\gamma} \lesssim 1\left(\frac{\Lambda}{1\text{ TeV}}\right). \tag{4.31}$$

It is easy to check that even if the couplings take the highest possible values allowed by these bounds, both (4.23) and (4.24) cannot be satisfied, implying that also these kind of contributions are not visible at MUonE. Some summary plots of the dependence of the two form factors $\mathcal{F}_1$ on the mass m_Φ and the parameters a or $c_{\gamma\gamma}$ are the following:

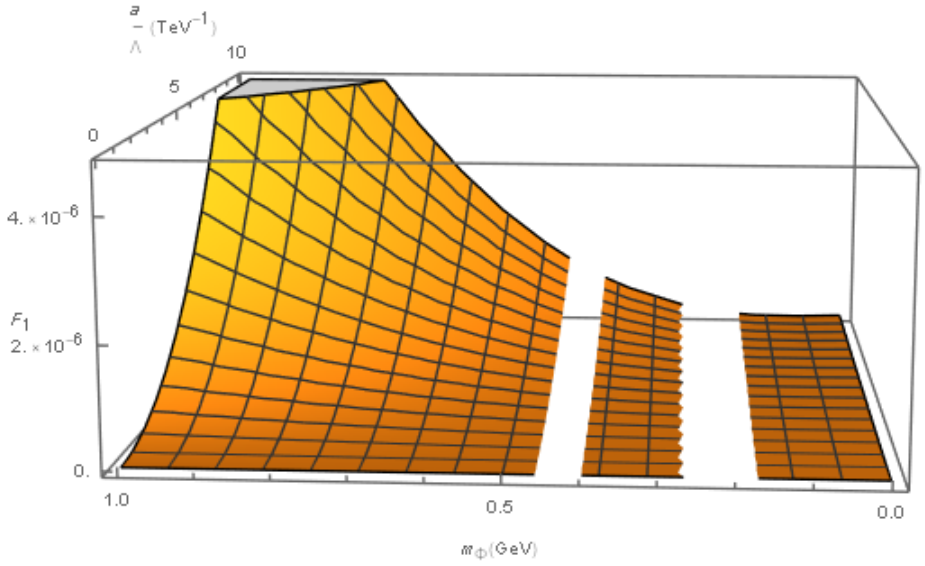

Figure 4.3: Dependence of the quadratic form factor $\mathcal{F}_1$ on the couple of parameters (a, m_Φ) in the range of interest for $t = -0.1$ Gev^2. As mentioned above, even saturating Eq. (4.28), $\delta_{\text{ALP}} = 2\mathcal{F}1 < 10^{-5}$. As for Fig. (4.1), the two white regions represent the couples of values (a, m_Φ) which are forbidden.

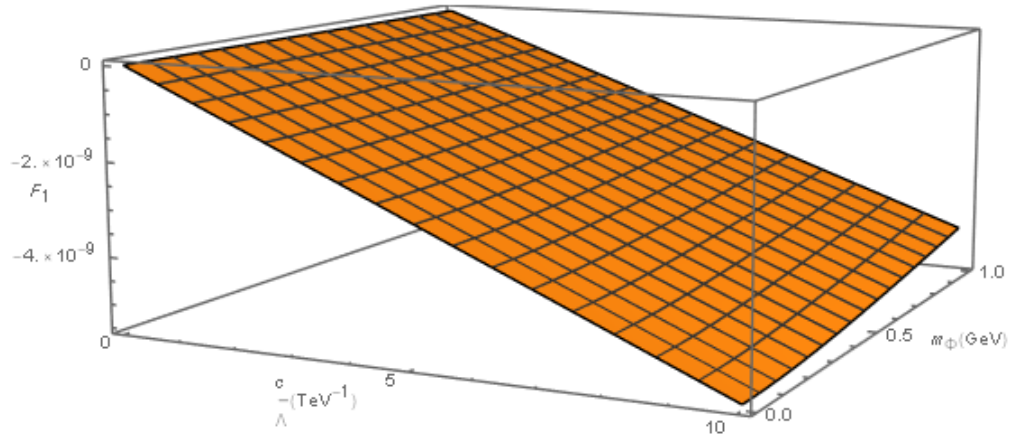

Figure 4.4: Dependence of the linear form factor $\mathcal{F}_1$ on the couple of parameters $(c_{\gamma\gamma}, m_\Phi)$ in the range of interest, with $t = -0.1$ Gev^2. Here the linear coupling a has been chosen as the maximum one according to the bound (4.28) but, as aforementioned, even saturating also Eq. (4.29), $\delta_{\text{ALP}} = 2\mathcal{F}1 < 10^{-5}$.

This analysis in the LFC context has been performed quite generally, assuming reasonable values for couplings and masses when needed. Similar conclusions can be reached also in the other case, where it is $y_{\Phi\mu}$ to tend to zero; as aforementioned the computations are the same, except for the substitution $M \to m$ and the fact that the $a = a_{ee}$ coupling should be constrained through the electron anomaly $|\Delta a_e| \lesssim 10^{-12}$.
An extension of this discussion can be found in [51], where it has been taken into account the possibility of LFV using $i \neq j$; it is possible to show that, taking the case $i = j$ from those general results, one recovers the expression (4.15) and (4.17), which have been found independently. Nevertheless, in this scenario an interesting discussion can be already carried out at the tree level; this will be done in a while, after a couple of comments.
In addition to the previous consistency check, it is possible to verify that the gauge invariance of the theory is still valid. In order to test this problem, it is firstly necessary to study the process $\ell_i \to \ell_i + \gamma$, where the photon is *on-shell* and satisfies $q^2 = 0$. The one-loop diagrams induced by ALPs are

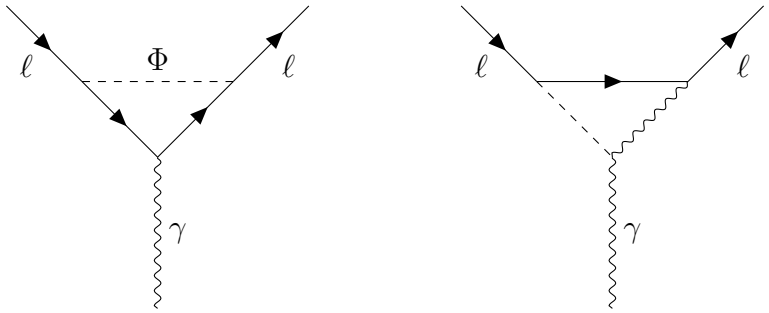

(4.32)

and, again, both the amplitudes can be generally Lorentz decomposed as

$$i\mathcal{M}^\rho\left(\ell_i \to \ell_i\gamma\right) = ie\bar{u}_i(p-q)\Sigma^\rho_{ii}(0)u_i(p), \tag{4.33}$$

where

$$\Sigma^\rho_{ii}(0) = \frac{i\sigma^{\rho\sigma}q_\sigma}{m_{\ell_i}}\mathcal{F}_{2\,ii}(0). \tag{4.34}$$

Therefore, a good check consists in verifying that in the limit $q^2 \to 0$ both the $\mathcal{F}_1(0) = 0$ and the two $\mathcal{F}_2(0)$ match with the corresponding form factors of this process. It is very easy to see that in this limit (4.17) satisfies immediately this condition, having factorised a q^2 factor; on the other side, the remaining three form factors requires the employment of numerical tools, being necessary to exploit all the PAVE functions; replacing the muon mass M with that of a generic lepton m_{ℓ_i}, by means of *Mathematica* it has been verified that also (4.15) vanishes in this limit, while the two $\mathcal{F}_2$ acquire the structure

$$\mathcal{F}_{2\,ii}^{\text{lin}}(0) = -\frac{\alpha m_{\ell_i}^2 a_{ii} c_{\gamma\gamma}}{2\pi\Lambda^2}\left[2\ln\left(\frac{\Lambda^2}{m_\Phi^2}\right) - \frac{\log x_i}{x_i - 1} - (x_i - 1)\log\left(\frac{x_i}{x_i - 1}\right) - 2\right] \tag{4.35}$$

$$\mathcal{F}_{2\,ii}^{\text{quad}}(0) = -\frac{m_{\ell_i}^2 a_{ii}^2}{16\pi^2\Lambda^2}\left[2x_i - 3 + (x_i^2 - 3x_i)\log x_i + 2x_i^{3/2}\sqrt{(x_i - 4)}\log\left(\frac{\sqrt{x_i} + \sqrt{x_i - 4}}{2}\right)\right] \tag{4.36}$$

which is precisely what we would get studying directly the decay $\ell_i \to \ell_j + \gamma$.
Lastly, it is possible to make another important remark in relation to the form factors, specifically on the two $\mathcal{F}_1(q^2)$. Indeed, if we are in the interesting regime $m_\Phi^2 \gg M^2 \gg q^2$, these two functions can be expanded around $q^2 = 0$ as

$$\mathcal{F}_1(q^2) = q^2\dot{\mathcal{F}}_1(0) + \mathcal{O}(q^4), \tag{4.37}$$

where $\dot{\mathcal{F}} \equiv \frac{d\mathcal{F}}{dq^2}$. Once again these computations are lengthy if performed by hand and they require a numerical resolution. Thanks the use of *Mathematica* and *Pakage-X* it has been possible to easily Taylor-expand around $q^2 = 0$ both the form factors, whose expressions read

$$\begin{aligned}\dot{\mathcal{F}}_1^{\text{lin}}(0) = \frac{a c_{\gamma\gamma}\alpha}{6\pi\Lambda^2}\Bigg[&6x^2\text{Li}_2\left(\frac{x-1}{x}\right) - \pi^2x^2 + 3\,(x+1) + 3\,(x-1)\,x\log\frac{x}{x-1} + \\ &+3x\frac{2x-1}{x-1}\log x\Bigg]\end{aligned} \tag{4.38}$$

$$\begin{aligned}\dot{\mathcal{F}}_2^{\text{quad}}(0) = -\frac{a^2}{16\pi^2\Lambda^2}\Bigg[&\frac{7x-48}{3} + \left(\frac{7}{3} - 4x + \frac{7x^2}{6}\right)\log x + \\ &+\frac{(3x-5)\sqrt{x(x-4)}}{2}\log\left(\frac{\sqrt{x} + \sqrt{x-4}}{2}\right)\Bigg],\end{aligned} \tag{4.39}$$

where $x = (m_\Phi/M)^2$ and $\text{Li}_2(z)$ is the Dilogarithm function defined as

$$\text{Li}_2(z) = \sum_{k=1}^{\infty}\frac{z^k}{k^2};\ |z| < 1.$$

Finally we can turn the attention on the LFV scenario; relaxing the hypothesis of lepton flavor conservation, the diagrams which would affect the μe scattering are

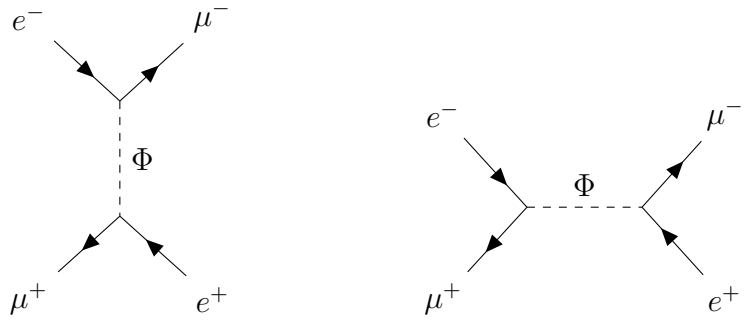

with amplitudes

$$\begin{aligned}\mathcal{M}^{\mathrm{t}}_{\mathrm{LFV}} &= \frac{C_X^{ij}C_{X'}^{ji}}{t-m_\Phi^2}\bar{u}(p_3)_i P u(p_1)_j \bar{v}(p_4)_j Q v(p_2)_i \\ \mathcal{M}^{\mathrm{s}}_{\mathrm{LFV}} &= \frac{C_X^{ij}C_{X'}^{ji}}{s-m_\Phi^2}\bar{u}(p_3)_i P v(p_4)_j \bar{v}(p_2)_j Q u(p_1)_i\end{aligned} \tag{4.40}$$

where $i,j=1,2$, $X,X^{'}=L,R$ and P,Q could be either $(1\pm\gamma_5)$. The computation of the two squared amplitudes $\left|\mathcal{M}^{\mathrm{s,t}}_{\mathrm{LFV}}\right|^2$ is very similar to that performed in (3.64); indeed they bring to the μe differential cross section the two NP contributions

$$\begin{aligned}\delta^{\mathrm{t}}_{\mathrm{LFV}} &= \left(\frac{tC_XC_{X'}}{8\pi\alpha(t-m_\Phi^2)}\right)^2\frac{m^2M^2}{f(s,t)} \\ \delta^{\mathrm{s}}_{\mathrm{LFV}} &= \left(\frac{tC_XC_{X'}}{8\pi\alpha(s-m_\Phi^2)}\right)^2\frac{m^2M^2}{f(s,t)}.\end{aligned} \tag{4.41}$$

A quick check with the bound imposed by the experimental value for the muonium-antimuonium oscillation probability leads to $|C_X^{ij}| \lesssim 10^{-4}(m_\Phi/0.1\,\mathrm{GeV})$, which makes (4.41) several orders of magnitude below MUonE resolution.
On the other side, the computation of the interference term strongly depends on the signs of the γ_5 in its (unique) trace. Depending on these factors, the trace can still be $64m^2M^2$ (as happens for the two contributions which give rise to (4.41)) or both $\sim 16m^2t$ and $\sim 16M^2t$; in each case, however, imposing the aforementioned bound for the C_X coefficients, it is simple to see that also the interference term lies several orders of magnitude below the sensitivity of MUonE.
Let's notice that in this discussion it has been implicitly assumed to work at energies different respect to the mass of the mediator; indeed, taking exactly the value $\sqrt{s}=m_\Phi$ all the amplitudes would diverge and, in order to avoid this issue, the loop treatment should be employed, leading to an additive factor $(i\Gamma_\Phi m_\Phi$, where Γ_Φ is the decay rate of the spin-zero field) in the denominator of the propagator. It is easy to take into account this improvement in the theoretical prediction and it can be done avoiding computations from the beginning; the results, however, is again the same, as shown in [52][17].

[17]Let's note that in this reference it has been used a different notation, based on quantities computed in (2.2.1).

4.2 Dark Photon

Another well motivated extension of the SM is the so called Dark Photon (DP) scenario, which consists in adding an extra $U(1)$ gauge group that mixes with the SM electromagnetic one. The Lagrangian needed to describe such an extension is

$$\mathcal{L}_{DP} = -\frac{1}{4}V_{\mu\nu}V^{\mu\nu} + \frac{1}{2}m_{\mathrm{DP}}^2 V_\mu V^\mu + e\epsilon J^\mu_{em} V_\mu, \tag{4.42}$$

where V_μ and $V_{\mu\nu}$ are, respectively, the DP and the corresponding field strength, ϵ is a dimensionless parameter which takes into account for the kinetic mixing and m_{DP} is the DP mass. The TL contribution to the μe differential cross section due to Eq. (4.42) is very simple to calculate and its corresponding diagram and amplitude read

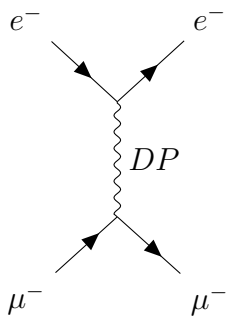

$$\mathcal{M}_{\mathrm{DP}} = e^2\epsilon^2\bar{u}(p_3)\gamma^\mu u(p_1)\frac{i(g_{\mu\nu} - \frac{k_\mu k_\nu}{m^2_{\mathrm{DP}}})}{t - m^2_{\mathrm{DP}}}\bar{u}(p_4)\gamma^\nu u(p_2) = \frac{ie^2\epsilon^2}{t - m^2_{\mathrm{DP}}}\bar{u}(p_3)\gamma^\mu u(p_1)\bar{u}(p_4)\gamma_\mu u(p_2), \tag{4.43}$$

where it has been used the facts that $k = p_1 - p_3 = p_2 - p_4$ and that the Dirac equation in the momentum space can be used either as $\not{p}u(p) = mu(p)$ and $\bar{u}(p)\not{p} = -m\bar{u}(p)$, implying:

$$\bar{u}(p_3)\gamma^\mu u(p_1)k_\mu k_\nu \bar{u}(p_4)\gamma^\nu u(p_2) = \bar{u}(p_3)(\not{p}_1 - \not{p}_3)u(p_1)\bar{u}(p_4)(\not{p}_2 - \not{p}_4)u(p_2) = 0. \tag{4.44}$$

In this scenario, then, the total unpolarized squared matrix element is

$$|\overline{\mathcal{M}}|^2 = |\overline{\mathcal{M}}_{\mathrm{DP}}|^2 + \overline{\mathcal{M}}_{\gamma\mathrm{DP}} \approx \overline{\mathcal{M}}_{\gamma\mathrm{DP}} \tag{4.45}$$

where the pure DP contribution can be safely neglected, having a ϵ^4 dependence; indeed, taking into account the fact that for DP in this range of masses it holds the experimental limit $\epsilon^2 \lesssim 2 \times 10^{-7}$ [54,55], this contribution is not visible at MUonE.
Computing the traces, Eq. (4.45) becomes explicitly

$$\overline{\mathcal{M}}_{\gamma\mathrm{DP}} = \frac{128\pi^2\alpha^2\epsilon^2 f(s,t)}{t(t - m^2_{\mathrm{DP}})}$$

leading to

$$\frac{d\sigma^\pm_{\mathrm{DP}}}{dt} = \frac{d\sigma_0}{dt}\delta^\pm_{\mathrm{DP}}, \tag{4.46}$$

with

$$\delta^\pm_{\mathrm{DP}} = \frac{2\epsilon^2 t}{t - m^2_{\mathrm{DP}}}. \tag{4.47}$$

Imposing the previous bound on the parameter ϵ it follows that $\delta_{\rm DP} \lesssim 4 \times 10^{-7}$ and, then, as it can be seen by Fig.(4.5) it is not visible at MUonE

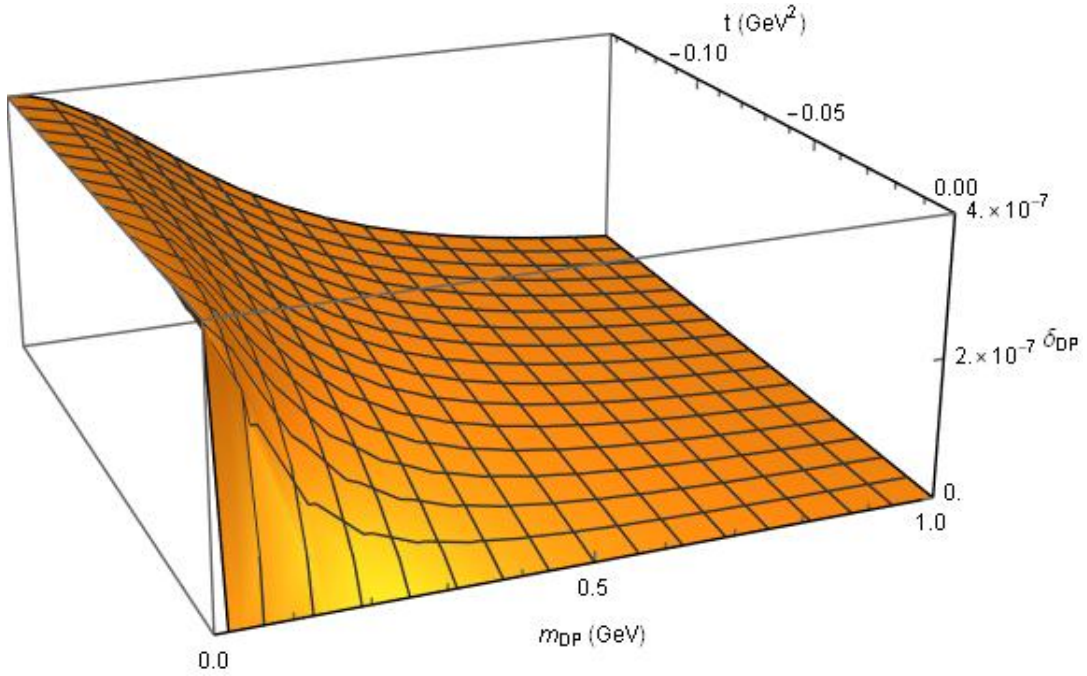

Figure 4.5: This plot shows how $\delta_{\rm DP}$ changes varying both t and $m_{\rm DP}$, once selected the upper bound $\epsilon = 2 \times 10^{-7}$. This contribution never reach the sensibility of MUonE and, in particular, in the limit $m^2_{\rm DP} \ll t$ it tends to the constant value $\delta_{\rm DP} = 4 \times 10^{-4}$.

4.3 Z' vector bosons

Models with an underlying $U(1)$ symmetry allow also direct couplings of SM particles with a new vector boson

$$\mathcal{L}_{Z'} = -\frac{1}{4} Z'_{\mu\nu} Z'^{\mu\nu} + \frac{1}{2} m^2_{Z'} Z'_\mu Z'^\mu + \bar{\ell}\gamma^\mu (g^\ell_V + g^\ell_A \gamma_5) \ell Z'_\mu, \tag{4.48}$$

where $g^\ell_{(A)V}$ are the (axial) vector coupling of leptons to the Z' [18].
Once again, the relevant and leading contribution to the μe differential cross section comes from the interference with the photon one of the SM. In particular, that due to Eq. (4.48) is

$$\mathcal{M}_{Z'} = i\bar{u}(p_3)\gamma^\mu (g^e_V + g^e_A\gamma_5) u(p_1) \frac{(\eta_{\mu\nu} - \frac{k_\mu k_\nu}{m^2_{Z'}})}{t - m^2_{Z'}} \bar{u}(p_4)\gamma^\nu (g^\mu_V + g^\mu_A \gamma_5) u(p_2)$$

which, again, can be simplified a lot exploiting the properties of the Dirac equation and the conservation of the four momenta, as for the DP scenario; nevertheless, while in the previous case the term $k_\mu k_\nu / m^2_{Z'}$ became null, here it provides a term suppressed by $\sim 4m^2/m^2_{Z'}$ which can be, however, safely neglected, leading to

$$\mathcal{M}_{Z'} = \frac{i}{t - m^2_{Z'}} \bar{u}(p_3)\gamma^\mu (g^e_V + g^e_A\gamma_5) u(p_1) \bar{u}(p_4)\gamma^\nu (g^\mu_V + g^\mu_A \gamma_5) u(p_2). \tag{4.49}$$

[18] These couplings should be not confused with those involved in the neutral weak current J_Z; nevertheless I will carry on this handler notation always omitting the superscript $'$, unless differently stated.

The total unpolarized squared matrix element is, then,

$$|\overline{\mathcal{M}}|^2 \approx \overline{\mathcal{M}}_{\gamma Z'} = \frac{32\pi\alpha}{t(t-m_{Z'}^2)}\left[g_V^e g_V^\mu f(s,t) + g_A^e g_A^\mu t(u-s)\right]$$

and exploiting the relations in (A.1), once defined $z^+ = s$ and $z^- = u$, leads to the final result

$$\frac{d\sigma^\pm}{dt} = \frac{d\sigma_0}{dt}\delta_{Z'}^\pm, \tag{4.50}$$

with

$$\delta_{Z'}^\pm = \frac{t}{2\pi\alpha\,(t-m_{Z'}^2)}\left[g_V^e g_V^\mu + g_A^e g_A^\mu \frac{t\,(z^\pm - z^\mp)}{2f(s,t)}\right]. \tag{4.51}$$

The most stringent bounds on the vector couplings $g_V^e g_V^\mu$ comes from the searches of light vector bosons in the process $e^+e^- \to \gamma Z' \to \ell^+\ell^-\gamma$ at BaBar [56] and KLOE [57]; actually these analyses were performed in the DP context but with a good approximation they can be still employed in this framework [19]. For the mass range $0.2 \leq m_{Z'} \leq 10$ GeV the experimental bounds provide the constraint $g_V^e g_V^\mu \lesssim 10^{-7}$, while under the dimuon mass threshold, in particular for $0.02 \leq m_{Z'} \leq 0.2$ GeV, only the electron vector coupling can be constrained, with $(g_V^e)^2 \lesssim 10^{-7}$ [56]. Focusing on the first mass range, it follows immediately that the shift induced by purely vector couplings satisfies

$$\delta_{Z'}^\pm \lesssim \mathcal{O}(10^{-6}) \tag{4.52}$$

so that it is not visible at MUonE.
Other constraints on these vector couplings and new bounds on the axial ones can be set by the leptonic $g-2$.
Let's see how to recover them. Firstly let's take the general interaction

$$\mathcal{L}_{\text{int}} = \sum_{F,X} \bar{\mu}\left[g_{\text{V}}\gamma^\mu + g_{\text{A}}\gamma^\mu\gamma^5\right] F X_\mu, \tag{4.53}$$

where the sum runs over all the possible fermions F and gauge bosons X; then, the contributions to the muonic anomalous magnetic moment are

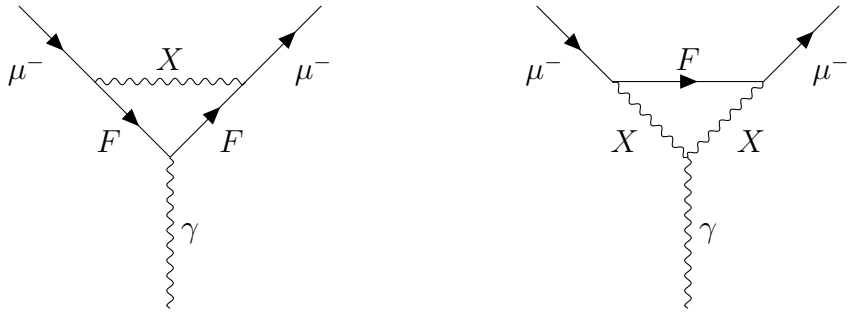

[19] In particular, the bounds for the product $g_V^e g_V^\mu$ can be identified with those of the $L_\mu - L_e$ model of [54].

whose analytical expressions [58] read[20]

$$[a_\mu]_{\rm a} = -\frac{q_{\rm F} m_\mu^2}{4\pi^2}\int_0^1 {\rm d}x \left[g_{\rm V}^2 \left\{ \left(x - x^2\right)\left(x + \frac{2m_{\rm F}}{m_\mu} - 2\right) - \frac{1}{2M_{\rm X}^2}\left(x^3\left(m_{\rm F} - m_\mu\right)^2 \right.\right.\right.$$
$$\left.\left.\left. + x^2\left(m_{\rm F}^2 - m_\mu^2\right)\left(1 - \frac{m_{\rm F}}{m_\mu}\right)\right\} + g_{\rm A}^2\left\{m_{\rm F} \to -m_{\rm F}\right\}\right]\left\{m_\mu^2 x^2 + M_{\rm X}^2(1-x) + x\left(m_{\rm F}^2 - m_\mu^2\right)\right\}^{-1} \tag{4.54}$$

$$[a_\mu]_b = \frac{q_X m_\mu^2}{8\pi^2}\int_0^1 dx \left[g_V^2 \left\{ \frac{4m_F}{m_\mu}x^2 - 2x^2(1+x) + \frac{m_\mu^2}{M_X^2}\left[-x^2(x-1) + \right.\right.\right.$$
$$\left.\left.\left. - \frac{m_F}{m_\mu}\left(-2x^3 + 3x^2 - x\right) - \frac{m_F^2}{m_\mu^2}\left(2x - 3x^2 + x^3\right) + \frac{m_F^3}{m_\mu^3}\left(x - x^2\right)\right]\right\} + g_{\rm A}^2\left\{m_{\rm F} \to -m_{\rm F}\right\}\right]$$
$$\left\{m_\mu^2 x^2 + \left(M_{\rm X}^2 - m_\mu^2\right)x + m_{\rm F}^2(1-x)\right\}^{-1}. \tag{4.55}$$

The computation of all the contributions is quite complicated to perform by hand and it is necessary to employ a numerical resolution. Nevertheless both Eq. (4.54) and (4.55) can be simplified for our purpose; indeed, imposing LFC (i.e. $F = \mu$) and taking the Z' as the only X boson, being the contribution of interest, they become

$$[a_\mu]_a = \frac{M^2}{4\pi^2}\int_0^1 {\rm d}x \left[g_V^{\mu 2}(x^2 - x^3) + g_A^{\mu^2}\left((5x^2 - 4x - x^3) - \frac{2x^3 M^2}{m_{Z'}^2}\right)\right] \times \{M^2 x^2 + m_{Z'}^2(1-x)\}^{-1} \tag{4.56}$$

and, since there is no $\gamma - Z'$ coupling in Eq. (4.48),

$$[a_\mu]_b = 0. \tag{4.57}$$

The same steps can be repeated to find $[a_e]_a$, but it is simple to notice that no calculations are needed since it is sufficient to perform the replacements $g_{V(A)}^{\mu 2} \to g_{V(A)}^{e2}$ and $M \to m$. Focusing on the mass range $m_{Z'} \lesssim 0.2$ GeV and imposing the bounds $|\Delta a_e| \leq 10^{-12}$ and $|\Delta a_\mu| \leq 10^{-8}$ it follows

$$g_V^\mu \lesssim 10^{-3}, \quad g_A^\mu \lesssim 5 \times 10^{-4} \tag{4.58}$$
$$g_V^e \lesssim 4 \times 10^{-3}, \quad g_A^e \lesssim 2 \times 10^{-3}. \tag{4.59}$$

It is possible to notice that in this case the constraints on the vector couplings are a little bit worse than those found through the data of BaBar experiment; nevertheless, also in this case the resulting shift turns out to be $\delta_{Z'}^{\pm} \lesssim \mathcal{O}(10^{-5})$ and, so, it lies below MUonE sensitivity. Contrary to the light vector boson searches mentioned before, direct searches of light Z' with also axial-vector couplings have not been yet performed but it is still reasonable to think that the bound for $g_V^e g_V^\mu$ found in [56] and [57] holds also for $g_A^e g_A^\mu$. Nevertheless, with the previous analysis based on the $g-2$ constraints, it still possible to verify that also the axial-vector contribution to Eq. (4.51) is of the order $\delta_{Z'}^{\pm} \lesssim \mathcal{O}(10^{-5})$. As for the ALP scenario, also in this model it is interesting to relax the hypothesis of flavor conservation and to check whether LFV effects induced by the Z' are visible at MUonE. At tree level the two relevant Feynman diagrams are

[20] Note that the g_A^2 contribution can be recovered from the g_V^2 one simply making the substitution $m_F \to -m_F$

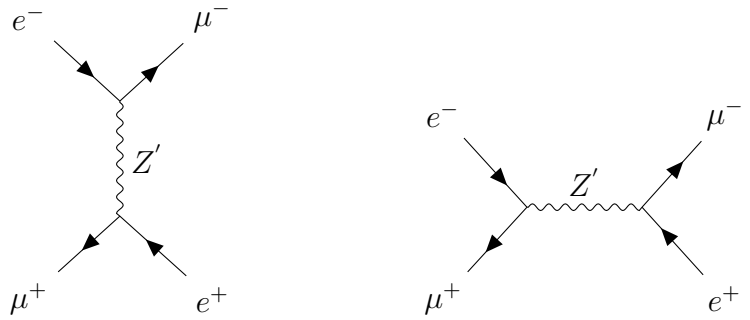

and the corresponding amplitudes read

$$\begin{aligned}\mathcal{M}^{\mathrm{t}}_{\mathrm{LFV}} &= \frac{-i(\eta_{\mu\nu}-\frac{k_\mu k_\nu}{m^2_{Z'}})}{t-m^2_{Z'}}\bar{u}(p_3)_i\gamma^\mu(g_V^{ij}+g_A^{ij}\gamma_5)u(p_1)_j\bar{v}(p_2)_j\gamma^\nu(g_V^{ji}+g_A^{ji}\gamma_5)v(p_4)_i \\ \mathcal{M}^{\mathrm{s}}_{\mathrm{LFV}} &= \frac{-i(\eta_{\mu\nu}-\frac{k_\mu k_\nu}{m^2_{Z'}})}{s-m^2_{Z'}}\bar{u}(p_3)_i\gamma^\mu(g_V^{ij}+g_A^{ij}\gamma_5)v(p_4)_j\bar{v}(p_2)_j\gamma^\nu(g_V^{ji}+g_A^{ji}\gamma_5)u(p_1)_i\end{aligned} \tag{4.60}$$

where, again, $i,j=1,2$. Ignoring suppressed terms, as the powers of m^2, the resulting shifts to the μe differential cross section read

$$\begin{aligned}\delta^{\mathrm{s}}_{\mathrm{LFV}} \approx \left(\frac{t}{16\pi\alpha(s-m^2_{Z'})}\right)^2 \frac{1}{f(s,t)}\Big[&32mM(g_V^{ij4}-g_A^{ij4})(s-M^2)+ \\ &8(g_V^{ij2}+g_A^{ij2})^2(2t^2+s^2+M^4-4M^2t+2st-2M^2s)+ \\ &32g_V^{ij2}g_A^{ij2}(s^2+2st-2M^2s-M^4)\Big] \\ \delta^{\mathrm{t}}_{\mathrm{LFV}} \approx \left(\frac{t}{16\pi\alpha(t-m^2_{Z'})}\right)^2 \frac{1}{f(s,t)}\Big[&32mM(g_V^{ij4}-g_A^{ij4})(t-M^2)+ \\ &16(g_V^{ij2}+g_A^{ij2})^2(f(s,t)-\frac{M^4}{2}-M^2t)+ \\ &32g_V^{ij2}g_A^{ij2}(f(s,t)-\frac{M^4}{2}-M^2t)\Big].\end{aligned} \tag{4.61}$$

The comparison with the probability of muonium-antimuonium oscillation provides also in this case the necessary bounds for the couplings; imposing the experimental bound (3.61) it is easy to find that, for the range $m_{Z'} \lesssim 0.2$ GeV, the axial-vector couplings must satisfy the condition $g^{ij}_{V,A} \lesssim 10^{-4}$, constraining $\delta^{\mathrm{t,\,s}}_{\mathrm{LFV}} \lesssim 10^{-14}$ and, so, it is absolutely not detectable at MUonE. The same conclusion is easily reached also for the interference term, whose contribution to the μe scattering differential cross section translates into the shift

$$\begin{aligned}\delta^{\mathrm{int}}_{\mathrm{LFV}} \approx \left(\frac{t}{8\pi\alpha}\right)^2 \frac{1}{(s-m^2_{Z'})(t-m^2_{Z'})f(s,t)}\Big[&mM(g_V^{ij4}-g_A^{ij2}g_V^{ij2})\left(M^2-\frac{s+t}{2}\right)+ \\ &(g_V^{ij4}-g_A^{ij4})\left(M^4-\frac{s^2+t^2+2st}{2}\right)\Big] \lesssim 10^{-15}.\end{aligned} \tag{4.62}$$

Chapter 5

Conclusions

The interpretation of the anomalous magnetic moment of the muon represents one of the most intriguing challenges of the Standard Model.
The discrepancy between the measurements and the theoretical prediction can be explained either with the large error in the leading hadronic contribution a_μ^{Had} or new physics effects. In order to solve this problem, it has been proposed the new experiment MUonE. The purpose of this project consists in measuring precisely a_μ^{Had} through the elastic scattering of energetic muons with electrons at rest. This analysis allows to avoid the problem of mass thresholds and resonances which affects the standard technique of dispersion integral, based on $e^+e^- \to hadrons$ data. As explained in Ch. (2), in order to be competitive enough, the sensitivity of MUonE should be $\mathcal{O}\left(10^{-5}\right)$ and it naturally raises the question whether the measure could be polluted by new physics.
In this thesis it has been analyzed in detail this problem considering both heavy and light NP degrees of freedom, depending on the fact that their mass is higher or lower $\mathcal{O}\left(1\text{ GeV}\right)$. In the former case it has been employed a model independent approach base on EFT, constructing the most general effective Lagrangians invariant under $U(1)_{em}$ (3.4.1) and $SU(2)_L \otimes U(1)_Y$ (3.6) up to dimension six. In both these scenarios the full set of NP contributions to the μe differential cross section has been computed, finding terms from vector and axial vector interactions. However, once analyzed their contributions to correlated observables and compared with the experimental bounds, it has been shown that their effects in the μe scattering at MUonE are strongly disfavoured. In the pure $U(1)_{em}$ case also scalar and tensor interactions appear, but their suppression due to the electron and muon masses do not allow them to pollute MUonE measurements. Moreover, in both cases pseudoscalar interactions provide vanishing interference contributions with the leading QED amplitude and, consequently, they do not contribute at dimension-six operators level.
In the $U(1)_{em}$ scenario it has been explored also the possibility of contamination in μe collisions due to LFV effects. Once again, however, it has been shown that, taking into account the current constraints on muonium-antimuonium oscillations, these contributions lies far beyond MUonE sensitivity.
Light NP has, instead, been analyzed specifying the spin and the interactions of the new particles with the SM ones, having no more the possibility to rely on the EFT approach. In particular, it has been considered the cases of both spin-0 and spin-1 dynamical fields. In the former case it has been studied the ALPs' scenario, where the field content of the SM is enriched with light (pseudo) scalars. Both LFC and LFV effects have been taken

into account: each one, however, using, respectively, the constraints from the electron's $g-2$ and the muonium-antimuonium oscillation probability, has been shown to be far below MUonE's sensitivity.
In the latter case there have been considered two very popular possibilities: the Dark Photon and the Z' boson. The first is introduced enlarging the SM group with an extra $U(1)$ and a kinetic mixing term which allows an interaction with the photon γ. However, the current bound on the kinetic mixing constrains NP effects in the μe scattering to be too small to be detected at MUonE. On the other hand, the same conclusions can be reached also for the Z' boson: indeed, as it has been shown, the bounds on its couplings due to direct searches do not allow for significant and measurable NP effects.
In conclusion, it can be safely stated that it is very unlikely that NP contributions will pollute MUonE's measurements of the μe scattering differential cross section and the corresponding extraction of $\Delta\alpha_{\rm h}(q^2)$; this confirmes and strongly reinforces the MUonE proposal.

Appendix A

A.1 Useful relations

Here I report some useful relations for the computation of all the results of this thesis:

$$
\begin{aligned}
&\mathrm{Tr}[\mathbb{1}] = 4 \\
&\mathrm{Tr}\left[\text{ any odd \# of } \gamma' s\right] = 0 \\
&\mathrm{Tr}\left[\gamma^\mu \gamma^\nu\right] = 4\eta^{\mu\nu} \\
&\mathrm{Tr}\left[\gamma^\mu \gamma^\nu \gamma^\rho \gamma^\sigma\right] = 4\left(\eta^{\mu\nu}\eta^{\rho\sigma} - \eta^{\mu\rho}\eta^{\nu\sigma} + \eta^{\mu\sigma}\eta^{\rho\nu}\right) \\
&\mathrm{Tr}\left[\gamma_5\right] = 0 \\
&\mathrm{Tr}\left[\gamma^\mu \gamma^\nu \gamma^\rho \gamma^\sigma \gamma_5\right] = -4i\varepsilon^{\mu\nu\rho\sigma} \\
&\mathrm{Tr}\left[\gamma^{\mu_1}\gamma^{\mu_2}\ldots\gamma^{\mu_n}\right] = \sum_{k=2}^{n}(-1)^k \eta^{\mu_1\mu_k} \times \mathrm{Tr}\left[\gamma^{\mu_2}\ldots\not{\gamma}^{\mu_k}\cdots\gamma^{\mu_n}\right] \text{ if } n \text{ even} \\
&\mathrm{Tr}\left[\gamma^{\mu_1}\ldots\gamma^{\mu_n}\gamma_5\right] = 0 \text{ if } n \text{ odd or } n \leq 3 \\
&\gamma^\mu\gamma_\mu = 4 \\
&\gamma^\mu\gamma^\nu\gamma_\mu = -2\gamma^\nu \\
&\gamma^\mu\gamma^\nu\gamma^\rho\gamma_\mu = 4\eta^{\nu\rho} \\
&\gamma^\mu\gamma^\nu\gamma^\rho\gamma^\sigma\gamma_\mu = -2\gamma^\sigma\gamma^\rho\gamma^\nu \\
&\varepsilon^{\alpha\beta\gamma\delta}\varepsilon_{\alpha\beta\gamma\delta} = -24 \\
&\varepsilon^{\alpha\beta\gamma\mu}\varepsilon_{\alpha\beta\gamma\nu} = -6\delta^\mu_\nu \\
&\varepsilon^{\alpha\beta\mu\nu}\varepsilon_{\alpha\beta\rho\sigma} = -2\left(\delta^\mu_\rho\delta^\nu_\sigma - \delta^\mu_\sigma\delta^\nu_\rho\right) \\
&\frac{d\sigma}{d\Omega} = \frac{1}{64\pi^2 s}\frac{|\vec{p_1}|}{|\vec{p_{1'}}|}|\overline{\mathcal{M}}|^2 \text{ for } 1+2 \to 1'+2' \text{ in the CM frame} \\
&\frac{d\sigma}{dt} = \frac{4\pi s}{\sqrt{\lambda_{12}\lambda_{34}}}\frac{d\sigma}{d\Omega} = \frac{4\pi s}{\lambda}\frac{d\sigma}{d\Omega}, \text{ with } \lambda = \lambda(s, m_i^2, m_j^2) = (s - m_i^2 - m_j^2)^2 - 4m_i^2 m_j^2
\end{aligned}
$$

Fierz identities for *commuting* spinors a, b, c and d:

$$(\bar{a}\gamma^\mu P_{L/R} b)(\bar{c}\gamma_\mu P_{L/R} d) = -(\bar{a}\gamma^\mu P_{L/R} d)(\bar{c}\gamma_\mu P_{L/R} b) \tag{A.1}$$

$$(\bar{a}\gamma^\mu P_{L/R} b)(\bar{c}\gamma_\mu P_{R/L} d) = 2(\bar{a} P_{R/L} d)(\bar{c} P_{L/R} b) \tag{A.2}$$

$$(\bar{a} P_{L/R} b)(\bar{c} P_{R/L} d) = \frac{1}{2}(\bar{a}\gamma^\mu P_{R/L} d)(\bar{c}\gamma_\mu P_{L/R} b) \tag{A.3}$$

$$\left(\bar{a}P_{L/R}b\right)\left(\bar{c}P_{L/R}d\right) = \frac{1}{2}\left(\bar{a}P_{L/R}d\right)\left(\bar{c}P_{L/R}b\right) + \frac{1}{8}\left(\bar{a}\sigma^{\mu\nu}P_{L/R}d\right)\left(\bar{c}\sigma_{\mu\nu}P_{L/R}b\right) \tag{A.4}$$

$$\left(\bar{a}\sigma^{\mu\nu}P_{L/R}b\right)\left(\bar{c}\sigma_{\mu\nu}P_{L/R}d\right) = 6\left(\bar{a}P_{L/R}d\right)\left(\bar{c}P_{L/R}b\right) - \frac{1}{2}\left(\bar{a}\sigma^{\mu\nu}P_{L/R}d\right)\left(\bar{c}\sigma_{\mu\nu}P_{L/R}b\right) \tag{A.5}$$

A.2 Detailed computation of NP contributions to μe scattering

The LFC Lagrangian of Eq. (3.38) is explicitly

$$\begin{aligned}\mathcal{L}_{\rm LFC} = \frac{1}{4\Lambda^2}\Big[&(a_1+ia_2)\bar{\mu}(1+\gamma_5)\mu\bar{e}(1+\gamma_5)e + h.c.+\\ &(a_3+ia_4)\bar{\mu}(1+\gamma_5)e\bar{e}(1+\gamma_5)\mu + h.c.+\\ &(a_5+ia_6)\bar{\mu}(1+\gamma_5)\mu\bar{e}(1-\gamma_5)e + h.c.+\\ &a_7\bar{\mu}(1+\gamma_5)\gamma^\mu\mu\bar{e}(1+\gamma_5)\gamma_\mu e+\\ &a_8\bar{\mu}(1-\gamma_5)\gamma^\mu\mu\bar{e}(1-\gamma_5)\gamma_\mu e+\\ &a_9\bar{\mu}(1+\gamma_5)\gamma^\mu\mu\bar{e}(1-\gamma_5)\gamma_\mu e+\\ &a_{10}\bar{\mu}(1-\gamma_5)\gamma^\mu\mu\bar{e}(1+\gamma_5)\gamma_\mu e\Big].\end{aligned} \tag{A.6}$$

All these terms can be represented with the Feynman diagram

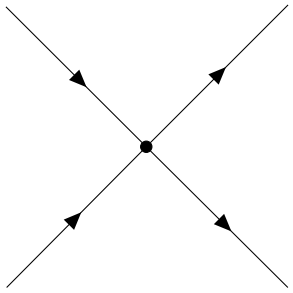

with different coefficients (and sign of γ_5) depending, clearly, on the operator which is taken into account. Since all of them have a factor $\propto 1/\Lambda^2$, in calculating the unpolarized squared Feynman amplitude $|\overline{\mathcal{M}}|^2$ it will be considered only the product of the amplitude of a given piece of Eq (A.6), $\mathcal{M}_i$ (i=1,...,10), with that of the photon. In other words [21]:

$$|\overline{\mathcal{M}}_{tot}|^2 = \frac{1}{4}\sum_{spins}(|\mathcal{M}_\gamma|^2 + 2\mathrm{Re}\mathcal{M}_\gamma^*\mathcal{M}_Z + 2\mathrm{Re}\sum_{i=1}^{10}\mathcal{M}_\gamma^*\mathcal{M}_i). \tag{A.7}$$

As already discussed in the main corpse of this thesis, all the $|\overline{\mathcal{M}}_i|^2$ have been neglected since they present a $1/\Lambda^4$ dependence, as well as $|\overline{\mathcal{M}}_Z|^2$, being suppressed by $G_F^2 s^2$ and all the amplitudes which involve the Higgs boson H.
Let's start the computation remembering that the amplitude of the diagram mediated by the photon is

$$\mathcal{M}_\gamma = \frac{ie^2}{t}\bar{u}(p_3)\gamma^\mu u(p_1)\bar{u}(p_4)\gamma_\mu u(p_2). \tag{A.8}$$

From the Lagrangian (A.6) it follows that the first operator provides an amplitude

$$\mathcal{M}_1 = \frac{i(a_1+ia_2)}{4\Lambda^2}\bar{u}(p_3)(1+\gamma_5)u(p_1)\bar{u}(p_4)(1+\gamma_5)u(p_2), \tag{A.9}$$

[21] In the following computations it will adopted the notation $\overline{\mathcal{M}}_{\gamma(Z)i} = \frac{1}{2}\,\mathrm{Re}\sum_{spins}\mathcal{M}_{\gamma(Z)}^*\mathcal{M}_i$.

so that

$$\overline{\mathcal{M}}_{\gamma 1} = \frac{e^2 a_1}{8\Lambda^2 t} \mathrm{Tr}\Big[\gamma^\mu (\not{p}_3 + m)(1+\gamma_5)(\not{p}_1 + m)\Big] \mathrm{Tr}\Big[\gamma_\mu (\not{p}_4 + M)(1+\gamma_5)(\not{p}_2 + M)\Big]. \quad \text{(A.10)}$$

The passages in the calculation of the first trace explicitly read

$$\begin{aligned}\mathrm{Tr}\Big[\gamma^\mu (\not{p}_3 + m)(1+\gamma_5)(\not{p}_1 + m)\Big] &= \mathrm{Tr}\Big[\gamma^\mu \not{p}_3 (1+\gamma_5)(\not{p}_1 + m)\Big] + m\,\mathrm{Tr}\Big[\gamma^\mu (1+\gamma_5)(\not{p}_1 + m)\Big] = \\ &= \mathrm{Tr}\Big[\gamma^\mu \not{p}_3 (\not{p}_1 + m)\Big] + m\,\mathrm{Tr}\Big[\gamma^\mu (\not{p}_1 + m)\Big] = m p_{3\alpha} Tr[\gamma^\mu \gamma^\alpha] + m p_{1\alpha} Tr[\gamma^\mu \gamma^\alpha] = 4m(p_3 + p_1)^\mu; \end{aligned} \quad \text{(A.11)}$$

the computation for the second trace, however, can be avoided simply observing that it can be directly recovered from the previous result applying the substitutions $p_3 \to p_4$, $p_1 \to p_2$, $m \to M$:

$$\mathrm{Tr}\Big[\gamma_\mu (\not{p}_4 + M)(1+\gamma_5)(\not{p}_2 + M)\Big] = 4M(p_2 + p_4)_\mu.$$

Putting all together and exploiting the relations between scalar products and the mandelstam variables, it can be found

$$\overline{\mathcal{M}}_{\gamma 1} = \frac{8\pi\alpha a_1 m M}{\Lambda^2 t}(s-u). \quad \text{(A.12)}$$

However it is possible to notice immediately one thing: in computing the trace (A.11) there is no renmant of the γ_5 and its signs. This means that the same result (with the coefficient a_5 instead of a_1) can be immediately recovered from the third term of the Lagrangian without any calculation:

$$\overline{\mathcal{M}}_{\gamma 5} = \frac{8\pi\alpha a_5 m M}{\Lambda^2 t}(s-u) \quad \text{(A.13)}$$

Summing these two contributions and defining $a_S = a_1 + a_5$, one easily finds the "scalar" shift to the μe differential cross section

$$\delta^{1+5}_{\mathrm{LFC}} = \frac{t}{8\pi\alpha\Lambda^2}\frac{1}{f(s,t)}[2mMa_S(s-u)]. \quad \text{(A.14)}$$

The second operator of (A.6) is a little bit subtle compared to the previous two, requiring the use of the Fierz identities; exploiting the fourth one in (A.1), it is possible to rewrite

$$\frac{(a_3 + ia_4)}{\Lambda^2}\left[\bar{\mu}_L e_R \bar{e}_L \mu_R\right] = -\frac{(a_3 + ia_4)}{2\Lambda^2}\left[\bar{\mu}_L \mu_R \bar{e}_L e_R + \frac{1}{4}\bar{\mu}_L \sigma^{\mu\nu} \mu_R \bar{e}_L \sigma_{\mu\nu} e_R\right]. \quad \text{(A.15)}$$

Let's analyze these two pieces separately.
In the case of the term with no gammas, the amplitude reads

$$\mathcal{M}_{3'} = -\frac{i(a_3 + ia_4)}{8\Lambda^2}\bar{u}(p_3)(1+\gamma_5)u(p_1)\bar{u}(p_4)(1+\gamma_5)u(p_2), \quad \text{(A.16)}$$

while the unpolarized one is

$$\overline{\mathcal{M}}_{\gamma 3'} = -\frac{e^2 a_3}{16 t \Lambda^2} \mathrm{Tr}\Big[\gamma^\mu (\not{p}_3 + m)(1+\gamma_5)(\not{p}_1 + m)\Big] \mathrm{Tr}\Big[\gamma_\mu (\not{p}_4 + M)(1+\gamma_5)(\not{p}_2 + M)\Big]. \tag{A.17}$$

The two traces are very simple and they turn out to respectively be

$$\mathrm{Tr}[1] = 4m[p_1^\mu + p_3^\mu]$$
$$\mathrm{Tr}[2] = 4M[p_{4\mu} + p_{2\mu}]$$

so that (A.17) becomes

$$\overline{\mathcal{M}}_{\gamma 3'} = -\frac{8\pi\alpha a_3}{t\Lambda^2} mM[2p_1 \cdot p_2 + 2p_3 \cdot p_4] = -\frac{8\pi\alpha a_3}{t\Lambda^2} mM[s-u]. \tag{A.18}$$

On the other side, the term with $\sigma^{\mu\nu}$ leads to the amplitude

$$\mathcal{M}_{3''} = \frac{(a_3 + i a_4)}{32\Lambda^2} \bar{u}(p_3)(1+\gamma_5)[\gamma^\mu, \gamma^\nu] u(p_1) \bar{u}(p_4)(1+\gamma_5)[\gamma^\mu, \gamma^\nu] u(p_2) \tag{A.19}$$

and, correspondingly, to the unpolarized one

$$\begin{aligned} \overline{\mathcal{M}}_{\gamma 3''} = \frac{e^2 a_3}{64 t \Lambda^2} \mathrm{Tr}\Big[\gamma^\rho (\not{p}_3 + m)(1+\gamma_5)[\gamma^\mu, \gamma^\nu](\not{p}_1 + m)\Big] \\ \mathrm{Tr}\Big[\gamma_\rho (\not{p}_4 + M)(1+\gamma_5)[\gamma_\mu, \gamma_\nu](\not{p}_2 + M)\Big]. \end{aligned} \tag{A.20}$$

As already done, it is sufficient to calculate only a trace and then making the correct substitutions in order to find the other one. Their explicit expressions are

$$\mathrm{Tr}[1] = 8m(p_3^\mu \eta^{\rho\nu} - p_3^\nu \eta^{\rho\mu} + p_1^\nu \eta^{\rho\mu} - p_1^\mu \eta^{\rho\nu}) \tag{A.21}$$

$$\mathrm{Tr}[2] = 8M(p_{4\mu}\eta_{\rho\nu} - p_{4\nu}\eta_{\rho\mu} + p_{2\nu}\eta_{\rho\mu} - p_{2\mu}\eta_{\rho\nu}), \tag{A.22}$$

so that the final unpolarized amplitude becomes

$$\overline{\mathcal{M}}_{\gamma 3''} = -\frac{24\pi\alpha a_3}{t\Lambda^2} mMt. \tag{A.23}$$

Finally, summing these two amplitudes, i.e. $\bar{\mathcal{M}}_{3'}$ and $\bar{\mathcal{M}}_{3''}$, the total contribution reads

$$\overline{\mathcal{M}}_3 = \overline{\mathcal{M}}_{3'} + \overline{\mathcal{M}}_{3''} = \frac{16\pi\alpha}{t\Lambda^2} mM(u - t - m^2 - M^2), \tag{A.24}$$

where it has been used $s + t + u = 2m^2 + 2M^2$; from this expression it follows the "tensor" shift to the total differential cross section $\frac{d\sigma}{dt}$, which is

$$\delta^3_{\mathrm{LFC}} = \frac{t a_T}{8\pi\alpha f(s,t)\Lambda^2} 2mM(u - t - m^2 - M^2), \tag{A.25}$$

where $a_T = a_3$.
Let's move on to the operators of (A.6) which involve a gamma matrix, starting from the fourth and the fifth; their amplitudes are

$$\mathcal{M}_7 = \frac{ia_7}{4\Lambda^2}\bar{u}(p_3)(1+\gamma_5)\gamma^\rho u(p_1)\bar{u}(p_4)(1+\gamma_5)\gamma_\rho u(p_2) \tag{A.26}$$

$$\mathcal{M}_8 = \frac{ia_8}{4\Lambda^2}\bar{u}(p_3)(1-\gamma_5)\gamma^\rho u(p_1)\bar{u}(p_4)(1-\gamma_5)\gamma_\rho u(p_2). \tag{A.27}$$

It is sufficient to compute $\mathcal{M}_7$ since, then, $\mathcal{M}_8$ can be found without making any effort using only a simple consideration (as done before for the a_5 coefficient); the unpolarized matrix element is

$$\overline{\mathcal{M}}_{\gamma 7} = \frac{e^2 a_7}{8\Lambda^2 t}\,\mathrm{Tr}\Big[\gamma^\mu(\not{p}_3+m)(1+\gamma_5)\gamma^\rho(\not{p}_1+m)\Big]\,\mathrm{Tr}\Big[\gamma_\mu(\not{p}_4+M)(1+\gamma_5)\gamma_\rho(\not{p}_2+M)\Big]. \tag{A.28}$$

The first trace is

$$\mathrm{Tr}\Big[\gamma^\mu(\not{p}_3+m)(1+\gamma_5)\gamma^\rho(\not{p}_1+m)\Big] = 4(m^2\eta^{\mu\rho} + p_1^\rho p_3^\mu + p_3^\rho p_1^\mu - p_1\cdot p_3\eta^{\mu\rho} - i\epsilon^{\mu\alpha\rho\beta}p_{3\alpha}p_{1\beta})$$

while the second, with the usual substitutions $p_3 \to p_4$, $p_1 \to p_2$, $m \to M$, reads

$$\mathrm{Tr}\Big[\gamma_\mu(\not{p}_4+M)(1+\gamma_5)\gamma_\rho(\not{p}_2+M)\Big] = 4(M^2\eta_{\mu\rho} + p_{1\rho}p_{3\mu} + p_{3\rho}p_{1\mu} - p_1\cdot p_3\eta_{\mu\rho} - i\epsilon_{\mu\gamma\rho\delta}p_4^\gamma p_2^\delta).$$

Using the properties of the Levi-Civita tensor, reported in (A.1), one easily arrives to the result

$$\overline{\mathcal{M}}_{\gamma 7} = \frac{8\pi\alpha a_7}{t\Lambda^2}[f(s,t) + \frac{t}{2}(u-s)]. \tag{A.29}$$

As anticipated, the amplitude $\bar{\mathcal{M}}_{\gamma 8}$ can be immediately recovered noticing a simple thing: the difference between (A.26) and (A.27) is only in the two signs of γ_5. This means that, repeating the various steps, the sames traces arise, now with the two Levi-Civita tensors both multiplied by i and no more by $-i$. However, being $i^2 = (-i)^2 = -1$, the product of the two traces remains the same and, then, the unpolarized amplitude is

$$\overline{\mathcal{M}}_{\gamma 8} = \frac{8\pi\alpha a_8}{t\Lambda^2}[f(s,t) + \frac{t}{2}(u-s)] \tag{A.30}$$

Finally, we are left with the last two operators of $\mathcal{L}_{\mathrm{LFC}}$, whose amplitudes now contain one $(1+\gamma_5)$ and one $(1-\gamma_5)$:

$$\mathcal{M}_9 = \frac{ia_9}{4\Lambda^2}\bar{u}(p_3)(1-\gamma_5)\gamma^\rho u(p_1)\bar{u}(p_4)(1+\gamma_5)\gamma_\rho u(p_2) \tag{A.31}$$

$$\mathcal{M}_{10} = \frac{ia_{10}}{4\Lambda^2}\bar{u}(p_3)(1+\gamma_5)\gamma^\rho u(p_1)\bar{u}(p_4)(1-\gamma_5)\gamma_\rho u(p_2). \tag{A.32}$$

Let's focus on (A.31), since the same will be clearly true also for the other amplitude. The fact that, this time, only one of the two γ_5 has different sign respect to those of (A.26) causes a change of sign of the Levi-Civita tensor in one of the two traces

$$\mathrm{Tr}\Big[\gamma^\mu(\not{p}_3 + m)(1+\gamma_5)\gamma^\rho(\not{p}_1 + m)\Big] = 4(m^2\eta^{\mu\rho} + p_1^\rho p_3^\mu + p_3^\rho p_1^\mu - p_1\cdot p_3\eta^{\mu\rho} + i\epsilon^{\mu\alpha\rho\beta}p_{3\alpha}p_{1\beta})$$

$$\mathrm{Tr}\Big[\gamma_\mu(\not{p}_4 + M)(1+\gamma_5)\gamma_\rho(\not{p}_2 + M)\Big] = 4(M^2\eta_{\mu\rho} + p_{1\rho}p_{3\mu} + p_{3\rho}p_{1\mu} - p_1\cdot p_3\eta_{\mu\rho} - i\epsilon_{\mu\gamma\rho\delta}p_4^\gamma p_2^\delta).$$

Consequently, taking again their product and repeating the usual steps, now it is no more the term $(p_1\cdot p_4)(p_2\cdot p_3)$ which disappears, but $(p_1\cdot p_2)(p_3\cdot p_4)$. Therefore

$$\begin{aligned}\overline{\mathcal{M}}_{\gamma 9} &= \frac{8\pi\alpha a_9}{t\Lambda^2}[4m^2M^2 + 4(p_1\cdot p_4)(p_2\cdot p_3) - 2M^2(p_1\cdot p_3) - 2m^2(p_2\cdot p_4)] = \\ &= \frac{8\pi\alpha a_9}{t\Lambda^2}[M^2t + m^2t + (s+t-m^2-M^2)^2] = \frac{8\pi\alpha a_9}{t\Lambda^2}[f(s,t) + \frac{t}{2}(s-u)]\end{aligned} \tag{A.33}$$

and, analogously,

$$\overline{\mathcal{M}}_{\gamma 10} = \frac{8\pi\alpha a_{10}}{t\Lambda^2}[f(s,t) + \frac{t}{2}(s-u)]. \tag{A.34}$$

Finally, summing $\overline{\mathcal{M}}_{\gamma 7}$, $\overline{\mathcal{M}}_{\gamma 8}$, $\overline{\mathcal{M}}_{\gamma 9}$ and $\overline{\mathcal{M}}_{\gamma 10}$ and defining $a_V = a_7 + a_8 + a_9 + a_{10}$ and $a_A = a_7 + a_8 - a_9 - a_{10}$, we recover also the "axial" and "vector" shifts

$$\delta_{\mathrm{LFC}}^{7+8+9+10} = \frac{t}{8\pi\alpha f(s,t)\Lambda^2}[a_V f(s,t) + \frac{a_A t}{2}(u-s)]. \tag{A.35}$$

This result concludes the calculations necessary to obtain Eq. (3.41).

A.3 Detailed Computation of the NP contributions to $\sigma(e^+e^- \to \mu^+\mu^-)$

This section is devoted to the computation of the total cross section of the scattering $e^+e^- \to \mu^+\mu^-$. First of all, in the pure SM the process is described by the Feynman diagrams

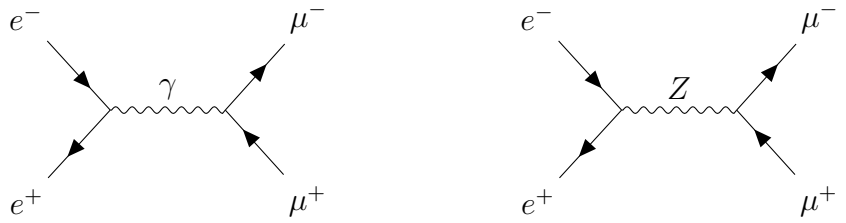

where the explicit amplitudes are

$$\mathcal{M}_\gamma = \frac{ie^2}{s}\bar{u}(p_3)\gamma^\mu v(p_4)\bar{v}(p_2)\gamma_\mu u(p_1) \tag{A.36}$$

and[22]

$$\mathcal{M}_Z = \frac{8iG_F}{\sqrt{2}}\bar{u}(p_3)\gamma^\mu(g_V - g_A\gamma_5)v(p_4)\frac{M_Z^2}{s-M_Z^2}\bar{v}(p_2)\gamma_\mu(g_V - g_A\gamma_5)u(p_1), \tag{A.37}$$

[22]Here the propagator should be modified with the vacuum polarization of the Z boson in order to avoid the divergence at $\sqrt{s} = M_Z$; nevertheless, working in energy ranges which do not include this scale, this correction can be ignored.

providing the unpolarized amplitude

$$|\overline{\mathcal{M}}|^2 = |\overline{\mathcal{M}_\gamma}|^2 + |\overline{\mathcal{M}_Z}|^2 + \overline{\mathcal{M}_{\gamma Z}}.$$

Let's notice that the term $\propto k_\mu k_\nu$ in the propagator has been neglected since it can be entirely rewritten in terms the lepton masses; however, working at energies much higher than these them allows to take $m = M = 0$, simplifying a lot the computation of the traces.
The final differential cross section can be rewritten in the same form of the QED one

$$\frac{d\sigma}{d\cos\theta} = \frac{\pi}{2}\frac{\alpha_{em}^2}{s}\left[A\left(1+\cos^2\theta\right) + B\cos\theta\right]$$

whit

$$A = 1 - \frac{8\sqrt{2}\,(G_F s)}{e^2}g_V^2 + \frac{32\,(G_F s)^2}{e^4}\left(g_V^2 + g_A^2\right)^2$$

$$B = -\frac{32\,(G_F s)}{\sqrt{2}e^2}g_A^2 + \frac{256\,(G_F s)^2}{e^4}g_V^2 g_A^2.$$

The total SM cross section, then, is simply

$$\sigma_{\text{SM}} = \frac{4\pi\alpha^2}{3s}A.$$

Now I turn the attention on NP contributions. Let's firstly notice that the a_1, a_3 and a_5 pieces don't contribute [23]: indeed the amplitude for the NP diagram is simply

$$\mathcal{M}_1 = \frac{i(a_1 + ia_2)}{4\Lambda^2}\bar{u}(p_3)(1+\gamma_5)v(p_4)\bar{v}(p_2)(1+\gamma_5)u(p_1) \tag{A.38}$$

so that

$$\overline{\mathcal{M}}_{\gamma 1} \propto \text{Tr}\Big[(1+\gamma_5)\not{p}_1\gamma^\mu\not{p}_2\Big]\,\text{Tr}\Big[(1+\gamma_5)\not{p}_3\gamma_\mu\not{p}_4\Big]. \tag{A.39}$$

However, due to the properties of the traces, this is clearly null. This statement holds also for the interference term with the Z boson, being

$$\overline{\mathcal{M}}_{Z1} \propto \text{Tr}\Big[(1+\gamma_5)\not{p}_1\gamma^\mu(g_V - g_A\gamma_5)\not{p}_2\Big]\,\text{Tr}\Big[(1+\gamma_5)\not{p}_3\gamma_\mu(g_V - g_A\gamma_5)\not{p}_4\Big].$$

Taking, for example, the first trace, it can be opened as

$$\text{Tr}[1] = \text{Tr}\Big[(g_V - g_A)\not{p}_1\gamma^\mu\not{p}_2\Big] + \text{Tr}\Big[(g_V - g_A)\gamma_5\not{p}_1\gamma^\mu\not{p}_2\Big]$$

which, again, vanishes.
The first operators which, then, provide a non zero contributions are those multiplied by the coefficients a_7 and a_8. The amplitude of the former is

$$\mathcal{M}_7 = \frac{ia_7}{4\Lambda^2}\bar{u}(p_3)(1+\gamma_5)\gamma^\nu v(p_4)\bar{v}(p_2)(1+\gamma_5)\gamma_\nu u(p_1) \tag{A.40}$$

and the unpolarized one reads

[23] This will be demonstrated only for a_1 but it is the same for all of them.

$$\overline{\mathcal{M}}_{\gamma 7} = \frac{a_7 e^2}{8\Lambda^2 s}\,\mathrm{Tr}\Big[(1+\gamma_5)\gamma^\nu \not{p}_1 \gamma^\mu \not{p}_2\Big]\,\mathrm{Tr}\Big[(1+\gamma_5)\gamma_\nu \not{p}_4 \gamma_\mu \not{p}_3\Big]. \tag{A.41}$$

As usual it is sufficient to compute the first trace and, then, the second can be straightforwardly obtained with the proper substitutions ($p_1 \to p_4, p_2 \to p_3, m \to M$):

$$\mathrm{Tr}[1] = 4\left(p_1^\nu p_2^\mu + p_2^\nu p_1^\mu - p_1 \cdot p_2 \eta^{\mu\nu} + i\epsilon^{\nu\alpha\mu\beta} p_{1\alpha} p_{2\beta}\right) \tag{A.42}$$

$$\mathrm{Tr}[2] = 4\left(p_{4\nu} p_{3\mu} + p_{3\nu} p_{4\mu} - p_3 \cdot p_4 \eta_{\mu\nu} + i\epsilon_{\nu\gamma\mu\delta} p_4^\gamma p_3^\delta\right). \tag{A.43}$$

Their product leads to the unpolarized squared amplitude

$$\overline{\mathcal{M}}_{\gamma 7} = \frac{8\pi\alpha a_7}{\Lambda^2 s}(s+t)^2 \tag{A.44}$$

and, exactly as happened in the computation of $\sigma(\mu^\pm e^- \to \mu^\pm e^-)$, it is equal to $\overline{\mathcal{M}}_{\gamma 8}$ (except, obviously, for a_8 instead of a_7).
Also for the last two operators of $\mathcal{L}_{\mathrm{LFC}}$ it is possible to rely on a reasoning similar to that made for the $\mu^\pm e^- \to \mu^\pm e^-$ scattering: respect to the case of the term multiplied by a_7, those multiplied by a_9 and a_{10} have one (and not two as for a_8) γ_5 with different sign. Consequently, the two traces will have the same form of (A.42) and (A.43) but, this time, one Levi-Civita tensor takes the minus sign; once computed their product, it follows

$$\overline{\mathcal{M}}_{\gamma 9} = \frac{8\pi\alpha a_9}{\Lambda^2 s} t^2 \tag{A.45}$$

$$\overline{\mathcal{M}}_{\gamma 10} = \frac{8\pi\alpha a_{10}}{\Lambda^2 s} t^2. \tag{A.46}$$

Finally, summing all the contributions it is possible to proceed to compute the total cross section for the interference with the photon; defining $x = \cos\theta$, in the CM frame $t = -s/2(1-x)$ and the total amplitude reads

$$\overline{\mathcal{M}}_{\gamma tot} = \frac{2\pi\alpha s}{\Lambda^2}\left[(a_7+a_8)(1+x)^2 + (a_9+a_{10})(1-x)^2\right].$$

Now, the differential cross section is simply

$$\begin{aligned}\frac{d\sigma_{\gamma tot}}{d\Omega} &= \frac{1}{64\pi^2 s} \times \frac{2\pi\alpha s}{\Lambda^2}\left[(a_7+a_8)(1+x)^2 + (a_9+a_{10})(1-x)^2\right] = \\ &= \frac{\alpha}{32\pi\Lambda^2}\left[(a_7+a_8)(1+x)^2 + (a_9+a_{10})(1-x)^2\right]\end{aligned} \tag{A.47}$$

and the resulting total one reads

$$\begin{aligned}\sigma_{\gamma tot} &= 2\pi\int_{-1}^{1}\frac{d\sigma_{\gamma tot}}{dx}dx = \frac{\alpha}{16\Lambda^2}\int_{-1}^{1} dx\left[(a_7+a_8)(1+x)^2 + (a_9+a_{10})(1-x)^2\right] = \\ &= \frac{\alpha a_V}{6\Lambda^2},\end{aligned} \tag{A.48}$$

where $a_V = a_7 + a_8 + a_9 + a_{10}$[24].
Let's now put the attention on the contribution coming from the interference with the Z

[24]NB: although one term is $(1-x)^2$ while the other $(1-x)^2$, since the interval of integration is symmetric the odd terms do not contribute. As a consequence since they differ exactly a odd terms, after the integration they gave the same result, which is 8/3.

boson. The Feynman amplitudes of interest are, now, (A.37) and (A.40). In the following computations (already characterized by a $1/\Lambda^2$ factor) I will neglect the g_V contribution, being $g_V = a_\theta/4 \sim -10^{-2}$; in this way (A.37) becomes simply

$$\mathcal{M}_Z = \frac{8iG_F g_A^2}{\sqrt{2}} \bar{u}(p_3)\gamma^\mu\gamma_5 v(p_4) \frac{M_Z^2}{s - M_Z^2} \bar{v}(p_2)\gamma_\mu\gamma_5 u(p_1) \tag{A.49}$$

and the unpolarized squared matrix element, then, reads

$$\overline{\mathcal{M}}_{Z7} = \frac{a_7 G_F g_A^2}{\sqrt{2}\Lambda^2} \frac{M_Z^2}{(s - M_Z^2)} \mathrm{Tr}\Big[(1+\gamma_5)\gamma^\nu \not{p}_1 \gamma^\mu \gamma_5 \not{p}_2\Big] \mathrm{Tr}\Big[(1+\gamma_5)\gamma_\nu \not{p}_4 \gamma_\mu \not{\gamma}_5 p_3\Big]. \tag{A.50}$$

Paying attention to use properly the anticommutation relation between γ_5 and the other gammas, the two traces turn out to be

$$\mathrm{Tr}[1] = -4\left(p_1^\nu p_2^\mu + p_2^\nu p_1^\mu - p_1 \cdot p_2 \eta^{\mu\nu} - i\epsilon^{\nu\alpha\mu\beta} p_{1\alpha} p_{2\beta}\right)$$

$$\mathrm{Tr}[2] = -4\left(p_{4\nu} p_{3\mu} + p_{3\nu} p_{4\mu} - p_3 \cdot p_4 \eta_{\mu\nu} - i\epsilon_{\nu\gamma\mu\delta} p_4^\gamma p_3^\delta\right),$$

providing the results

$$\overline{\mathcal{M}}_{Z7} = \frac{a_7 G_F}{4\sqrt{2}\Lambda^2} \frac{M_Z^2}{(s - M_Z^2)} s^2 (1+x)^2 \tag{A.51}$$

and

$$\overline{\mathcal{M}}_{Z8} = \frac{a_8 G_F}{4\sqrt{2}\Lambda^2} \frac{M_Z^2}{(s - M_Z^2)} s^2 (1+x)^2. \tag{A.52}$$

Thus, the differential cross section due to these two terms is

$$\frac{d\sigma_{Z(7+8)}}{d\Omega} = \frac{1}{64\pi^2 s} \times \frac{(a_7 + a_8) G_F}{4\sqrt{2}\Lambda^2} \frac{M_Z^2}{(s - M_Z^2)} s^2 (1+x)^2 = \frac{(a_7 + a_8) G_F s}{256\pi^2\sqrt{2}\Lambda^2} \frac{M_Z^2}{(s - M_Z^2)} (1+x)^2 \tag{A.53}$$

and the corresponding total one reads

$$\begin{aligned} \sigma_{Z(7+8)} &= 2\pi \int_{-1}^{1} \frac{d\sigma_{Z(7+8)}}{dx} dx = \frac{(a_7 + a_8) G_F s}{128\pi\sqrt{2}\Lambda^2} \frac{M_Z^2}{(s - M_Z^2)} \int_{-1}^{1} dx (1+x)^2 = \\ &= \frac{(a_7 + a_8) G_F s}{48\pi\sqrt{2}\Lambda^2} \frac{M_Z^2}{(s - M_Z^2)}. \end{aligned} \tag{A.54}$$

Also this computation is almost ended, but we have firstly to deal with the last two operators of $\mathcal{L}_{\mathrm{LFC}}$. Their amplitudes are

$$\mathcal{M}_9 = \frac{i a_9}{4\Lambda^2} \bar{u}(p_3)(1-\gamma_5)\gamma^\rho u(p_1) \bar{u}(p_4)(1+\gamma_5)\gamma_\rho u(p_2) \tag{A.55}$$

$$\mathcal{M}_{10} = \frac{i a_{10}}{4\Lambda^2} \bar{u}(p_3)(1+\gamma_5)\gamma^\rho u(p_1) \bar{u}(p_4)(1-\gamma_5)\gamma_\rho u(p_2), \tag{A.56}$$

which have both a $(1+\gamma_5)$ and a $(1-\gamma_5)$ terms, differently from the previous contributions in which there were two $(1+\gamma_5)$ or two $(1-\gamma_5)$. This difference has two effects: as

usual, the Levi-Civita tensors in the two traces have opposite signs but, this time, as a consequence of the different channel of interaction, the unpolarized matrix element gains a minus sign, becoming

$$\overline{\mathcal{M}}_{Z9} - \frac{a_9 G_F}{4\sqrt{2}\Lambda^2}\frac{M_Z^2}{(s-M_Z^2)}s^2(1-x)^2 \tag{A.57}$$

and, similarly,

$$\overline{\mathcal{M}}_{Z10} = -\frac{a_{10} G_F}{4\sqrt{2}\Lambda^2}\frac{M_Z^2}{(s-M_Z^2)}s^2(1-x)^2. \tag{A.58}$$

Once summed these two contributions, the related shift to the differential cross section takes the form

$$\frac{d\sigma_{Z(9+10)}}{d\Omega} = -\frac{1}{64\pi^2 s}\times\frac{(a_9+a_{10})G_F}{4\sqrt{2}\Lambda^2}\frac{M_Z^2}{(s-M_Z^2)}s^2(1-x)^2 = -\frac{(a_9+a_{10})G_F s}{256\pi^2\sqrt{2}\Lambda^2}\frac{M_Z^2}{(s-M_Z^2)}(1-x)^2 \tag{A.59}$$

which, if integrated, provides the corresponding total one

$$\begin{aligned}\sigma_{Z(9+10)} &= 2\pi\int_{-1}^{1}\frac{d\sigma_{Z(9+10)}}{dx}dx = -\frac{(a_9+a_{10})G_F s}{128\pi\sqrt{2}\Lambda^2}\frac{M_Z^2}{(s-M_Z^2)}\int_{-1}^{1}dx(1-x)^2 = \\ &= -\frac{(a_9+a_{10})G_F s}{48\pi\sqrt{2}\Lambda^2}\frac{M_Z^2}{(s-M_Z^2)}.\end{aligned} \tag{A.60}$$

Combining the previous results, the final interference term between the NP Lagrangian and the SM Z boson reads

$$\sigma_{Ztot} = \frac{a_A G_F s}{48\pi\sqrt{2}\Lambda^2}\frac{M_Z^2}{(s-M_Z^2)} \tag{A.61}$$

where $a_A = a_7 + a_8 - a_9 - a_{10}$.
Finally, the total correction to the SM cross section obtained summing (A.48) and (A.61) becomes

$$\sigma_{\rm NP} = \frac{1}{\Lambda^2}\left[\frac{\alpha a_V}{6} + \frac{a_A G_F s}{48\pi\sqrt{2}}\frac{M_Z^2}{(s-M_Z^2)}\right] \tag{A.62}$$

A.4 Detailed computation of NP contributions to $A_{\rm FB}$ of $e^+e^- \to \mu^+\mu^-$

Here it will be shown the explicit computations for the NP contribution to the forward-backward asymmetry of the $e^+e^- \to \mu^+\mu^-$ process; nevertheless, as for the previous section, let's firstly recall the SM result.
The forward-backward asymmetry is defined as

$$A_{\rm FB} = \frac{\sigma_{\rm F} - \sigma_{\rm B}}{\sigma_{\rm F} + \sigma_{\rm B}} = \frac{\int_0^1 \frac{d\sigma}{dx} dx - \int_{-1}^0 \frac{d\sigma}{dx} dx}{\sigma_{tot}} \tag{A.63}$$

and the SM prediction is simply

$$A_{\rm FB} = \frac{3B}{8A}. \tag{A.64}$$

However, since in the NP contribution there is already the suppression due to Λ^2, I directly neglect a_θ (and its powers) in A and B, i.e. in the following computations it will be used

$$A = \frac{128\pi^2\alpha^2(s - M_Z^2)^2 + G_F^2 s^2 M_Z^4}{128\pi^2\alpha^2(s - M_Z^2)^2}$$

$$B = -\frac{G_F s M_Z^2}{2\sqrt{2}\pi\alpha(s - M_Z^2)}.$$

Now we are ready to deal with the corrections to the asymmetry.
The NP differential cross sections are explicitly

$$\frac{d\sigma_Z}{dx}|_{\rm NP} = \frac{G_F s}{128\pi\sqrt{2}\Lambda^2} \frac{M_Z^2}{(s - M_Z^2)} \left[(a_7 + a_8)(1 + x)^2 - (a_9 + a_{10})(1 - x)^2\right]$$

$$\frac{d\sigma_\gamma}{dx}|_{\rm NP} = \frac{\alpha}{16\Lambda^2} \left[(a_7 + a_8)(1 + x)^2 + (a_9 + a_{10})(1 - x)^2\right].$$

The integration of both of them is very easy to perform and it brings to the difference

$$\sigma_{\rm F} - \sigma_{\rm B}|_{\rm NP} = \frac{1}{\Lambda^2}\left[a_A \frac{\alpha}{8} + a_V \frac{G_F s}{64\sqrt{2}\pi} \frac{M_Z^2}{(s - M_Z^2)}\right],$$

so that the forward-backward asymmetry due to NP contributions is

$$A_{\rm FB}^{\rm NP} = \frac{1}{\sigma_{tot}} \times \frac{1}{\Lambda^2}\left[a_A \frac{\alpha}{8} + a_V \frac{G_F s}{64\sqrt{2}\pi} \frac{M_Z^2}{(s - M_Z^2)}\right]. \tag{A.65}$$

Now, in order to find the result of Eq. (3.49) it is necessary to rewrite the total asymmetry factorizing the SM contribution as

$$A_{\rm FB}^{tot} = A_{\rm FB}^{\rm SM}\left[1 + \delta_{\rm FB}^{\rm NP}\right] \tag{A.66}$$

with

$$\delta_{\rm FB}^{\rm NP} = \frac{A_{\rm FB}^{\rm NP}}{A_{\rm FB}^{\rm SM}}. \tag{A.67}$$

For this purpose let's firstly rewrite the total asymmetry as

$$A_{\rm FB}^{tot} = \frac{(\sigma_{\rm F}-\sigma_{\rm B})|_{\rm SM} + (\sigma_{\rm F}-\sigma_{\rm B})|_{\rm NP}}{\sigma_{\rm SM}\left[1+\frac{3s}{4\pi\alpha^2 A}\sigma_{\rm NP}\right]} = \\ = A_{\rm FB}^{\rm SM}\left[\frac{1}{\left(1+\frac{3s}{4\pi\alpha^2 A}\sigma_{\rm NP}\right)} + \frac{(\sigma_{\rm F}-\sigma_{\rm B})|_{\rm NP}}{(\sigma_{\rm F}-\sigma_{\rm B})|_{\rm SM}\left(1+\frac{3s}{4\pi\alpha^2 A}\sigma_{\rm NP}\right)}\right],$$

where the denominator in the first equality is nothing else that the total cross section in which the SM part has been factorized. Eq. (A.66) and the explicit expression of (A.67) are immediately recovered and found after the expansion

$$\frac{1}{\left(1+\frac{3s}{4\pi\alpha^2 A}\sigma_{\rm NP}\right)} \approx \left(1-\frac{3s}{4\pi\alpha^2 A}\sigma_{\rm NP}\right),$$

which provides

$$\delta_{\rm FB}^{\rm NP} = -\frac{3s}{4\pi\alpha^2 A}\sigma_{\rm NP} + \frac{(\sigma_{\rm F}-\sigma_{\rm B}\,)|_{\rm NP}}{(\sigma_{\rm F}-\sigma_{\rm B})|_{\rm SM}}. \tag{A.68}$$

Exploiting the approximated expressions of A and B aforementioned, these two term read explicitly

$$\frac{3s}{4\pi\alpha^2 A}\sigma_{\rm NP} = \frac{2s(s-M_Z^2)}{[128\pi^2\alpha^2(s-M_Z^2)^2 + G_F^2 s^2 M_Z^4]}\left[\frac{8\sqrt{2}\pi\alpha a_V(s-M_Z^2)+a_A G_F s M_Z^2}{\Lambda^2\sqrt{2}}\right]$$

$$\frac{(\sigma_{\rm F}-\sigma_{\rm B})|_{\rm NP}}{(\sigma_{\rm F}-\sigma_{\rm B})|_{\rm SM}} = -\frac{1}{16\pi\alpha G_F M_Z^2\Lambda^2}\left[8\sqrt{2}\pi\alpha a_A(s-M_Z^2)+a_V G_F s M_Z^2\right].$$

In Eq. (3.49) the term $\delta_{\rm FB}^{\rm NP}$ is expressed by factorizing the function

$$r(s) = \frac{[128\pi^2\alpha^2(s-M_Z^2)^2 - G_F^2 s^2 M_Z^4]}{[128\pi^2\alpha^2(s-M_Z^2)^2 + G_F^2 s^2 M_Z^4]}$$

and, as it can been seen from the previous expressions, there are some efforts to deal with in trying to do the same also in (A.68). Since the computation is very long (although conceptually simple) and having just explained how it should be done, I will report directly the result, which is

$$\delta_{\rm FB}^{\rm NP} = -\frac{r(s)}{\Lambda^2}\frac{1}{[128\pi^2\alpha^2(s-M_Z^2)^2 - G_F^2 s^2 M_Z^4]}\times \\ \times\left[-\frac{64\sqrt{2}\pi^2\alpha^2 a_A(s-M_Z^2)^3}{G_F M_Z^2} + \frac{a_V G_F^2 s^3 M_Z^4}{48\pi\alpha} + \frac{3a_A G_F s M_Z^2(s-M_Z^2)}{\sqrt{2}} + 24\pi\alpha a_V(s-M_Z^2)^2\right] \tag{A.69}$$

The last passage consists in making a division between polynomials. Defining

- $y = s - M_Z^2$

- $P(y) = \left[-\frac{64\sqrt{2}\pi^2\alpha^2 a_A y^3}{G_F M_Z^2} + \frac{a_V G_F^2 s^3 M_Z^4}{48\pi\alpha} + \frac{3a_A G_F s M_Z^2 y}{\sqrt{2}} + 24\pi\alpha a_V y^2\right]$
- $D(y) = [128\pi^2\alpha^2 y^2 - G_F^2 s^2 M_Z^4]$
- $R(y)$ what remains from the division
- $Q(y)$ the quotient

the following relation holds:

$$\frac{P(y)}{D(y)} = Q(y) + \frac{R(y)}{D(y)}.$$

In particular

- The quotient results
$$Q(y) = \frac{a_V s}{16\pi\alpha} - \frac{a_A y}{\sqrt{2}G_F M_Z^2} \tag{A.70}$$
- The rest is
$$R(y) = \frac{4a_A s^2 G_F M_Z^2 y}{\sqrt{2}} + \frac{a_V G_F^2 s^3 M_Z^4}{4\pi\alpha} \tag{A.71}$$

Neglecting $R(y)$, [25] then it follows

$$\delta_{\rm FB}^{\rm NP} = \frac{r(s)}{\Lambda^2}\left(\frac{a_A(s-M_Z^2)}{\sqrt{2}G_F M_Z^2} - \frac{a_V s}{16\pi\alpha}\right). \tag{A.72}$$

which is precisely Eq. (3.49).
Although this seems to be the only way to proceed, there is a better and faster approach which can be employed: the idea is to directly sum the amplitudes $\mathcal{M}_Z$ and all the $\mathcal{M}_i$, with $i = 7, 8, 9, 10$, obtaining something which has the same structure of the weak amplitude but with redefined chiral coefficients. This way requires firstly to rewrite $\mathcal{M}_Z$ in terms of $g_{R,L}$ rather than $g_{V,A}$, which is

$$\begin{aligned}\mathcal{M}_Z = \frac{2iG_F}{\sqrt{2}}\frac{M_Z^2}{s-M_Z^2}[&g_L^2\bar{\mu}(p_3)\gamma^\mu(1-\gamma_5)\mu(p_4)\bar{e}\gamma_\mu(1-\gamma_5)e(p_1)+\\ &g_R^2\bar{\mu}(p_3)\gamma^\mu(1+\gamma_5)\mu(p_4)\bar{e}\gamma_\mu(1+\gamma_5)e(p_1)+\\ &g_L g_R\bar{\mu}(p_3)\gamma^\mu(1-\gamma_5)\mu(p_4)\bar{e}\gamma_\mu(1+\gamma_5)e(p_1)+\\ &g_L g_R\bar{\mu}(p_3)\gamma^\mu(1+\gamma_5)\mu(p_4)\bar{e}\gamma_\mu(1-\gamma_5)e(p_1)].\end{aligned} \tag{A.73}$$

Then, summing all the non vanishing NP contributions, the total amplitude reads

$$\begin{aligned}\mathcal{M}_{tot} = \frac{2iG_F}{\sqrt{2}}\frac{M_Z^2}{s-M_Z^2}[&C\bar{\mu}(p_3)\gamma^\mu(1-\gamma_5)\mu(p_4)\bar{e}\gamma_\mu(1-\gamma_5)e(p_1)+\\ &D\bar{\mu}(p_3)\gamma^\mu(1+\gamma_5)\mu(p_4)\bar{e}\gamma_\mu(1+\gamma_5)e(p_1)+\\ &E\bar{\mu}(p_3)\gamma^\mu(1-\gamma_5)\mu(p_4)\bar{e}\gamma_\mu(1+\gamma_5)e(p_1)+\\ &E\bar{\mu}(p_3)\gamma^\mu(1+\gamma_5)\mu(p_4)\bar{e}\gamma_\mu(1-\gamma_5)e(p_1)]\end{aligned} \tag{A.74}$$

[25] I checked for different energy ranges and I found that $\frac{R(y)}{D(y)}$ is really suppressed respect to $Q(y)$ unless $\sqrt{s} = M_Z$ or very closed to M_Z; howeve,r in that case computations must be done again in order to consider the factor $i\Gamma_Z M_Z$, as previously explained, has been removed.

where

$$C = g_L^2 + \frac{\sqrt{2}a_7}{8G_F\Lambda^2}\frac{s - M_Z^2}{M_Z^2}$$

$$D = g_R^2 + \frac{\sqrt{2}a_8}{8G_F\Lambda^2}\frac{s - M_Z^2}{M_Z^2}$$

$$E = g_L g_R + \frac{\sqrt{2}(a_9 + a_{10})}{8G_F\Lambda^2}\frac{s - M_Z^2}{M_Z^2}.$$

It is easy, now, to understand how one should proceed: the SM prediction of the asymmetry must be firstly rewritten in terms of the usual $g_{L,R}$ by means of the definitions of $g_{V,A}$ and, then, they must be substituted in terms of the new coefficients C, D, E and of the NP pieces trough the above relations.

A.5 LFV computation

In this section I will provide details on the derivation of Eq. (3.59) [64]. I rename the five operators as

$$\begin{aligned}\mathcal{Q}_1 &= (\bar{\mu}_L e_R)(\bar{\mu}_L e_R)\\ \mathcal{Q}_2 &= (\bar{\mu}_R e_L)(\bar{\mu}_R e_L)\\ \mathcal{Q}_3 &= (\bar{\mu}_L e_R)(\bar{\mu}_R e_L)\\ \mathcal{Q}_4 &= (\bar{\mu}_L \gamma^\alpha e_L)(\bar{\mu}_L \gamma_\alpha e_L)\\ \mathcal{Q}_5 &= (\bar{\mu}_R \gamma^\alpha e_R)(\bar{\mu}_R \gamma_\alpha e_R)\end{aligned}$$

and in the following I will focus $\mathcal{Q}_3$; nevertheless, the computation is perfectly analogous also for the other four operators and for this reason it will be only sketched.
First of all, let's notice that this operator can be rewritten in a different way by means of the third Fierz identity in (A.1) as

$$(\bar{\mu}_L e_R)(\bar{\mu}_R e_L) = -\frac{1}{2}(\bar{\mu}_R \gamma^\mu e_R)(\bar{\mu}_L \gamma_\mu e_L). \tag{A.75}$$

However, although the result must (and indeed it is) the same in both cases, the computation is much more simple without exploiting such an identity. The corresponding matrix element, then, is simply

$$\langle \overline{\mathrm{Mu}}|\mathcal{Q}_3|\mathrm{Mu}\rangle = \langle \overline{\mathrm{Mu}}|\frac{b_3(\bar{\mu}_L e_R)(\bar{\mu}_R e_L)}{\Lambda^2}|\mathrm{Mu}\rangle. \tag{A.76}$$

Here the non-relativistic (NR) bound states are normalized as $\langle \mathrm{Mu}(\vec{p})|\mathrm{Mu}(\vec{p'})\rangle = 2E_p(2\pi)^3\delta^3(\vec{p}-\vec{p'})$ and, being the Muonium essentially a Coulomb bound state of μ^+ and e^-, it can be expressed as [65]

$$|\mathrm{Mu}\rangle = \sqrt{\frac{2M_M}{2m2M}}\int \frac{d^3p}{(2\pi)^3}\sqrt{2E_p}\sqrt{2E'_p}\tilde{\varphi}(p)a_p^{(e)\dagger}b_{p'}^{(\mu)\dagger}|0\rangle, \tag{A.77}$$

where M_M is the Muonium mass and $\tilde{\varphi}$ is the Fourier transform of the spatial wave function describing the bound state, i.e.

$$\tilde{\varphi}(p)\int dr\varphi(\vec{r})e^{i\vec{p}\cdot\vec{r}}.$$

Exploiting also the electron and muon fields as

$$\psi(x) = \int \frac{d^3p}{(2\pi)^3}\frac{1}{\sqrt{2E_p}}\sum_s\left[a_p^s u^s(p)e^{-ipx} + b_p^{\dagger s}v^s(p)e^{ipx}\right]$$

and using the anticommutation relation among the ladder operators $\{a_p, a^\dagger_{p'}\} = (2\pi)^3\delta^3(p-p')$, it is possible to rewrite Eq. (A.76) in the form

$$\begin{aligned}\langle Q_3\rangle = &[(\bar{u}P_L v)(\bar{v}P_R u) + (\bar{v}P_L u)(\bar{u}P_R v)\\ &-(\bar{v}P_L v)(\bar{u}P_R u) - (\bar{u}P_L u)(\bar{v}P_R v)]\times\left|\int\frac{d^3p}{(2\pi)^3}\widetilde{\varphi}(p)\right|^2.\end{aligned} \tag{A.78}$$

Here u and v are nothing else that spinors, whose dependence on the momentum has been neglected being in the NR regime; their explicit expressions are

$$u(m) = \sqrt{m}\begin{pmatrix}\xi\\ \xi\end{pmatrix} \qquad v(m) = \sqrt{m}\begin{pmatrix}\eta\\ -\eta\end{pmatrix}$$
$$\bar{u}(M) = \sqrt{M}(\xi^\dagger, \xi^\dagger)\gamma^0 \quad \bar{v}(M) = \sqrt{M}(\eta^\dagger, -\eta^\dagger)\gamma^0,$$

where ξ and η are two-component spinor such that $\xi^\dagger\xi = \eta^\dagger\eta = 1$; moreover, in the Weyl chiral basis the γ's have the form

$$\gamma_0 = \begin{pmatrix}\mathbb{0} & \mathbb{1}\\ \mathbb{1} & \mathbb{0}\end{pmatrix} \quad \gamma_\alpha = \begin{pmatrix}\mathbb{0} & \sigma_\alpha\\ \bar{\sigma_\alpha} & \mathbb{0}\end{pmatrix} \quad \gamma_5 = \begin{pmatrix}-\mathbb{1} & \mathbb{0}\\ \mathbb{0} & \mathbb{1}\end{pmatrix},$$

with $\sigma^\alpha = (\mathbf{1}, \vec{\sigma})$ and $\bar{\sigma}^\alpha = (\mathbf{1}, -\vec{\sigma})$.
Then, the first term in the squared brackets of Eq. is explicitly

$$\begin{aligned}(\bar{u}P_L v)\,(\bar{v}P_R u) &= \frac{1}{4}mM\left(\xi^\dagger, \xi^\dagger\right)\gamma^0\left(1-\gamma^5\right)\begin{pmatrix}\eta\\ -\eta\end{pmatrix}\left(\eta^\dagger, -\eta^\dagger\right)\gamma^0\left(1+\gamma^5\right)\begin{pmatrix}\xi\\ \xi\end{pmatrix} =\\ &= mM\left(\xi^\dagger, \xi^\dagger\right)\begin{pmatrix}\eta\\ 0\end{pmatrix}\left(\eta^\dagger, -\eta^\dagger\right)\begin{pmatrix}0\\ \xi\end{pmatrix} =\\ &= -mM\left(\xi^\dagger\eta\right)\left(\eta^\dagger\xi\right).\end{aligned} \tag{A.79}$$

Focusing only on the projection onto the singlet state, which can be obtained by means of the substitution [65] $\xi^\dagger\eta = 1/(\sqrt{2})$, the previous result simply reads $-mM/2$. Notice that these steps are precisely the same that have to be followed in computing the scond piece in (A.5).
For what concerns the third term, its computation is

$$\begin{aligned}(\bar{v}P_L v)\,(\bar{u}P_R u) &= \frac{1}{4}mM\left(\eta^\dagger, -\eta^\dagger\right)\gamma^0\left(1-\gamma^5\right)\begin{pmatrix}\eta\\ -\eta\end{pmatrix}\left(\xi^\dagger, \xi^\dagger\right)\gamma^0\left(1+\gamma^5\right)\begin{pmatrix}\xi\\ \xi\end{pmatrix} =\\ &= mM\left(\eta^\dagger, -\eta^\dagger\right)\begin{pmatrix}\eta\\ 0\end{pmatrix}\left(\xi^\dagger, \xi^\dagger\right)\begin{pmatrix}0\\ \xi\end{pmatrix} = mM\left(\eta^\dagger\eta\right)\left(\xi^\dagger\xi\right) = mM.\end{aligned} \tag{A.80}$$

Also in this case, these steps are the same of those necessary for the forth piece in (A.5). Summing all the four contributions, we end up with

$$\langle Q_3\rangle = -6mM\left|\int\frac{d^3p}{(2\pi)^3}\tilde{\varphi}(p)\right|^2. \tag{A.81}$$

On the other side, the term $\left|\int\frac{d^3p}{(2\pi)^3}\tilde{\varphi}(p)\right|^2$ is, almost by definition, the squared modulus of the spatial wavefunction at zero distance, properly normalized with the fermion masses as $|\varphi(0)|^2/4mM$. Remembering that for a NR Coulombic bound state the wave function in the ground state is

$$\varphi(r) = \frac{1}{\sqrt{\pi a_0^3}}e^{-r/a_0},$$

the final expression for this matrix element reads

$$\langle\overline{\mathrm{Mu}}|\frac{b_3(\bar{\mu}_L e_R)(\bar{\mu}_R e_L)}{\Lambda^2}|\mathrm{Mu}\rangle = -\frac{b_3}{\Lambda^2}\frac{|\varphi(0)|^2}{4mM}6mM = -\frac{3b_3}{2\pi\Lambda^2 a_0^3} \tag{A.82}$$

where $a_0 = (m\alpha)^{-1}$ is the Bohr radius [26].
The computation for operators $\mathcal{Q}_1$ and $\mathcal{Q}_2$ is almost identical; the only difference that has to be taken into account is the fact that in these cases there are either two P_L or two P_R and not one of both of them. Take, for example, $\mathcal{Q}_2$; its matrix element reads

$$\begin{aligned}\langle Q_2\rangle = &\left[(\bar{u}P_L v)\,(\bar{v}P_L u) + (\bar{v}P_L u)\,(\bar{u}P_L v)\right.\\ &\left. - (\bar{v}P_L v)\,(\bar{u}P_L u) - (\bar{u}P_L u)\,(\bar{v}P_L v)\right] \times \left|\int \frac{d^3p}{(2\pi)^3}\widetilde{\varphi}(p)\right|^2.\end{aligned}$$

The computation of the first term in the squared brackets follows the sames steps of (A.79), but with a difference in the final sign due to the mentioned difference in the projectors:

$$\begin{aligned}(\bar{u}P_L v)\,(\bar{v}P_L u) &= \frac{1}{4}mM\left(\xi^\dagger,\xi^\dagger\right)\gamma^0\left(1-\gamma^5\right)\begin{pmatrix}\eta\\-\eta\end{pmatrix}\left(\eta^\dagger,-\eta^\dagger\right)\gamma^0\left(1-\gamma^5\right)\begin{pmatrix}\xi\\\xi\end{pmatrix} =\\ &= mM\left(\xi^\dagger,\xi^\dagger\right)\begin{pmatrix}\eta\\0\end{pmatrix}\left(\eta^\dagger,-\eta^\dagger\right)\begin{pmatrix}\xi\\0\end{pmatrix} =\\ &= mM\left(\xi^\dagger\eta\right)\left(\eta^\dagger\xi\right) = \frac{mM}{2}.\end{aligned}$$

The final matrix elements for these two operators are

$$\begin{aligned}\langle\overline{\mathrm{Mu}}|\frac{b_1(\bar{\mu}_L e_R)(\bar{\mu}_L e_R)}{\Lambda^2}|\mathrm{Mu}\rangle &= \frac{b_1}{2\pi\Lambda^2 a_0^3}\\ \langle\overline{\mathrm{Mu}}|\frac{b_2(\bar{\mu}_R e_L)(\bar{\mu}_R e_L)}{\Lambda^2}|\mathrm{Mu}\rangle &= \frac{b_2}{2\pi\Lambda^2 a_0^3}.\end{aligned} \tag{A.83}$$

Finally, let's briefly see $\mathcal{Q}_4$ and $\mathcal{Q}_5$. As already pointed out, as well as for the computations already performed, the *modus operandi* is the same. The only difference is only the presence of the γ's, whose presence is not so problematic as it could appear. Let's take $\mathcal{Q}_4$ (the reasonment holds also for $\mathcal{Q}_5$); its matrix element is

$$\begin{aligned}\langle Q_4\rangle = &\left[(\bar{u}\gamma_\alpha P_L v)\,(\bar{v}\gamma^\alpha P_L u) + (\bar{v}\gamma_\alpha P_L u)\,(\bar{u}\gamma^\alpha P_L v)\right.\\ &\left. - (\bar{v}\gamma_\alpha P_L v)\,(\bar{u}\gamma^\alpha P_L u) - (\bar{u}\gamma_\alpha P_L u)\,(\bar{v}\gamma^\alpha P_L v)\right] \times \left|\int \frac{d^3p}{(2\pi)^3}\widetilde{\varphi}(p)\right|^2.\end{aligned}$$

Focusing, again, on the first term in the squared brakets, it turns out to be

$$\begin{aligned}(\bar{u}\gamma_\alpha P_L v)\,(\bar{v}\gamma^\alpha P_L u) &= \frac{1}{4}mM\left(\xi^\dagger,\xi^\dagger\right)\gamma^0\gamma^\alpha\left(1-\gamma^5\right)\begin{pmatrix}\eta\\-\eta\end{pmatrix}\left(\eta^\dagger,-\eta^\dagger\right)\gamma^0\gamma_\alpha\left(1-\gamma^5\right)\begin{pmatrix}\xi\\\xi\end{pmatrix} =\\ &= mM\left(\xi^\dagger,\xi^\dagger\right)\begin{pmatrix}\bar{\sigma}^\alpha & 0\\0 & \sigma^\alpha\end{pmatrix}\begin{pmatrix}\eta\\0\end{pmatrix}\left(\eta^\dagger,-\eta^\dagger\right)\begin{pmatrix}\bar{\sigma}^\alpha & 0\\0 & \sigma^\alpha\end{pmatrix}\begin{pmatrix}\xi\\0\end{pmatrix} =\\ &= mM\left(\xi^\dagger\bar{\sigma}^\alpha\eta\right)\left(\eta^\dagger\sigma_\alpha\xi\right) = mM\,\mathrm{Tr}\left[\eta\xi^\dagger\bar{\sigma}^\alpha\right]\mathrm{Tr}\left[\xi\eta^\dagger\sigma_\alpha\right].\end{aligned}$$

[26] Actually it should be $a_0 = \mu\alpha$, with μ the reduced mass of the system; nevertheless, being $m \ll M$, it is a very good approximation to take $\mu \approx m$

Projecting onto the singlet state, i.e. using the relation

$$\eta\xi^\dagger = \frac{1}{\sqrt{2}}\mathbb{1},$$

the previous term becomes simply

$$(\bar{u}\gamma_\alpha P_L v)\,(\bar{v}\gamma^\alpha P_L u) = \frac{mM}{2}\,\mathrm{Tr}\,[\bar{\sigma}^\alpha]\,\mathrm{Tr}\,[\sigma_\alpha] = 2mM,$$

being only the $\alpha = 0$ contribution not traceless.
Finally, the two amplitudes explicitly read

$$\begin{aligned}\langle\overline{\mathrm{Mu}}|\frac{b_4(\bar{\mu}_L\gamma_\alpha e_L)(\bar{\mu}_R\gamma^\alpha e_R)}{\Lambda^2}|\mathrm{Mu}\rangle &= \frac{4b_4}{2\pi\Lambda^2 a_0^3}\\ \langle\overline{\mathrm{Mu}}|\frac{b_5(\bar{\mu}_R\gamma_\alpha e_R)(\bar{\mu}_R\gamma^\alpha e_R)}{\Lambda^2}|\mathrm{Mu}\rangle &= \frac{4b_5}{2\pi\Lambda^2 a_0^3}.\end{aligned} \tag{A.84}$$

A.6 Dimension six $U(1)_{em}$ invariant operators

Here I provide the $U(1)_{em}$ dimension-six operators made of the field content of the Standard Model which allow to construct the most general LEFT [63].

$(\bar{L}L)(\bar{R}R)$	
$Q^{V}_{\nu e}$	$(\bar{\nu}_{Lp}\gamma^{\mu}\nu_{Lr})(\bar{e}_{Rs}\gamma_{\mu}e_{Rt})$
Q^{V}_{ee}	$(\bar{e}_{Lp}\gamma^{\mu}e_{Lr})(\bar{e}_{Rs}\gamma_{\mu}e_{Rt})$
$Q^{V}_{\nu u}$	$(\bar{\nu}_{Lp}\gamma^{\mu}\nu_{Lr})(\bar{u}_{Rs}\gamma_{\mu}u_{Rt})$
$Q^{V}_{\nu d}$	$(\bar{\nu}_{Lp}\gamma^{\mu}\nu_{Lr})(\bar{d}_{Rs}\gamma_{\mu}d_{Rt})$
Q^{V}_{eu}	$(\bar{e}_{Lp}\gamma^{\mu}e_{Lr})(\bar{u}_{Rs}\gamma_{\mu}u_{Rt})$
Q^{V}_{ed}	$(\bar{e}_{Lp}\gamma^{\mu}e_{Lr})(\bar{d}_{Rs}\gamma_{\mu}d_{Rt})$
Q^{V}_{ue}	$(\bar{u}_{Lp}\gamma^{\mu}u_{Lr})(\bar{e}_{Rs}\gamma_{\mu}e_{Rt})$
Q^{V}_{de}	$(\bar{d}_{Lp}\gamma^{\mu}d_{Lr})(\bar{e}_{Rs}\gamma_{\mu}e_{Rt})$
$Q^{V}_{\nu edu}$	$(\bar{\nu}_{Lp}\gamma^{\mu}e_{Lr})(\bar{d}_{Rs}\gamma_{\mu}u_{Rt})$
$Q^{V(1)}_{uu}$	$(\bar{u}_{Lp}\gamma^{\mu}u_{Lr})(\bar{u}_{Rs}\gamma_{\mu}u_{Rt})$
$Q^{V(8)}_{uu}$	$(\bar{u}_{Lp}\gamma^{\mu}T^{A}u_{Lr})(\bar{u}_{Rs}\gamma_{\mu}T^{A}u_{Rt})$
$Q^{V(1)}_{ud}$	$(\bar{u}_{Lp}\gamma^{\mu}u_{Lr})(\bar{d}_{Rs}\gamma_{\mu}d_{Rt})$
$Q^{V(8)}_{ud}$	$(\bar{u}_{Lp}\gamma^{\mu}T^{A}u_{Lr})(\bar{d}_{Rs}\gamma_{\mu}T^{A}d_{Rt})$
$Q^{(1)}_{du}$	$(\bar{d}_{Lp}\gamma^{\mu}d_{Lr})(\bar{u}_{Rs}\gamma_{\mu}u_{Rt})$
$Q^{V(8)}_{du}$	$(\bar{d}_{Lp}\gamma^{\mu}T^{A}d_{Lr})(\bar{u}_{Rs}\gamma_{\mu}T^{A}u_{Rt})$
$Q^{V(1)}_{dd}$	$(\bar{d}_{Lp}\gamma^{\mu}d_{Lr})(\bar{d}_{Rs}\gamma_{\mu}d_{Rt})$
$Q^{V(8)}_{dd}$	$(\bar{d}_{Lp}\gamma^{\mu}T^{A}d_{Lr})(\bar{d}_{Rs}\gamma_{\mu}T^{A}d_{Rt})$
$Q^{V(1)}_{uddu}$	$(\bar{u}_{Lp}\gamma^{\mu}d_{Lr})(\bar{d}_{Rs}\gamma_{\mu}u_{Rt})$
$Q^{V(8)}_{uddu}$	$(\bar{u}_{Lp}\gamma^{\mu}T^{A}d_{Lr})(\bar{d}_{Rs}\gamma_{\mu}T^{A}u_{Rt})$

$(\bar{L}L)(\bar{L}L)$ and $(\bar{R}R)(\bar{R}R)$	
$Q^{V}_{\nu\nu}$	$(\bar{\nu}_{Lp}\gamma^{\mu}\nu_{Lr})(\bar{\nu}_{Ls}\gamma_{\mu}\nu_{Lt})$
Q^{V}_{ee}	$(\bar{e}_{Lp}\gamma^{\mu}e_{Lr})(\bar{e}_{Ls}\gamma_{\mu}e_{Lt})$
$Q^{V}_{\nu e}$	$(\bar{\nu}_{Lp}\gamma^{\mu}\nu_{Lr})(\bar{e}_{Ls}\gamma_{\mu}e_{Lt})$
$Q^{V}_{\nu u}$	$(\bar{\nu}_{Lp}\gamma^{\mu}\nu_{Lr})(\bar{u}_{Ls}\gamma_{\mu}u_{Lt})$
$Q^{V}_{\nu d}$	$(\bar{\nu}_{Lp}\gamma^{\mu}\nu_{Lr})(\bar{d}_{Ls}\gamma_{\mu}d_{Lt})$
Q^{V}_{eu}	$(\bar{e}_{Lp}\gamma^{\mu}e_{Lr})(\bar{u}_{Ls}\gamma_{\mu}u_{Lt})$
Q^{V}_{ed}	$(\bar{e}_{Lp}\gamma^{\mu}e_{Lr})(\bar{d}_{Ls}\gamma_{\mu}d_{Lt})$
$Q^{V}_{\nu edu}$	$(\bar{\nu}_{Lp}\gamma^{\mu}e_{Lr})(\bar{d}_{Ls}\gamma_{\mu}u_{Lt})$
Q^{V}_{uu}	$(\bar{u}_{Lp}\gamma^{\mu}u_{Lr})(\bar{u}_{Ls}\gamma_{\mu}u_{Lt})$
Q^{V}_{dd}	$(\bar{d}_{Lp}\gamma^{\mu}d_{Lr})(\bar{d}_{Ls}\gamma_{\mu}d_{Lt})$
$Q^{V(1)}_{ud}$	$(\bar{u}_{Lp}\gamma^{\mu}u_{Lr})(\bar{d}_{Ls}\gamma_{\mu}d_{Lt})$
$Q^{V(8)}_{ud}$	$(\bar{u}_{Lp}\gamma^{\mu}T^{A}u_{Lr})(\bar{d}_{Ls}\gamma_{\mu}T^{A}d_{Lt})$
Q^{V}_{ee}	$(\bar{e}_{Rp}\gamma^{\mu}e_{Rr})(\bar{e}_{Rs}\gamma_{\mu}e_{Rt})$
Q^{V}_{ee}	$(\bar{e}_{Rp}\gamma^{\mu}e_{Rr})(\bar{e}_{Rs}\gamma_{\mu}e_{Rt})$
Q^{V}_{eu}	$(\bar{e}_{Rp}\gamma^{\mu}e_{Rr})(\bar{u}_{Rs}\gamma_{\mu}u_{Rt})$
Q^{V}_{ed}	$(\bar{e}_{Rp}\gamma^{\mu}e_{Rr})(\bar{d}_{Rs}\gamma_{\mu}d_{Rt})$
Q^{V}_{uu}	$(\bar{u}_{Rp}\gamma^{\mu}u_{Rr})(\bar{u}_{Rs}\gamma_{\mu}u_{Rt})$
Q^{V}_{dd}	$(\bar{d}_{Rp}\gamma^{\mu}d_{Rr})(\bar{d}_{Rs}\gamma_{\mu}d_{Rt})$
$Q^{V(1)}_{ud}$	$(\bar{u}_{Rp}\gamma^{\mu}u_{Rr})(\bar{d}_{Rs}\gamma_{\mu}d_{Rt})$
$Q^{V(8)}_{ud}$	$(\bar{u}_{Rp}\gamma^{\mu}T^{A}u_{Rr})(\bar{d}_{Rs}\gamma_{\mu}T^{A}d_{Rt})$

$(\bar{L}R)(\bar{L}R)$	
Q^{S}_{ee}	$(\bar{e}_{Lp}e_{Rr})(\bar{e}_{Ls}e_{Rt})$
Q^{S}_{eu}	$(\bar{e}_{Lp}e_{Rr})(\bar{u}_{Ls}u_{Rt})$
Q^{T}_{eu}	$(\bar{e}_{Lp}\sigma^{\mu\nu}e_{Rr})(\bar{u}_{Ls}\sigma_{\mu\nu}u_{Rt})$
Q^{S}_{ed}	$(\bar{e}_{Lp}e_{Rr})(\bar{d}_{Ls}d_{Rt})$
Q^{T}_{ed}	$(\bar{e}_{Lp}\sigma^{\mu\nu}e_{Rr})(\bar{d}_{Ls}\sigma_{\mu\nu}d_{Rt})$
$Q^{S}_{\nu edu}$	$(\bar{\nu}_{Lp}e_{Rr})(\bar{d}_{Ls}u_{Rt})$
$Q^{T}_{\nu edu}$	$(\bar{\nu}_{Lp}\sigma^{\mu\nu}e_{Rr})(\bar{d}_{Ls}\sigma_{\mu\nu}u_{Rt})$
$Q^{S(1)}_{uu}$	$(\bar{u}_{Lp}u_{Rr})(\bar{u}_{Ls}u_{Rt})$

$(\bar{L}R)(\bar{L}R)$	
$Q^{S(8)}_{uu}$	$(\bar{u}_{Lp}T^{A}u_{Rr})(\bar{u}_{Ls}T^{A}u_{Rt})$
$Q^{S(1)}_{ud}$	$(\bar{u}_{Lp}u_{Rr})(\bar{d}_{Ls}d_{Rt})$
$Q^{S(8)}_{ud}$	$(\bar{u}_{Lp}T^{A}u_{Rr})(\bar{d}_{Ls}T^{A}d_{Rt})$
$Q^{S(1)}_{dd}$	$(\bar{d}_{Lp}d_{Rr})(\bar{d}_{Ls}d_{Rt})$
$Q^{S(8)}_{dd}$	$(\bar{d}_{Lp}T^{A}d_{Rr})(\bar{d}_{Ls}T^{A}d_{Rt})$
$Q^{S(1)}_{uddu}$	$(\bar{u}_{Lp}d_{Rr})(\bar{d}_{Ls}u_{Rt})$
$Q^{S(8)}_{uddu}$	$(\bar{u}_{Lp}T^{A}d_{Rr})(\bar{d}_{Ls}T^{A}u_{Rt})$

X^3 and $(\bar{L}R)(\bar{R}L)$	
Q_{G}	$f^{ABC}G^{A\nu}_{\mu}G^{B\rho}_{\nu}G^{C\mu}_{\rho}$
$Q_{\tilde{G}}$	$f^{ABC}\tilde{G}^{A\nu}_{\mu}G^{B\rho}_{\nu}G^{C\mu}_{\rho}$
Q^{S}_{eu}	$(\bar{e}_{Lp}e_{Rr})(\bar{u}_{Rs}u_{Lt})$
Q^{S}_{ed}	$(\bar{e}_{Lp}e_{Rr})(\bar{d}_{Rs}d_{Lt})$
$Q^{S}_{\nu edu}$	$(\bar{\nu}_{Lp}e_{Rr})(\bar{d}_{Rs}u_{Lt})$

A.7 Dimension six $SU(3)_C \otimes SU(2)_L \otimes U(1)_Y$ invariant operators

Here I provide the 59 $SU(3)_C \otimes SU(2)_L \otimes U(1)_Y$ dimension-six operators made of the field content of the Standard Model which allow to construct the most general SMEFT.

X^3	
Q_G	$f^{ABC}G^{A\nu}_{\mu}G^{B\rho}_{\nu}G^{C\mu}_{\rho}$
$Q_{\tilde{G}}$	$f^{ABC}\tilde{G}^{A\nu}_{\mu}G^{B\rho}_{\nu}G^{C\mu}_{\rho}$
Q_W	$\epsilon^{IJK}W^{I\nu}_{\mu}W^{J\rho}_{\nu}W^{K\mu}_{\rho}$
$Q_{\tilde{W}}$	$\epsilon^{IJK}\tilde{W}^{I\nu}_{\mu}W^{J\rho}_{\nu}W^{K\mu}_{\rho}$

ϕ^6 and $\phi^4 D^2$	
Q_ϕ	$(\phi^\dagger\phi)^3$
$Q_{\phi\Box}$	$(\phi^\dagger\phi)\Box(\phi^\dagger\phi)$
$Q_{\phi D}$	$(\phi^\dagger D^\mu\phi)^*(\phi^\dagger D^\mu\phi)$

$\psi^2\phi^3$	
$Q_{e\phi}$	$(\phi^\dagger\phi)(\bar{l}_p e_r\phi)$
$Q_{u\phi}$	$(\phi^\dagger\phi)(\bar{q}_p u_r\phi)$
Q_ϕ	$(\phi^\dagger\phi)(\bar{q}_p d_r\phi)$

$\psi^2 X\phi + h.c.$	
$Q_{\phi G}$	$(\phi^\dagger\phi)G^A_{\mu\nu}G^{A\mu\nu}$
$Q_{\phi\tilde{G}}$	$(\phi^\dagger\phi)\tilde{G}^A_{\mu\nu}G^{A\mu\nu}$
$Q_{\phi W}$	$(\phi^\dagger\phi)W^I_{\mu\nu}W^{I\mu\nu}$
$Q_{\phi\tilde{W}}$	$(\phi^\dagger\phi)\tilde{W}^I_{\mu\nu}W^{I\mu\nu}$
$Q_{\phi B}$	$(\phi^\dagger\phi)B^I_{\mu\nu}B^{I\mu\nu}$
$Q_{\phi\tilde{B}}$	$(\phi^\dagger\phi)\tilde{B}^I_{\mu\nu}B^{I\mu\nu}$
$Q_{\phi WB}$	$(\phi^\dagger\tau^I\phi)W^I_{\mu\nu}B_{\mu\nu}$
$Q_{\phi\tilde{W}B}$	$(\phi^\dagger\tau^I\phi)\tilde{W}^I_{\mu\nu}B_{\mu\nu}$

$X^2\phi^2$	
Q_{eW}	$(\bar{\ell}_p\sigma^{\mu\nu}e_r)\tau^I\phi W^I_{\mu\nu}$
Q_{eB}	$(\bar{\ell}_p\sigma^{\mu\nu}e_r)\phi B_{\mu\nu}$
Q_{uG}	$(\bar{q}_p\sigma^{\mu\nu}u_r)T^A\tilde{\phi}G^A_{\mu\nu}$
Q_{uW}	$(\bar{q}_p\sigma^{\mu\nu}u_r)\tau^I\tilde{\phi}W^I_{\mu\nu}$
Q_{uB}	$(\bar{q}_p\sigma^{\mu\nu}u_r)\tilde{\phi}B_{\mu\nu}$
Q_{dG}	$(\bar{q}_p\sigma^{\mu\nu}d_r)T^A\phi G^A_{\mu\nu}$
Q_{dW}	$(\bar{q}_p\sigma^{\mu\nu}d_r)\tau^I\phi W^I_{\mu\nu}$
Q_{dB}	$(\bar{q}_p\sigma^{\mu\nu}u_r)\phi B_{\mu\nu}$

$\psi^2\phi^2 D$	
$Q^{(1)}_{\phi\ell}$	$(\phi^\dagger i\bar{D}^\mu\phi)(\bar{\ell}_p\gamma_\mu\ell_r)$
$Q^{(3)}_{\phi\ell}$	$(\phi^\dagger i\bar{D}^{I\mu}\phi)(\bar{\ell}_p\tau^I\gamma_\mu\ell_r)$
$Q_{\phi e}$	$(\phi^\dagger i\bar{D}^\mu\phi)(\bar{e}_p\gamma_\mu e_r)$
$Q^{(1)}_{\phi q}$	$(\phi^\dagger i\bar{D}^\mu\phi)(\bar{q}_p\gamma_\mu q_r)$
$Q^{(3)}_{\phi q}$	$(\phi^\dagger i\bar{D}^{I\mu}\phi)(\bar{q}_p\tau^I\gamma_\mu q_r)$
$Q_{\phi u}$	$(\phi^\dagger i\bar{D}^\mu\phi)(\bar{u}_p\gamma_\mu u_r)$
$Q_{\phi d}$	$(\phi^\dagger i\bar{D}^\mu\phi)(\bar{d}_p\gamma_\mu d_r)$
$Q_{\phi ud}$	$(\phi^\dagger i\bar{D}^\mu\phi)(\bar{u}_p\gamma_\mu d_r)$

$(\bar{L}L)(\bar{R}R)$	
$Q_{\ell e}$	$(\bar{\ell}_p\gamma^\mu\ell_r)(\bar{e}_s\gamma_\mu e_t)$
$Q_{\ell u}$	$(\bar{\ell}_p\gamma^\mu\ell_r)(\bar{u}_s\gamma_\mu u_t)$
$Q_{\ell d}$	$(\bar{\ell}_p\gamma^\mu\ell_r)(\bar{d}_s\gamma_\mu d_t)$
Q_{qe}	$(\bar{q}_p\gamma^\mu q_r)(\bar{e}_s\gamma_\mu e_t)$
$Q^{(1)}_{qu}$	$(\bar{q}_p\gamma^\mu q_r)(\bar{u}_s\gamma_\mu u_t)$
$Q^{(8)}_{qu}$	$(\bar{q}_p\gamma^\mu T^A q_r)(\bar{u}_s\gamma_\mu T^A u_t)$
$Q^{(1)}_{qd}$	$(\bar{q}_p\gamma^\mu q_r)(\bar{d}_s\gamma_\mu d_t)$
$Q^{(8)}_{qd}$	$(\bar{q}_p\gamma^\mu T^A q_r)(\bar{d}_s\gamma_\mu T^A d_t)$

$(\bar{R}R)(\bar{R}R)$	
Q_{ee}	$(\bar{e}_p\gamma^\mu e_r)(\bar{e}_s\gamma_\mu e_t)$
Q_{uu}	$(\bar{u}_p\gamma^\mu u_r)(\bar{u}_s\gamma_\mu u_t)$
Q_{dd}	$(\bar{d}_p\gamma^\mu d_r)(\bar{d}_s\gamma_\mu d_t)$
Q_{eu}	$(\bar{e}_p\gamma^\mu e_r)(\bar{u}_s\gamma_\mu u_t)$
Q_{ed}	$(\bar{e}_p\gamma^\mu d_r)(\bar{d}_s\gamma_\mu d_t)$
$Q^{(1)}_{ud}$	$(\bar{u}_p\gamma^\mu u_r)(\bar{d}_s\gamma_\mu d_t)$
$Q^{(8)}_{ud}$	$(\bar{u}_p\gamma^\mu T^A u_r)(\bar{d}_s\gamma_\mu T^A d_t)$

$(\bar{L}L)(\bar{L}L)$	
$Q_{\ell\ell}$	$(\bar{\ell}_p\gamma^\mu\ell_r)(\bar{\ell}_s\gamma_\mu\ell_t)$
$Q^{(1)}_{qq}$	$(\bar{q}_p\gamma^\mu q_r)(\bar{q}_s\gamma_\mu q_t)$
$Q^{(3)}_{qq}$	$(\bar{q}_p\gamma^\mu\tau^i q_r)(\bar{q}_s\gamma_\mu\tau^i q_t)$
$Q^{(1)}_{\ell q}$	$(\bar{\ell}_p\gamma^\mu\ell_r)(\bar{q}_s\gamma_\mu q_t)$
$Q^{(3)}_{\ell q}$	$(\bar{\ell}_p\gamma^\mu\tau^i\ell_r)(\bar{q}_s\gamma_\mu\tau^i q_t)$

$(\bar{L}R)(\bar{R}L)$ and $(\bar{L}R)(\bar{L}R)$	
$Q_{\ell edq}$	$(\bar{\ell}_p^{\,j}e_r)(\bar{d}_s q_t^j)$
$Q^{(1)}_{quqd}$	$(\bar{q}_p^{\,j}u_r)\epsilon_{jk}(\bar{q}_s^k d_t)$
$Q^{(8)}_{quqd}$	$(\bar{q}_p^{\,j}T^A u_r)\epsilon_{jk}(\bar{q}_s^k T^A d_t)$
$Q^{(1)}_{\ell equ}$	$(\bar{\ell}_p^{\,j}e_r)\epsilon_{jk}(\bar{q}_s^k u_t)$
$Q^{(3)}_{\ell equ}$	$(\bar{\ell}_p^{\,j}\sigma^{\mu\nu}e_r)\epsilon_{jk}(\bar{q}_s^k\sigma_{\mu\nu}u_t)$

where $\phi^\dagger i\bar{D}_\mu\phi \equiv \phi^\dagger(D_\mu - \overleftarrow{D}_\mu)\phi$ and $\phi^\dagger i\bar{D}^I_\mu\phi \equiv \phi^\dagger(\tau^I D_\mu - \overleftarrow{D}_\mu\tau^I)\phi$, with $\varphi^\dagger\overleftarrow{D}_\mu\varphi \equiv (D_\mu\varphi)^\dagger\varphi$.

Acknowledgments

At the end of this work I want to thank all the people without whom this thesis wouldn't be complete.

I thank my supervisor Prof. Paride Paradisi for having accepted to be my guide in this last step of my master degree; it has been an honour to be his student and to work with him.

I thank my mom, for having taught me that a light shines as more as around becomes darker, and my dad, who incited me to not give up when all seemed to go wrong.

I want to thank also the friends who supported me during this path: I am very lucky to have a lot of people who care for me and who didn't disappear when I need their help. I will be always here for you. A special thanks goes, in particular, to my lifelong friends Matteo, Gabriele, Andrea and Nicole; to Camilla, the most similar person to me who I've ever met; to the "Gang of Padova", a group of six friends who encountered almost casually but who share a very strong connection.

Lastly, I want to dedicate this goal to myself. I am very proud for all the passion and hard work that I put into this thesis, for which I dedicated everything. I hope this will be only the beginning of a bright and rich future in this field.

Bibliography

[1] ATLAS Collaboration, *Observation of a New Particle in the Search for the Standard Model Higgs Boson with the ATLAS Detector at the LHC*, https://arxiv.org/pdf/1207.7214.pdf, (2012)

[2] CMS Collaboration, *Observation of a new boson at a mass of 125 GeV with the CMS experiment at the LHC*, https://arxiv.org/pdf/1207.7235.pdf, (2012)

[3] Wolfenstein, *Parametrization of the Kobayashi-Maskawa matrix*, Phys. Rev. Lett. **51**, 1945 (1983).

[4] UTfit collaboration, *Standard Model Fit results: Summer 2016*, www.utt.org

[5] G. W. Bennet *et al.*, *Final Report of the Muon E821 Anomalous Magnetic Moment Measurement at BNL*, https://arxiv.org/pdf/hep-ex/0602035.pdf, (2006)

[6] M. Passera, *The Standard Model Prediction of the Muon Anomalous Magnetic Moment*, arXiv:hep-ph/0411168, (2004)

[7] A. Petermann, *Fourth order magnetic moment of the electron*, (1957), Helv. Phys. Acta 30, pp. 407-408

[8] Charles M. Sommerfield, *Magnetic Dipole Moment of the Electron*, https://link.aps.org/doi/10.1103/PhysRev.107.328, (1957)

[9] H. H. Elend, *On the anomalous magnetic moment of the muon*, http://www.sciencedirect.com/science/article/pii/0031916366911711, (1966)

[10] S. Laporta, *The analytical contribution of thes ixth-order graphs with vacuum polarization insertions to the muon* $(g-2)$ *in QED*, https://doi.org/10.1007/BF02787236. Il Nuovo Cimento A (1965-1970) 106.5(1993), pp.675– 683. ISSN: 1826-9869.

[11] S. Laporta, E. Remiddi, *The analytical value of the electron light-light graphs contribution to the muon* $(g-2)$ *in QED*, Physics Letters B 301.4 (1993), pp. 440 –446. ISSN: 0370-2693. http://www.sciencedirect.com/science/article/pii/037026939391176N

[12] A. Czarnecki, M. Skrzypek, *The muon anomalous magnetic moment in QED: three-loop electron and tau contributions*, https://arxiv.org/pdf/hep-ph/9812394.pdf, (1998)

[13] S. Laporta, *High-precision calculation of the 4-loop contribution to the electron g-2 in QED*, https://arxiv.org/pdf/1704.06996.pdf, (2017)

[14] T. Aoyama, M. Hayakawa, T. Kinoshita,M. Nio, *Complete Tenth Order QED Contribution to the Muon $g-2$*, https://arxiv.org/pdf/1205.5370.pdf, (2012)

[15] T. Aoyama, M. Hayakawa, T. Kinoshita, M. Nio, *Tenth-Order QED Contribution to the Electron $g-2$ and an Improved Value of the Fine Structure Constant*, https://link.aps.org/doi/10.1103/PhysRevLett.109.111807, (2012)

[16] R. Jackiw, S. Weinberg, *Weak-Interaction Corrections to the Muon Magnetic Moment and to Muonic-Atom Energy Levels*, https://link.aps.org/doi/10.1103/PhysRevD.5.2396, Phys.Rev.D5(91972), pp.2396–2398

[17] I. Bars, M. Yoshimura, *Muon Magnetic Moment in a Finite Theory of Weak and Electromagnetic Interactions*, https://link.aps.org/doi/10.1103/PhysRevD.6.374 Phys. Rev. D 6 (1 1972), pp. 374–376

[18] G. Altarelli, N. Cabibbo, L. Maiani *The Drell-Hearn sum rule and the lepton magnetic moment in the Weinberg model of weak and electromagnetic interactions*, http://www.sciencedirect.com/science/article/pii/0370269372908337, Physics Letters B 40.3 (1972), pp. 415 –419. ISSN: 0370-2693

[19] W.A. Bardeen, R. Gastmans, B. Lautrup, *Static quantities in Weinberg's model of weak and electromagnetic interactions*, http://www.sciencedirect.com/science/article/pii/0550321372902180, Nuclear Physics B46.1(1972),pp.319–331. ISSN:05503213

[20] K. Fujikawa, B. W. Lee, A. I. Sanda *Generalized Renormalizable Gauge Formulation of Spontaneously Broken Gauge Theories*, https://link.aps.org/doi/10.1103/PhysRevD.6.2923, Phys.Rev.D6(101972),pp.2923– 2943

[21] T. V. Kukhto, E. A. Kuraev, A. Schiller, Z.K. Silagadze, *The dominant two-loop electroweak contributions to the anomalous magnetic moment of the muon*, http://www.sciencedirect.com/science/article/pii/0550321392906877, Nuclear Physics B 371.3 (1992), pp. 567 –596. ISSN: 0550-3213

[22] F. Jegerlehner, *Muon $g-2$ Theory: the Hadronic Part*, https://arxiv.org/pdf/1705.00263.pdf, (2017)

[23] T. Blum, N. Christ, M. Hayakawa, T. Izubuchi, L. Jin, Chulwoo Jung, C Lehner, *Connected and leading disconnected hadronic light-by-light contribution to the muon anomalous magnetic moment with physical pion mass*, https://arxiv.org/pdf/1610.04603.pdf, (2016)

[24] C. M. Carloni Calame, M. Passera, L. Trentadue, and G. Venanzoni *A new approach to eval- uate the leading hadronic corrections to the muon g-2*, https://arxiv.org/pdf/1504.02228.pdf, (2015)

[25] L.Bouchiat Claude et Michel, *La r´esonance dans la diffusion m´eson π^- m´eson π et le moment magn´etique anormal du m´eson μ*, J. Phys. Radium 22 (1961), pp. 121–121

[26] L. Durand, *Pionic Contributions to the Magnetic Moment of the Muon*, https://link.aps.org/doi/10.1103/PhysRev.128.441, Phys. Rev. 128 (1 1962), pp. 441–448

[27] M.Gourdin, E. De Rafael, *Hadronic contributions to the muon g-factor*, http://www.sciencedirect.com/science/article/pii/0550321369903332, NuclearPhysics B 10.4 (1969), pp. 667 –674. ISSN: 0550-3213

[28] T. Blum, N. Christ, M. Hayakawa, T. Izubuchi, L. Jin, C. Jung, C. Lehner, *Connected and leading disconnected hadronic light-by-light contribution to the muon anomalous magnetic moment with physical pion mass*, https://arxiv.org/pdf/1610.04603.pdf, (2016)

[29] G. Abbiendi *et al.*, *Measuring the leading hadronic contribution to the muon g-2 via μe scattering* , https://arxiv.org/pdf/1609.08987.pdf, (2017)

[30] M.Davier, A.Hoecker, B.Malaescu and Z. Zhang, Eur. Phys. J. **C71**, (2011)

[31] K. Hagiwara, R. Liao, A. D. Martin, D. Nomura and T. Teubner, J. Phys. **G38**, (2011)

[32] D. Babusci *et al.*, *Proposal for taking data with the KLOE-2 detector at the DAΦNE collider upgraded in energy*, https://arxiv.org/pdf/1007.5219.pdf, (2010)

[33] T. Blum *et al. A novel precision measurement of muon $g-2$ and EDM at J-PARC*, , (2012)

[34] G. Venanzoni, *The New Muon $g-2$ experiment at Fermilab*, https://arxiv.org/pdf/1411.2555.pdf, (2014)

[35] C. M. Carloni Calame, M. Passera, L. Trentadue, G. Venanzoni *A new approach to evaluate the leading hadronic corrections to the muon g-2*, https://arxiv.org/pdf/1504.02228.pdf, (2015)

[36] B.E. Lautrup, A. Peterman, E. de Rafael *Recent developments in the comparison between theory and experiments in quantum electrodynamics*, http://www.sciencedirect.com/science/article/pii/0370157372900117, (1972)

[37] G. Venanzoni, *The MUonE experiment: a novel way to measure the leading order hadronic contribution to the muon $g-2$*, https://arxiv.org/pdf/1811.11466.pdf, (2018)

[38] S. Schael *et al.* [ALEPH, DELPHI, L3 and OPAL, and LEP Electroweak Collaborations], *Electroweak Measurements in Electron-Positron Collisions at W-Boson-Pair Energies at LEP*, arXiv:1302.3415, (2013)

[39] M. Derrick *et al.*, *New results on the reaction $e^+e^- \to \mu^+\mu^-$ at $\sqrt{s} = 29$ GeV* Phys. Rev. D **31**(1985) 2352

[40] S. Hegner *et al.* [JADE Collaboration], *Final results on muon and tau pair production by the JADE Collaboration at PETRA* , Z. Phys. C **46** (1990) 547

[41] M. Miura *et al.* [VENUS Collaboration], *Precise measurement of the $e^+e- \to \mu^+\mu^-$ reaction at $\sqrt{s} = 57.77$ GeV*, Phys. Rev. D **57** (1998) 5345

[42] J. L. Rainbolt, M. Schmitt, *Branching fraction for Z decays to four leptons and constraints on new physics* , https://arxiv.org/pdf/1805.05791.pdf, (2019)

[43] J. P. Lees *et al.* [BaBar Collaboration], *Search for a muonic dark force at BABAR*, https://arxiv.org/pdf/1606.03501.pdf, (2016)

[44] B. Pontecorvo, Sov. Phys. JETP 6 (1957) 429 [Zh. Eksp. Teor. Fiz. 33 (1957) 549]

[45] V. W. Hughes *et al.*, *Formation of muonium and observation of its Larmor precession*, Phys. Rev. Lett. 5 (1960) 63

[46] G. Feinberg, S. Weinberg, *Conversion of Muonium into Antimuonium*, Phys. Rev. Lett. 6 (1961) 381; Phys. Rev. 123 (1961) 1439

[47] L. Willmann *et al.*, *New Bounds from a Search for Muonium to Antimuonium Conversion*, Phys. Rev. Lett. 82 (1999) 49

[48] M. Bauer, M. Neubert, S. Renner, M. Schnubel, A. Thamm, *Axion-like particles, lepton-flavor violation and a new explanation of a_μ and a_e*, https://arxiv.org/pdf/1908.00008.pdf, (2019)

[49] M. Bauer, M. Heiles, M. Neubert, A. Thamm, *Axion-like particles at future colliders*, https://link.springer.com/content/pdf/10.1140/epjc/s10052-019-6587-9.pdf, (2019)

[50] M. Tanabashi *et al.* [Particle Data Group], Phys. Rev. D **98**, no. 3, 030001 (2018).

[51] C. Cornella, P. Paradisi, O. Sumensari, *Hunting for ALPs with Lepton Flavor Violation*, https://arxiv.org/pdf/1911.06279.pdf, (2020)

[52] P. S. Bhupal Dev, W. Rodejohann, Xun-Jie Xu, Y. Zhanga, *MUonE sensitivity to new physics explanations of the muon anomalous magnetic moment* , https://arxiv.org/pdf/2002.04822.pdf, (2020)

[53] B. Batell, N. Lange, D. McKeen, M. Pospelov, A. Ritz, *The Leptonic Higgs Portal*, https://arxiv.org/pdf/1606.04943.pdf, (2016)

[54] M. Bauer, P. Foldenauer, J. Jaeckel, *Hunting All the Hidden Photons*, https://arxiv.org/abs/1803.05466, (2018)

[55] R. Alemany *et al.*, *Summary Report of Physics Beyond Colliders at CERN*, https://arxiv.org/pdf/1902.00260.pdf), (2019)

[56] J. P. Lees *et al.* [BaBar Collaboration], *Search for a dark photon in e^+e^- collisions at BABAR*, https://arxiv.org/pdf/1406.2980.pdf, (2014)

[57] A. Anastasi *et al.* [KLOE-2 Collaboration], *Combined limit on the production of a light gauge boson decaying into $\mu^+\mu^-$ and $\pi^+\pi^-$*, https://arxiv.org/pdf/1807.02691.p, (2018)

[58] J. P. Leveille, *The second order weak correction to $g-2$ of the muon in arbitrary gauge models*, Nucl. Phys. B **137** (1978) 63

[59] M. Alacevich *et al.*, *Muon-electron scattering at NLO*, https://arxiv.org/pdf/1811.06743.pdf, (2019)

[60] A. Crivellin, S. Davidson, G. M. Pruna, A. Signer, *Renormalisation-group improved analysis of $\mu \to e$ processes in a systematic effective-field-theory approach*, https://arxiv.org/pdf/1702.03020.pdf, (2018)

[61] W. Buchmuller, D. Wyler, *Effective Lagrangian analysis of new interactions and flavour conservation*, https://inspirehep.net/literature/218149, (1986)

[62] B. Grzadkowski, M. Iskrzyński, M. Misiak, and J. Rosiek , *Dimension-Six Terms in the Standard Model Lagrangian*, https://arxiv.org/pdf/1008.4884.pdf, (2017)

[63] Elizabeth E. Jenkins, Aneesh V. Manohar, Peter Stoffer, *Low-Energy Effective Field Theory below the Electroweak Scale: Operators and Matching* , https://arxiv.org/pdf/1709.04486.pdf, (2018)

[64] R. Conlin, A. A. Petrov, *Muonium-antimuonium oscillations in effective field theory*, https://arxiv.org/pdf/2005.10276.pdf, (2020)

[65] M. E. Peskin, D. V. Schroeder, *An Introduction to quantum field theory*